

# RO ADIOLOGY AND NCOLOGY



September 1999  
Vol. 33 No. 3  
Ljubljana

ISSN 1318-2099

# Ω

*preprosto  
neboleče*

*Napolnjene injekcijske brizge  
za samoaplikacijo*

volumen (ml)	jakost (I.E.)
1	EPOMAX™ 4000
0,5	EPOMAX™ 2000
0,5	EPOMAX™ 1000



# EPOMAX™



EPOETIN OMEGA

lek  
v sodelovanju z  
*Elanor*

Podrobnejše informacije o zdravilu dobite pri proizvajalcu.

# RADIOLOGY AND ONCOLOGY



## Editorial office

### **Radiology and Oncology**

*Institute of Oncology*

*Vrazov trg 4*

*SI-1000 Ljubljana*

*Slovenia*

*Phone: +386 61 1320 068*

*Phone/Fax: +386 61 1337 410*

*E-mail: gsertsa@onko-i.si*

*September 1999*

*Vol. 33 No. 3*

*Pages 179-255*

*ISSN 1318-2099*

*UDC 616-006*

*CODEN: RONCEM*

## Aims and scope

*Radiology and Oncology is a journal devoted to publication of original contributions in diagnostic and interventional radiology, computerized tomography, ultrasound, magnetic resonance, nuclear medicine, radiotherapy, clinical and experimental oncology, radiobiology, radiophysics and radiation protection.*

## Editor-in-Chief

**Gregor Serša**

*Ljubljana, Slovenia*

## Editor-in-Chief Emeritus

**Tomaž Benulič**

*Ljubljana, Slovenia*

## Executive Editor

**Viljem Kovač**

*Ljubljana, Slovenia*

## Editor

**Uroš Smrdel**

*Ljubljana, Slovenia*

## Editorial board

**Marija Auersperg**

*Ljubljana, Slovenia*

**Nada Bešenski**

*Zagreb, Croatia*

**Karl H. Bohuslavizki**

*Hamburg, Germany*

**Haris Boko**

*Zagreb, Croatia*

**Nataša V. Budihna**

*Ljubljana, Slovenia*

**Marjan Budihna**

*Ljubljana, Slovenia*

**Malte Clausen**

*Hamburg, Germany*

**Christoph Clemm**

*München, Germany*

**Mario Corsi**

*Udine, Italy*

**Christian Dittrich**

*Vienna, Austria*

**Ivan Drinković**

*Zagreb, Croatia*

**Gillian Duchesne**

*Melbourne, Australia*

**Béla Fornet**

*Budapest, Hungary*

**Tullio Giraldi**

*Trieste, Italy*

**Andrija Hebrang**

*Zagreb, Croatia*

**László Horváth**

*Pécs, Hungary*

**Berta Jereb**

*Ljubljana, Slovenia*

**Vladimir Jevtič**

*Ljubljana, Slovenia*

**H. Dieter Kogelnik**

*Salzburg, Austria*

**Jurij Lindtner**

*Ljubljana, Slovenia*

**Ivan Lovasić**

*Rijeka, Croatia*

**Marijan Lovrenčić**

*Zagreb, Croatia*

**Luka Milas**

*Houston, USA*

**Metka Milčinski**

*Ljubljana, Slovenia*

**Maja Osmak**

*Zagreb, Croatia*

**Branko Palčič**

*Vancouver, Canada*

**Jurica Papa**

*Zagreb, Croatia*

**Dušan Pavčnik**

*Portland, USA*

**Stojan Plesničar**

*Ljubljana, Slovenia*

**Ervin B. Podgoršak**

*Montreal, Canada*

**Jan C. Roos**

*Amsterdam, Netherlands*

**Slavko Šimunić**

*Zagreb, Croatia*

**Lojze Šmid**

*Ljubljana, Slovenia*

**Borut Štabuc**

*Ljubljana, Slovenia*

**Andrea Veronesi**

*Aviano, Italy*

**Živa Zupančič**

*Ljubljana, Slovenia*

**Publishers**

*Slovenian Medical Association - Slovenian Association of Radiology, Nuclear Medicine Society,  
Slovenian Society for Radiotherapy and Oncology, and Slovenian Cancer Society  
Croatian Medical Association - Croatian Society of Radiology*

**Affiliated with**

*Societas Radiologorum Hungarorum  
Friuli-Venezia Giulia regional groups of S.I.R.M.  
(Italian Society of Medical Radiology)*

*Copyright © Radiology and Oncology. All rights reserved.*

**Reader for English**

*Olga Shrestha  
Mojca Čakš*

**Key words**

*Eva Klemenčič*

**Secretaries**

*Milica Harisch  
Betka Savski*

**Design**

*Monika Fink-Serša*

**Printed by**

*Imprint d.o.o., Ljubljana, Slovenia*

*Published quarterly in 750 copies*

*Bank account number 50101 679 901608*

*Foreign currency account number*

*50100-620-133-900-27620-978-515266/6*

*NLB - Ljubljanska banka d.d. - Ljubljana*

*Subscription fee for institutions \$ 100 (16000 SIT), individuals \$ 50 (5000 SIT)*

*The publication of this journal is subsidized by the Ministry of Science and Technology of the Republic of Slovenia.*

*According to the opinion of the Government of the Republic of Slovenia, Public Relation and Media Office.*

*The journal Radiology and Oncology is a publication of informative value, and as such subject to taxation by 5 % sales tax.*

**Indexed and abstracted by:**

*BIOMEDICINA SLOVENICA*

*CHEMICAL ABSTRACTS*

*EMBASE / Excerpta Medica*

*This journal is printed on acid-free paper*

*Radiology and Oncology is available on the internet at: <http://www.onko-i.si/radiolog/rno.htm>*



## CONTENTS

### ULTRASOUND

---

- Treatment of hyperfunctioning thyroid nodules with ultrasound guided percutaneous ethanol injection - 30 months experience** 179  
*Brkljačić B, Sučić M, Božikov V, Hebrang A*
- Sonographic diagnosis of soft-tissue foreign bodies in children** 189  
*Ročić G, Ercegović S, Vlahović T, Čop S, Bumči I, Višnjić S*
- Ultrasonographic diagnosis of obstructive ileus in a patient with Meckel's diverticulum (case report)** 193  
*Alenka Višnar-Perovič A, Koren A*

### COMPUTERIZED TOMOGRAPHY

---

- When do heterogeneous splenic enhancement patterns occur in contrast-enhanced CT studies of the abdomen ?** 199  
*Groell R, Rienmüller R, Uggowitzer MM, Kugler C, Stauber RE, Fickert P*

### NUCLEAR MEDICINE

---

- Value of F-18-FDG PET in patients with cervical lymph node metastases of unknown origin** 207  
*Bohuslavizki KH, Klutmann S, Buchert R, Kröger S, Werner JA, Mester J, Clausen M*

<b>Renal transplant blood flow in patients with acute tubular necrosis</b>	<b>215</b>
<i>Huić D, Grošev D, Bubić-Filipi L, Crnković S, Dodig D, Poropat M, Puretić Z</i>	

---

## EXPERIMENTAL ONCOLOGY

---

<b>Cryosurgery combined with radiotherapy of tumors in mice</b>	<b>221</b>
<i>Fras AP, Kranjc S, Čemažar M, Serša G</i>	

---

## RADIOPHYSICS

---

<b>A modified half-block breast irradiation technique using a CT-simulator</b>	<b>227</b>
<i>Evans MDC, Benk V, Freeman C, Gosselin M, Olivares M, Podgorsak EB</i>	
<b>Evaluation of silicon microstrip detectors as X-ray sensors in digital mammography</b>	<b>237</b>
<i>Mali T, Cindro V, Mikuž M, Zdešar U, Jančar B</i>	

<b>SLOVENIAN ABSTRACTS</b>	<b>245</b>
----------------------------	------------

---

<b>NOTICES</b>	<b>253</b>
----------------	------------

---

## Treatment of hyperfunctioning thyroid nodules with ultrasound guided percutaneous ethanol injection - 30 months experience

Boris Brkljačić<sup>1</sup>, Mate Sučić<sup>2</sup>, Veljko Božikov<sup>2</sup>, Andrija Hebrang<sup>1</sup>

<sup>1</sup>Department of Radiology, University Hospital "Merkur" and <sup>2</sup>Department of Internal Medicine, Division of Endocrinology, University Hospital "Dubrava", Zagreb, Croatia

---

**Background.** Our technique of performing percutaneous ethanol injection (PEI) and results after 30 months are presented and compared with results from the literature.

**Material and methods.** PEI was performed in 40 patients (37 female, 3 male, age range 28-76 years); in 35 cases, there was a solitary, scintigraphically "hot" nodule, and in 5 cases a toxic nodular goiter was found. The volume of treated nodules was in the range from 2.5 to 38 ccm (mean volume  $20.7 \pm 14.1$  ccm). Ethanol was injected with the "free-hand" technique, usually in multiple sessions, with the color and power Doppler ultrasound guidance. The total injected volume of ethanol was 1.5 times the volume of the treated nodule.

**Results.** The procedure was technically successful in 37 patients (92.5%). Pain during injection was observed in all cases, subcutaneous hematoma in 6 cases, and transitory dysphonia in one patient. There were no long-term complications. In 36 patients, the successfulness of the treatment was evaluated after 3-4 months on the basis of scintigraphy, hormonal status and ultrasonographic findings. A complete and partial cure was achieved in 22 (61.1%) and in 10 patients (27.8%) of patients, respectively, whereas in 4 patients (11.1%) the result was unsatisfactory, since only a moderate hormonal remission was observed after the completion of the procedure. A satisfactory result was observed in 32/36 patients (88.9%). Significant reduction of nodular volume was noted in all cases. A better result was observed in smaller nodules and in cases of autonomous adenomas. No cases of recurrent hyperthyreosis were detected.

**Conclusions.** Percutaneous ethanol injection under ultrasound guidance is an efficient and safe method in the treatment of autonomous thyroid nodules, that enables inactivation of nodules with minimal and/or transitory complications, without permanent or serious complications that can be observed after radioiodine or surgical therapy.

**Key words:** thyroid nodule - drug therapy; ethanol; thyroid neoplasms - ultrasonography; autonomous adenoma

---

Correspondence to: Doc. Boris Brkljačić, MD, PhD, Ultrasonic Center, Department of Radiology, University Hospital "Merkur", Zajčeva 19, 10000 Zagreb, Croatia; Phone: 385 1 2431 413; Fax: 2431 397; E-mail: boris.brkljacic@zg.tel.hr

Received 28 January 1999

Accepted 6 April 1999



## Introduction

Thyroid toxic adenomas and toxic nodular goiters have until recently been exclusively treated with radioiodine therapy or surgical resection.<sup>1,2</sup> According to the numerous reports in the literature, both of these methods are known to have potentially serious and/or permanent and relatively frequent complications.<sup>2-6</sup> Ethanol is percutaneously being instilled in hepatocellular carcinomas using ultrasound guidance,<sup>7</sup> and, in the region of the neck, Solbiati started to use ethanol for parathyroid glands sclerosations in cases of the secondary hyperparathyroidism.<sup>8</sup> In 1990, Livraghi started with the ultrasound-guided percutaneous ethanol injections (PEI) for sclerosation of autonomous and toxic thyroid adenomas.<sup>9</sup> Reported results were promising and the method spread fast throughout Italy.<sup>10-16</sup> Surprisingly, the method is not frequently used in other countries; there are only two published articles about its utilization outside Italy - one from Turkey<sup>17</sup> and one from Germany.<sup>18</sup>

Our two institutions (University Hospitals "Merkur" and "Dubrava") started jointly with the percutaneous ethanol injection of thyroid autonomous and toxic nodules under the ultrasound color and power Doppler guidance in August of 1996. In this paper, our technique of performing PEI and results after 30 months are presented and compared with the results from the literature.

## Patients and methods

Percutaneous ethanol injection is performed under the ultrasound guidance, using linear electronic high-frequency probes with a frequency range between 7.5 and 10 MHz. Color and power Doppler are used to evaluate increased vascularisation which can be observed in the vast majority of autonomous (scintigraphically "hot") thyroid nodules. All

PEI procedures were performed by the first author (BB), using US scanner Acuson 128 XP4 with a linear 7.5 MHz probe (from August 1996 until September 1997) and Acuson 128 XP10 with a linear multifrequency probe 7.5-10 MHz (from September 1997 onwards). Both scanners are equipped with color and power Doppler capabilities and provide high-quality visualization of thyroid nodules in B-mode and visualization of intra and perinodular vascularisation. PEI under color and power Doppler guidance was especially valuable in cases of multinodular thyroids, when only one (or some) of nodules was autonomous; in these cases, such nodules can be differentiated from adjacent non-functioning nodules that are less vascularized.

The needle is introduced into the nodule using the "free-hand" technique, without the local anesthesia. We used 22-gauge needles with the end-hole and a 96% sterile ethanol (prepared in the State Institute of Transfusiology). The total volume of ethanol instilled was 1.5 times of the nodular volume, with a maximum of 10 ml of ethanol that could be injected in a single session (personal communication by Livraghi to the first author). The nodular volume (in ccm) was calculated in a usual fashion ( $a \times b \times c \times 0.5$ ;  $a$ =length,  $b$ =width,  $c$ =depth in centimeters). The number of injections (sessions) was calculated according to the nodular size and varied from 1 to 8 injections per therapy cycle. The volume of ethanol being injected per session was determined depending on the individual patient's compliance with the procedure; in larger nodules, it was at most 30% of the nodular volume, while in small nodules, the total ethanol volume required could be injected either in one or two sessions.

In each session, the ethanol was injected once or twice, with the needle being directed to different areas of the nodule to insure an equal distribution of the ethanol. The utilization of the side-hole needles simplifies the procedure and ensures an equal ethanol dis-



tribution with no need to move the needle within the nodule. The procedure was repeated twice per week until the total planned volume of ethanol was injected into the nodule. The injection and distribution of ethanol within the nodule were clearly visible in real-time under the ultrasound guidance, as tiny brightly echogenic dots within the nodule. Occasionally, a rapid wash-out of ethanol in a highly vascularized nodule could be observed; in these cases, a larger volume of ethanol could be injected, until its distribution within the nodule was observed. During the ethanol injection to the posteriorly located nodules, special care should be taken in order to avoid possible impairment of the recurrent laryngeal nerve with the ethanol.

The thyreostatic medication was not applied routinely prior to PEI; the therapy being taken was not altered because of the procedure. In all patients T3, T4, FT3, FT4, TSH and thyroid antibodies in the serum were determined using standard laboratory methods. In all patients the thyroid scintigraphy with Tc-99m pertechnetate was performed and scintigraphic and US/color Doppler findings compared prior to the commencement of the PEI, so that the ethanol could be injected into the right nodule, which proved to be particularly beneficial in cases of multinodular thyroids.

PEI was performed in the period from August 1996 to January 1999 in 40 patients (37 women and 3 men) with the age range of 28-76 (mean  $54.2 \pm 12.8$ ) years. Thirty-five patients had the solitary "hot" nodule, and five patients the toxic nodular goiter, with 2 scintigraphically "hot" nodules which were both sclerosed with ethanol. All the procedures were performed on the out-patient basis.

All the patients, who were referred for the PEI by endocrinologists, and who had multinodular thyroids with scintigraphically visible multiple "hot" nodules, and in whom particular nodules could not be ultrasonographically

reliably differentiated from cold nodules, were refused from the PEI and referred for the radioiodine therapy. Thirty-four patients were hyperthyroid, with elevated FT3 and FT4 levels and suppressed TSH level, and scintigraphically suppressed extranodular tissue. Six patients had only minimal extranodular uptake of the Technetium on scintigraphy (developing autonomous adenomas); three of them had normal TSH level, and three had suppressed TSH and thyroid hormones within the normal range.

The smallest treated nodule had a volume of 2.5 ccm, and the largest of 38 ccm (mean  $20.7 \pm 14.1$  ccm). The injected volume varied from 4 ml to 57 ml of ethanol, with the maximum volume of 1.5 times the nodular volume. Maximum number of injections in one cycle was 10. The largest single volume of ethanol injected in one session was 10 ml. It was injected exclusively to the patients living far away for whom frequent travels to our Institution for the injection, would present a problem. Usually single volumes of up to 5-6 ml per session were administered. PEI procedure was as a rule performed in two sessions per week, with 3 or 4 days between each session.

The follow-up of patients after PEI was performed under the following protocol: serum thyroid hormones were assessed after 1, 3, 6 and 12 months; the control ultrasound examinations were performed in the same intervals. Thyroid scintigraphy was performed for the first time 3-4 months after the completion of PEI, which proved to be a sufficient period in the majority of cases to evaluate the treatment successfulness.

After the successful PEI, the hormonal status was normalized, as well as scintigraphic finding. The majority of patients did not take thyreostatic medications after the therapy and the evaluation of the successfulness of PEI could be performed on the basis of hormonal status. However, we always analyzed scintigraphic findings to evaluate definitely

the successfulness of the procedure. Color and power Doppler US played important role in the follow-up, since the successfully sclerosed nodules exhibited considerably less or even no vascularization, as compared to the pre-procedure findings. B-mode US showed, as a rule, the shrinking of nodules and changing of echogenicity: the nodules became hyperechogenic (due to the ethanol-induced coagulation necrosis<sup>9</sup>) as compared to the pre-procedure echogenicity. If residual hypervascularisation was observed with color and power Doppler, the additional ethanol was injected into the region. If the procedure was not successful upon the completion of the first cycle of injections, the ethanol could be injected again; the volume of ethanol needed in the second or the third cycle was determined arbitrarily according to the size of the nodule, degree of hypervascularization and hormonal status. In the presented group of patients we performed at most two cycles of PEI (one patient with unsuccessful outcome after the second cycle refused the proposed third cycle).

Results

*Technical successfulness of the procedure and complications*

Six patients developed subcutaneous neck hematomas after the procedure; two of these patients were hospitalized, one for two days and the other for five days. In both patients

hematomas resolved completely without therapy, and without permanent sequels. In one of the latter two patients, hematoma developed after the last session in the second PEI cycle, and the final result of the procedure was complete cure of the toxic adenoma. In the other patient, hematoma occurred after the second of the four planned sessions. She refused further treatment. Another patient refused the treatment after the first session; she had a minimal subcutaneous hematoma, but could not tolerate the pain during and after the injection. The latter two patients were included in the group of patients, where the procedure was considered as technically unsuccessful. The third patient in this "technical failure" group could not tolerate the pain during the injection, and she immediately refused further treatment.

All patients complained of the pain of varying degree during the injection. The pain was projected toward the jaw, ear or sternum, and lasted several minutes after the procedure. Many patients experienced some pain also 1-2 days after the session (as a rule, the pain was stronger when more ethanol was injected). Nevertheless, significant complications were not noted, and patients tolerated the procedure well. One patient had a transient dysphonia, which passed after 7 days. Transient dysphonia occurred due to the unilateral vocal cord paresis, most probably caused by the ethanol when injected in nodules adjacent to the posterior contour of the thyroid lobe and coming in contact with the recurrent laryngeal nerve. It is assumed that a chemically or compression induced lesion of

**Table 1.** Technical successfulness of the PEI procedure

No. of pts in whom PEI was performed	40
No. of pts where PEI was technically successful	37 (92.5%)
No. of pts where PEI was technically unsuccessful	3 (7.5%)
Reasons for the failure of the procedure	(1) refusing after 1st session due to pain; (2) minimal subcut. hematoma and pain after 1st injection; (3) major subcutaneous hematoma after 2nd injection

the nerve occurs.<sup>19</sup> This was a reversible paresis without anatomical break of the nerve, as opposed to surgical impairment in which transection of the nerve causes permanent nerve damage.<sup>2,19</sup>

There were no cases of thyreotoxicosis or hyperthyreosis observed after the procedure. In all 37 patients, ultrasonography showed a satisfactory and even distribution of ethanol within the nodule.

**Table 2.** Complications in 37 patients where PEI was technically successful

Pain during injection	37/37
Pain 1-2 days after the injection	15/37
Subcutaneous hematoma, hospitalization	1/37
Minor subcutaneous hematoma	3/37
Transient dysphonia	1/37

### Results (outcome) of the PEI procedure

The outcome of the PEI in our patients could be categorized into three groups, according to the literature<sup>8-18</sup>:

- 1.) *Complete cure* with the normalization of serum thyroid hormones and TSH levels, normalization of clinical status and reappearance of extranodular uptake on scintigraphy, while the node is either "cold", or non-visible on the scan;
- 2.) *Partial recovery* with the remission of clinical symptoms, normalization of serum thyroid hormones and TSH levels, reappearance of extranodular uptake on scintigraphy, with the node (or part of the node) still "hot" on the scan;

3.) *Hormonal remission* - clinical status improved, serum thyroid hormone levels normal, TSH still suppressed; scintigraphically "hot" nodule, with suppressed extranodular uptake.

Our results include 40 patients in whom procedure was started during the last 30 months, and was technically successfully completed in 37 (92.5%). In 36 patients, the definite successfulness of the procedure could be evaluated 3-4 months after the completion of the procedure. In these 36 patients, the successfulness of the PEI was assessed on the basis of scintigraphic and ultrasonographic findings and of hormonal status. In 32 patients, a solitary nodule was observed (6 autonomous adenomas and 26 toxic adenomas), and 4 patients had toxic nodular goiter. The results of the procedure in these 36 patients are presented in the Table 3.

A complete cure was achieved in 22 patients, and partial recovery in 10 patients; both outcomes are considered favourable result of the PEI. Therefore, the overall success of the procedure was achieved in 32/36 patients (88.9%). A complete cure was obtained in all 6 patients who developed autonomous adenomas. The initial nodule volume in patients in whom complete cure (I), partial cure (II) and hormonal remission (III) was obtained, was  $18.2 \pm 12.7$  ccm,  $22.4 \pm 13.9$  ccm, and  $30.1 \pm 21.1$  ccm, respectively. One cycle of therapy was applied in 19/22 patients with complete cure and 7/10 patients with partial recovery and in one patient with hormonal remission. In the remaining nine patients, two cycles of PEI were performed.

**Table 3.** Outcome of PEI in 36 patients

Outcome	No. of patients	%	Solitary nodules	TNG
I	22/36	61.1	22/22	0/22
II	10/36	27.8	8/10	2/10
III	4/36	11.1	2/4	2/4

I-complete cure, II- partial recovery, III-hormonal remission

In four patients, the procedure was not successful. One patient with toxic nodular goiter was referred for radioiodine therapy after the completion of the first cycle, and the procedure was not repeated; in three patients PEI was repeated with the new cycle of treatment and was not successful. In two cases of toxic nodular goiters, a partial recovery was achieved after the second cycle, and, in one case, the procedure was unsuccessful after the second cycle.

Overall, out of 36 patients with solitary "hot" nodules the PEI was successful in 32 (88.9%), while in 4 patients with toxic nodular goiter, the procedure was successful in two patients (50%).

The longest follow-up after the procedure was 26 months. The largest observed reduction in the volume of the nodule after the procedure was observed in the patient with the largest treated nodule; the initial volume of 38 ccm was reduced to 6 ccm (15.8% of the initial volume) 6 months after PEI. During the follow-up of 3-26 months, the initial nodular volume was reduced more than 50% in 34 of 36 patients. In the follow-up period, no recurrence was noted in the cases of complete or partial recovery after PEI.

In all patients with the successful outcome of the procedure, a considerable reduction of flow or even disappearance of intranodular flow was observed with color and power Doppler ultrasound. Moreover, B-mode ultrasonography showed a markedly increased echogenicity of the treated nodules in these patients.

## Discussion

There are three published studies in the literature, comprising larger number of treated patients, with longer follow-up and evaluation of the successfulness of the therapy.

Livraghi was the first to commence with PEI; in 1994 he published his results on a

group of 101 patients, with the mean age of  $50.8 \pm 12.4$  years.<sup>19</sup>

In ten patients with developing autonomous adenomas, PEI was successful in all cases. Out of 91 patients with suppressed TSH, a complete cure was observed in 49 (53.9%); the initial nodular volume in this group was  $16.8 \pm 10.3$  ccm, and after PEI it was reduced to  $2.8 \pm 1.6$  ccm (16.7% of the initial volume). Color Doppler showed complete lack of nodular hypervascularization. In 42 patients PEI was performed in a single cycle, and in 7 patients in two cycles. A partial recovery, also considered as successful outcome, was observed in 34 (37.4%) patients. The nodular volume was reduced to 24.5% of initial volume (from  $20.8 \pm 12.2$  ccm to  $5.1 \pm 4.0$  ccm). In this group, one, two and three cycles of PEI were performed in 23, 9 and 2 patients, respectively. A hormonal remission, considered as failure of PEI, was noted in 9 patients (9.9%); the nodules in this group were mainly large, with an average volume of  $30.4 \pm 19.9$  ccm, that was reduced to 26.6% of the initial volume after PEI ( $8.1 \pm 7.9$  ccm). Three patients had 3 PEI cycles, four had two cycles, and one had one cycle. As a rule, the results are more favorable in small nodules as compared to large ones. The satisfactory response can be expected in the nodules below 40 ccm. TSH in serum is detectable usually 1-3 months after the therapy is finished. Livraghi's results are excellent, and even in 9 patients with unsuccessful procedure a significant decrease of serum FT3 and FT4 levels was observed. A significant reduction of the nodular volume was observed in all cases. In the follow-up period of 6 months to 4 years, no recurrence was noted in cases of complete or partial recovery after PEI.

In 1997, a group from Pisa published their results of five-year follow up of 111 patients after PEI.<sup>20</sup> Seventy-seven had a toxic adenoma, and 40 developing autonomous adenomas. The results are similar to Livraghi's, with all autonomous adenoma patients being

successfully treated. In 77 patients with TA, a complete cure was noted in 60 (78%), partial recovery in 7 (9%), and PEI was unsuccessful in 10 patients (13%). PEI was equally successful in the case of solitary "hot" nodule or two "hot" nodules. A significant reduction of nodular volume was observed in all cases, and no recurrences of hyperthyreosis occurred during the follow-up period. Only one patient developed subclinical hypothyreosis after five years; however, that patient had considerably elevated thyroid antibodies serum levels prior to the therapy. Unlike Livraghi, these authors did not observe any differences in the outcome related to the volume of the nodules.

The results of Italian multicentric study were published in 1996.<sup>21</sup> It comprised 429 patients with PEI performed in solitary autonomous nodules (242 toxic adenomas, 187 autonomous adenomas). Complete cure was observed in 2/3 of patients with toxic adenoma, and 83.4% of patients with autonomous adenomas. In remaining patients, where no changes on scintigraphy were observed and/or TSH remained suppressed, the procedure was considered as a failure. In all treated patients, a significant reduction of nodular volume was noted, and there was no recurrence of hyperthyreosis or occurrence of hypothyreosis. Almost all successful results were obtained in nodules with a volume of < 15 ccms. Somewhat inferior results of this study as compared to previous two studies may be due to the recruitment of patients from a large number of centers, and one can assume that the procedure was not technically optimally performed in all institutions.

Although our group of patients is relatively small, the initial results are comparable with those reported by Livraghi, and other larger studies.<sup>19-21</sup> Complications are rare and acceptable. Pain during the injection is the inevitable component of the procedure, and should not be considered as complication.

Transient dysphonia is not a major complication either. We had relatively high number of clinically significant subcutaneous hematomas (6/40, 15%), higher than in other studies. It can be attributed to the utilization of an end-hole needles in our patients; the usage of side-hole needles probably reduces hematoma and enables equal distribution of ethanol within the nodule. All patients should keep the injection site compressed for 1-2 hours after the procedure, and avoid physical activity for at least 24 hrs to prevent bleeding. Early physical activity can increase the number of hematomas. Initial good results increased the interest of endocrinologists for the procedure, and the number of patients referred for the procedure has been lately increasing.

One might speculate whether PEI should be used only in patients with toxic adenomas, because patients with autonomous adenomas seldom have clinical symptoms and autonomous adenomas can undergo spontaneous degeneration, involution and self-healing. According to Livraghi, PEI is indicated in developing autonomous adenomas, because it can prevent the development of overt hyperthyreosis in the future.<sup>19</sup> All studies previously discussed and our study have shown very favorable outcome of PEI in patients with autonomous adenomas. Since the procedure has no permanent or significant complications, we believe that treating patients with autonomous adenomas, even when they are euthyroid, is justifiable.

In addition to laboratory tests and scintigraphy, ultrasound itself proved useful in evaluating successfulness of the treatment. B-mode echogenicity increases in successfully sclerosed nodules due to the ethanol induced fibrosis after the coagulation necrosis.<sup>9</sup> We observed this phenomenon clearly in all cases. Ultrasound is indispensable as a guidance modality even in palpable solitary nodules, to insure the equal distribution of ethanol, which is clearly visible in real-time

during the injection. Color and power Doppler have also proved to be very useful in assessing the reduction of vascularization in sclerosed parts of the nodule. If we observed the area of residual intranodular hypervascularisation, we were able to inject ethanol in that particular area in subsequent sessions or cycles.

We observed favourable outcome only in 1/2 of patients (2/4) with toxic nodular goiter (TNG). Bearing in mind that we refused to start the procedure in several patients where it was hard to determine accurately scintigraphically "hot" nodules with ultrasound, we consider TNG to be inappropriate for the PEI treatment. These patients can be treated with radioiodine therapy. On the other hand, young female patients with solitary hyperfunctioning nodules seem to be ideal candidates for PEI procedure, especially those with autonomous adenomas. This is a group of patients where exposure to radioactive isotope therapy should be avoided because of long-lasting hypothyreosis that follows this kind of the therapy.

Hypothyreosis after PEI is extremely rare. In a study of 101 patients, only one case was noted,<sup>19</sup> as well as in a study of 111 patients.<sup>20</sup> Both patients had elevated thyroid antibodies prior to the treatment, which was most probably due to the progression of already existing autoimmune thyroiditis.

Unlike PEI, radioiodine therapy causes hypothyreosis in 5-30% of patients,<sup>3-5</sup> and it is also known to increase the risk of gastric carcinoma occurrence.<sup>6</sup> After the surgical resection of the thyroid gland, hypothyreosis can be observed in 11% of cases; other serious complications may occur, such as permanent damage of the recurrent laryngeal nerve and of the parathyroid glands.<sup>2</sup> Both radioiodine therapy and surgery are considerably more expensive as than PEI.

Only one case of thyreotoxicosis induced by PEI was described in the literature,<sup>14</sup> indicating very low rate of this complication.

Shortly after the PEI, one can observe only mild elevation of thyroid hormones and thyreoglobulin levels.<sup>9-19</sup>

We conclude that the percutaneous ethanol injection under ultrasound, color and power Doppler guidance is a safe and effective method for the treatment of autonomous and toxic thyroid nodules, in spite of the fact that all patients experience pain during the procedure. The best results are observed in the patients with small and solitary nodules. The recurrence (hyperthyreosis) does not occur in patients in whom complete cure or partial recovery are achieved. PEI is less efficient in the treatment of patients with toxic nodular goiters. The first choice of treatment of autonomous thyroid nodules in the most countries is still radioiodine therapy. However, we believe that PEI should become the treatment of choice for toxic and autonomous solitary nodules, specially in the younger age-groups of patients. The procedure enables permanent inactivation of autonomous nodules in up to 90% of patients, with minimal and transitory complications. Significant and/or permanent complications were not observed. Radioiodine therapy and surgery are the methods associated with higher proportion of serious and/or permanent complications. We believe that it should be reserved as the first-choice treatment modality for the patients with toxic nodular goiter. For the patients with solitary autonomous nodules, radioiodine therapy should be given only to the patients in whom PEI is not successful, to uncooperative patients, and patients with anxious reactions, intolerance of pain during injection of ethanol.

## References

1. Reinwein D, Roehrer H-D, Emrich D. Therapie der hyperthyreose. *Dtsch Med Wchsr* 1993; **118**: 1036-43.
2. O'Brien T, Gharib H, Suman VJ, Van Heerden JA.

- Treatment of toxic solitary nodules: surgery versus radioactive iodine. *Surgery* 1992; **112**: 1166-70.
3. Goldstein R, Hart IR. Follow-up of solitary autonomous thyroid nodules treated with I-131. *N Engl J Med* 1983; **309**: 1473-6.
  4. Huysmans DA, Corstens FH, Kloppenborg PW. Long-term follow-up in toxic solitary autonomous thyroid nodules treated with radioactive iodine. *J Nucl Med* 1991; **32**: 27-30.
  5. Leisner B. Radiojodtherapie hyperthyreoter zustaende. *Dtsch Med Wschr* 1991; **116**: 423-5.
  6. Hall P, Berg G, Bjelkengren G, Boice JD, Ericsson UB, Hallquist A, et al. Cancer mortality after iodine-131 therapy for hyperthyroidism. *Int J Cancer* 1992; **50**: 886-90.
  7. Livraghi T, Salmi A, Bolondi L, Marin G, Arienti V, Monti E, et al. Small hepatocellular carcinoma: percutaneous alcohol injection - results in 23 patients. *Radiology* 1988; **168**: 313-7.
  8. Solbiati L, Giangrande A, DePra L, Bellotti E, Cantu P, Ravetto C. Percutaneous ethanol injection of parathyroid tumors under US guidance: treatment for secondary hyperparathyroidism. *Radiology* 1985; **155**: 607-10.
  9. Livraghi T, Paracchi A, Ferrari C, Bergonzi M, Garavaglia G, Raineri P, et al. Treatment of autonomous thyroid nodules with percutaneous ethanol injection: preliminary results. *Radiology* 1990; **175**: 827-9.
  10. Paracchi A, Ferrari C, Livraghi T, Reschini E, Macchi RM, Bergonzi M, et al. Percutaneous intranodular ethanol injection: a new method for autonomous thyroid adenoma. *J Endocrinol Invest* 1992; **15**: 353-62.
  11. Monzani F, Goletti O, Caraccio N, DelGuerra P, Ferdeghini M, Pucci E, et al. Percutaneous ethanol injection treatment of autonomous thyroid adenoma: hormonal and clinical evaluation. *Clin Endocrinol* 1992; **36**: 491-7.
  12. Goletti O, Monzani F, Caraccio N, DelGuerra P, Lippolis PV, Pucciarelli M, et al. Percutaneous ethanol injection treatment of autonomously functioning single thyroid nodules: optimization of treatment and short outcome. *World J Surg* 1992; **16**: 784-90.
  13. Martino E, Murtas ML, Loviselli A, Piga M, Petrini L, Miccoli P, et al. Percutaneous intranodular ethanol injection for treatment of toxic autonomously functioning thyroid nodules. *Surgery* 1992; **112**: 1161-5.
  14. Papini E, Panunzi C, Pacella CM, Bizzarri G, Fabbri R, Petrucci L, et al. Percutaneous ultrasound guided ethanol injection: a new treatment of toxic autonomously functioning thyroid nodules? *J Clin Endocrinol Metab* 1993; 411-6.
  15. Di Lelio A, Rivolta M, Casati M, Capra M. Treatment of autonomous thyroid nodules: value of percutaneous ethanol injection. *Am J Roentgenol* 1995; **164**: 207-13.
  16. Mazzeo S, Toni MG, De Gaudio C, Caramella D, Pinto F, Lencioni R, et al. Percutaneous injection of ethanol to treat autonomous thyroid nodules. *Am J Roentgenol* 1993; **161**: 871-6.
  17. Ozdemir H, Ilgit ET, Yucel C, Atilla S, Isik S, Cakir N, Gokcora N. Treatment of autonomous thyroid nodules: safety and efficacy of sonographically guided percutaneous injection of ethanol. *Am J Roentgenol* 1994; **163**: 929-32.
  18. Braun B, Blank W. Farbdopplersonographisch gesteuerte perkutane alkoholinsitllation zur therapie der funktionellen Schilddruesenautonomie. *Dtsch Med Wschr* 1994; **119**: 1607-12.
  19. Livraghi T, Paracchi A, Ferrari C, Reschini E, Macchi RM, Bonifacino A. Treatment of autonomous thyroid nodules with percutaneous ethanol injection: 4-year experience. *Radiology* 1994; **190**: 529-33.
  20. Monzani F, Caraccio N, Goletti O, Lippolis PV, Casolaro A, DelGuerra P, et al. Five-year follow-up of percutaneous ethanol injection for the treatment of hyperfunctioning thyroid nodules - a study of 117 patients. *Clin Endocrinol* 1997; **46**: 9-15.
  21. Lippi F, Ferrari C, Manetti L, Rago T, Santini F, Monzani F, et al. Treatment of solitary autonomous thyroid nodules by percutaneous ethanol injection - results of an Italian multicentric study. *J Clin Endocrin Metabol* 1996; **81**: 3261-4.





## Sonographic diagnosis of soft-tissue foreign bodies in children

Goran Roić<sup>1</sup>, Suzana Ercegović<sup>1</sup>, Tomislav Vlahović<sup>2</sup>, Slavko Čop<sup>1</sup>,  
Igor Bumčić<sup>2</sup>, Stjepan Višnjić<sup>2</sup>

<sup>1</sup>Department of Pediatric Radiology, <sup>2</sup>Department of Pediatric Surgery, Children's Hospital  
Zagreb, Croatia

---

**Background.** The aim of our study was to establish the successfulness of the ultrasound (US) method in diagnosing a soft-tissue foreign body.

**Patients and methods.** We analysed US findings of 14 children with a foreign body in soft-tissue structures. In 6 patients with negative X-ray findings of a foreign body, the identification and extraction of the foreign body during the surgical excision did not succeed. In 5 patients with a small superficial punctured wound, soreness and swelling of soft-tissue structures appeared after a few weeks to a few months and after a negative X-ray finding the US examination was done to diagnose a possible soft-tissue foreign body. In 2 children with foreign body granuloma, which developed after the foreign body had been in soft tissue for a few months, a soft-tissue solid tumour was suspected. In just 1 patient the foreign body was visible on X-ray too (glass), but it was impossible to define its position and depth.

**Results.** According to the US diagnosis and the precise localisation and marking of a foreign body immediately before a surgical excision, the operation was successful in all examined patients. Only in patients with multiple foreign bodies it was necessary to repeat the surgical excision to remove the remaining pieces of the foreign body.

**Conclusions.** The US has indubitably shown the presence of the foreign body and a surrounding granulomatous inflammatory reaction.

*Key words:* foreign bodies-ultrasonography; child

---

### Introduction

The detection of a foreign body in superficial soft-tissue at the children age, which are not visible on X-ray, can cause a diagnostic problem. Namely, a foreign body in soft-tissue

provokes and supports the surrounding inflammatory reaction and soreness, thus the localisation of a foreign body which is not visible on X-ray can be very difficult during the primary wound closure or subsequent surgery. High resolution ultrasound (US) enables reliable detection, preoperative localisation and marking even of very small pieces of foreign bodies, which significantly facilitates the detection of foreign bodies during the surgical excision.<sup>1,2</sup> As distinguished from X-ray,

Received 2 February 1999  
Accepted 6 July 1999

Correspondence to: Dr Goran Roić, Department of Pediatric Radiology, Children's Hospital Zagreb, Klaićeva 16, 10000 Zagreb, Croatia.

the US diagnosis of a foreign body does not depend on the type and size of it.

The aim of our study was to establish the successfulness of the US method in diagnosing a soft-tissue foreign body.

### Patients and methods

In our study, we reviewed US findings of 14 children with a foreign body in soft-tissue structures.

The equipment used was ACUSON 128/Xp10 and ALOKA 1700, using linear array transducers of 5-7,5 MHz. In all the patients we also used colour and power Doppler in order to estimate local inflammatory hypervascularity.

Eleven children with anamnestic and clinical suspicion of a foreign body were sent to the US examination. In 6 of these patients the identification and removal of a foreign body during the surgical excision was unsuccessful twice or three times.

In other 5 patients the foreign body entered the soft-tissue through a small entrance wound on the skin surface, and due to uncertain anamnestic data about foreign body, a surgical excision was not done. After a few weeks or months due to swelling and soreness, these patients were also sent, after a negative X-ray, to the US examination in order to detect a possible foreign body.

Two children were sent to the US examination in case a solid tumour process on the calf was suspected.

In all children discussed in our study, an X-ray was done before the US examination, while the foreign body was visible in only 1 patient (glass), but it was impossible to define its depth and precise position.

### Results

During the first US examination the foreign

body was localised in all children, and the position of it was marked down on the skin surface in all patients just before the surgical excision. The removal of a foreign body was successful in all patients.

In all patients we performed the US control 1 week and 2 weeks after the surgical excision in order to control the success of the operation and soothing of inflammatory reaction. In only one patient with US finding of multiple pieces of glass in the upper eyelid there were two pieces of glass left after the excision, so it was necessary to repeat the intervention.

In 8 of 14 patients the foreign body was of organic origin (wood), in 4 patients of pieces of metal, in 2 patients of pieces of glass. Eleven patients had only one piece of a foreign body, 2 patients each had two separated foreign bodies and 1 patient had multiple pieces of glass.

In 7 patients the foreign body was located on the foot, in 1 patient on the knee, in 2 patients on the calf, in 3 patients on the hand and in 1 patient in the upper eyelid.

The size of foreign bodies in our study ranged from 3 to 22 mm. In 12 patients a local inflammatory reaction around the foreign body was observed; in only 1 patient with a piece of glass subcutaneously there was no signs of local inflammation.

In 2 patients - who were sent to the US examination due to the clinical suspicion of the solid tumour in the calf - the ultrasound examination showed the foreign body (thorn) with surrounding granuloma (*"foreign body granuloma"*), which was surgically confirmed.

### Discussion

Foreign bodies in the soft tissues of children are usually pieces of wood, glass or metal. Diagnostically, the most frequent problem are pieces of wood because they are visible on X-ray only in 15% of the patients.<sup>3-5</sup> Glass and

metal, although often visible on X-ray, can also be a diagnostic problem because of their localisation, size and structure.<sup>3</sup> Due to its physical characteristic, the US is a very useful method in detection and preoperative localisation of foreign bodies regardless of their types and dimensions. Linear array transducers of high frequency and resolution enable the localisation of even the smallest pieces of a foreign body. A foreign body in soft-tissue almost always causes the inflammatory reaction of surrounding soft tissue with clinically present swelling and soreness of that region.<sup>1</sup> The US enables the precise and reliable localisation and marking of the foreign body before the surgical excision.<sup>6</sup> It frequently happens that, in spite of anamnestic information about a possible foreign body, it cannot be located and removed even after the repeated surgical intervention. The US gives precise information about the localisation of a foreign body in all three levels which simplifies the surgical excision very much. On the US foreign body it is most commonly shown as a hyperechoic linear band with or without associated shadowing or reverberating "comet-tail" artifacts<sup>1</sup> (Figures 1,2). As a rule there is almost always inflammatory reaction of surrounding soft-tissue structures which is shown as hypoechoic zone around the foreign body. The analysis by colour and power Doppler shows focal inflammatory hypervascularity around the foreign body.

The granuloma of the foreign body results from the inflammatory reaction of tissue to the foreign body. Thus, it is most frequently shown on the US as a hypoechoic solid mass of complex structure with the marked demonstration of hyperechoic focus of foreign body in the middle of formation (Figure 3). The analysis by colour and power Doppler shows the increased flow around the foreign body in inflamed soft-tissue (Figure 4).

In conclusion, the ultrasound is a method of choice in detection and preoperative localisation of a foreign body in superficial soft-tis-

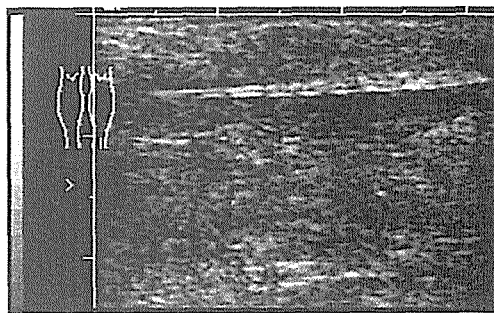


**Figure 1a.** Foreign body. Longitudinal scan of the soft-tissue (foot) shows a hyperechoic band (piece of wood).

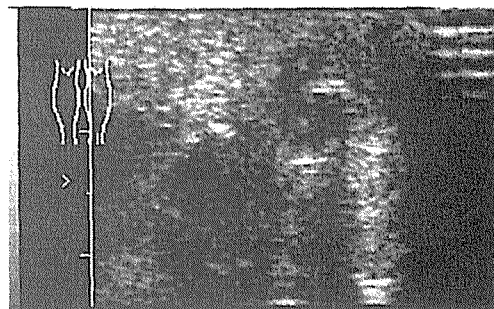


**Figure 1b.** Foreign body. Transverse scan shows hyperechoic focus.

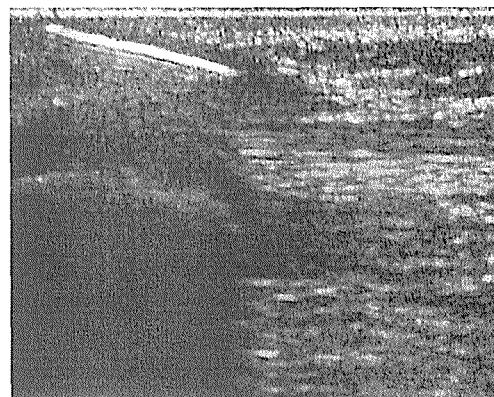


**Figure 2.** Foreign body - reverberation artefacts. Longitudinal scan shows a hyperechoic band (glass) with reverberation artefacts.

sue in case the foreign body is not visible on X ray. The US helps to detect even small pieces of a foreign body. According to our experience, the high resolution US should be routinely used in case of clinical and anamnestic suspicion of the foreign body

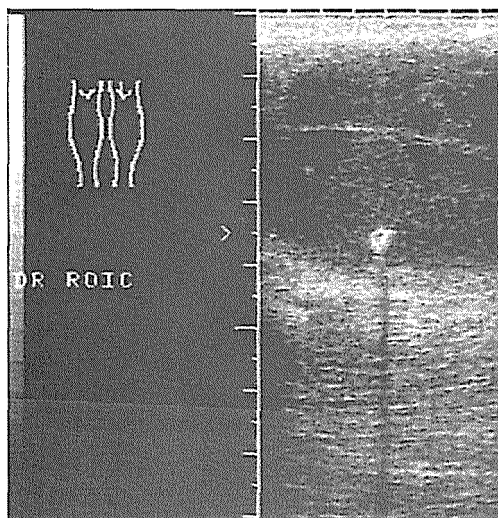


Figure 3. Foreign body - granuloma. Hyperechoic band (thorn) with surrounding hypoechoic mass and through transmission.

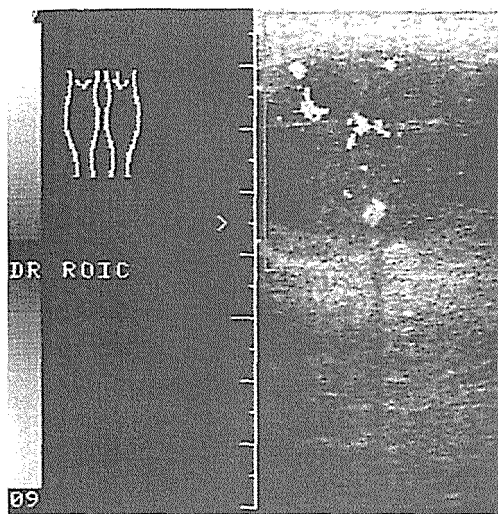


Figure 4. Foreign body - colour Doppler. Colour flow Doppler imaging shows increased blood flow in the hypoechoic mass; central hyperechoic focus with acoustic shadowing - foreign body (metal silver).

which is not visible on the X-ray film. Colour and power Doppler study is a useful adjunct to the grey-scale US in evaluating a focal inflammatory reaction around the foreign body and can aid in defining and clarifying grey-scale abnormalities.

*Radiol Oncol* 1999; 33(3): 189-92.

## References

1. Siegel MJ. Soft tissue. In: Siegel MJ, editor. *Pediatric sonography*. New York: Raven Press; 1995. p. 368.
2. Fornage BD, Schernberg FL. Sonographic diagnosis of foreign bodies of the distal extremities. *AJR* 1986; **147**: 567-9.
3. Bray H, Stringer DA, Poskitt K, Newman DE, MacKenzie WG. Maple tree knee: a unique foreign body - value of ultrasound and CT examination. *Pediatr Radiol* 1991; **21**: 457-8.
4. Ginsburg MJ, Ellis GL, Flom LL. Detection of soft-tissue foreign bodies by plain radiography, computed tomography, and ultrasonography. *Ann Emerg Med* 1990; **19**: 136-8.
5. Gooding GAW, Hardiman T, Summers M, Stress R, Graf P, Grunfeld C. Sonography of the hand and foot in foreign body detection. *J Ultrasound Med* 1988; **7**: 225-6.
6. Shiels WE II, Babcock DS, Wilson JL, Burch RA. Localization and guided removal of soft-tissue foreign bodies with sonography. *AJR* 1990; **155**: 1277-81.

## case report

# Ultrasonographic diagnosis of obstructive ileus in a patient with Meckel's diverticulum

Alenka Višnar-Perovič and Aleš Koren

*Institute of Radiology, University Medical Center, Ljubljana, Slovenia*

---

**Introduction.** Despite the use of modern imaging techniques, the reliable preoperative assessment of Meckel's diverticulum and related complications with this rare congenital anomaly of the gastrointestinal tract in adults is uncommon.

**Case presentation.** This report presents the case of a 25 year old man who presented with a sudden onset of pain in the right lower abdomen and vomiting. On clinical examination the affected area was tender to palpation which revealed an elastic cylindrical formation situated deeply in the abdomen. Blumberg's sign was positive while the laboratory findings were still within normal limits. An ultrasonography of the abdomen revealed an ileocaecal fluid collection containing thicker residue, which was suspicious for Meckel's diverticulum or a duplication cyst and ileus of the small bowel proximally from the formation described. Native radiogram of the abdomen in supine position has confirmed the presence of obstructive ileus at the level of the distal part of the small bowel. Surgery revealed an ileus and compression of the distal part of the small bowel due to the presence of an edematous Meckel's diverticulum.

**Conclusion.** In view of the frequent use of ultrasonography in the evaluation of acute abdomen, the diagnostic procedures could be rationalized and the time to surgery reduced if possible complications due to Meckel's diverticulum would be considered in the differential diagnosis.

*Key words:* Meckel's diverticulum - complications; interstitial obstruction - ultrasonography

---

## Introduction

Meckel's diverticulum (MD) is a congenital anomaly of the gastrointestinal tract. It occurs due to incomplete obliteration of the omphalomesenteric duct (vitelline duct)

which would normally close during the 5<sup>th</sup> to 7<sup>th</sup> embryonic week. MD represents 90% of all anomalies of the omphalomesenteric duct.<sup>1, 2</sup> During the embryonic development, the omphalomesenteric duct forms a communication between the yolk sac and the midgut.

With its incidence of 0.3-4% as evident from autopsy reports, the presence of MD is the most frequent anomaly of the gastrointestinal tract.<sup>3</sup> Progressive obliteration can be incomplete, leading to various anomalies, such as: a fibrous cord between the umbilicus

Received: 4 May 1999

Accepted: 20 July 1999

Correspondence to: Alenka Višnar-Perovič, MD, Institute of Radiology, University Medical Center, Ljubljana, Zaloška 7, SI-1000 Ljubljana, Slovenia. Phone: +386 61 325-570; Fax: +386 61 1331-044.

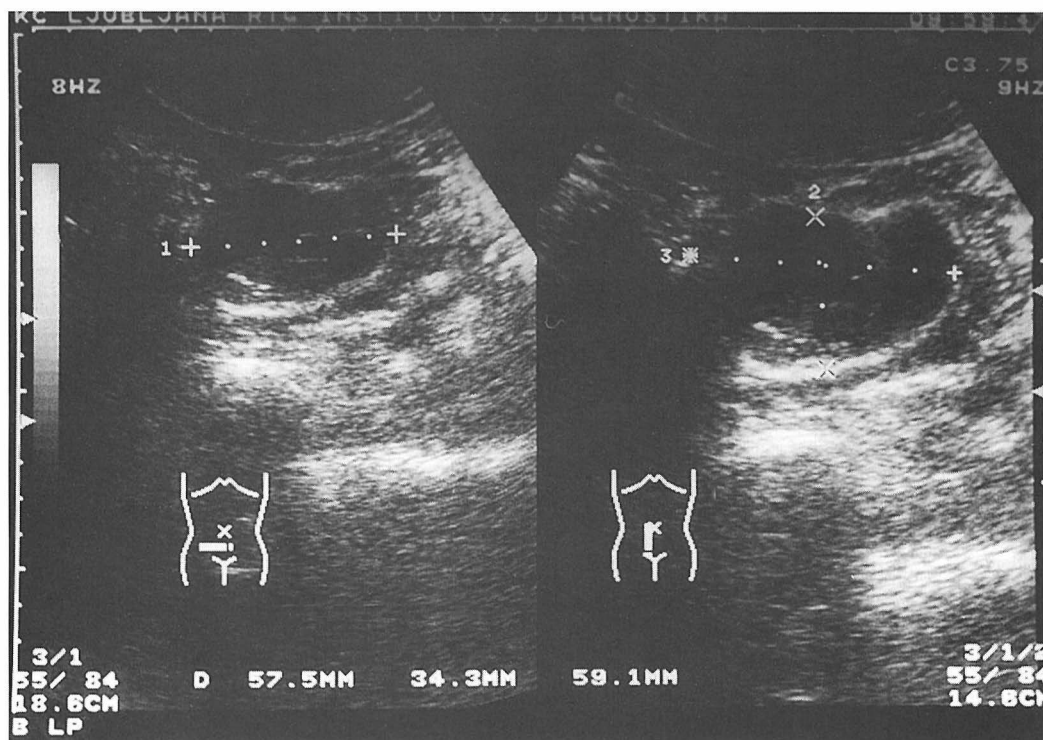


Figure 1. Meckel's diverticulum: The ileocaecal cystic formation with a layer of echogenic tissue at the bottom - edematous heterotopic gastric mucosa.

and the ileum which can contain cystic remnants of the lumen. MD occurs when the intestinal end of the omphalomesenteric duct fails to close. When no bliteration of omphalomesenteric duct occurs the anomaly is ileumbilical fistula.

Only 20-30% of all MD are symptomatic.<sup>4,5</sup> MD is a true diverticulum containing all the layers of the ileal wall, including heterotopic islets of the gastric mucosa, pancreas, and rarely also other parts of the gastrointestinal tract mucosa.<sup>6</sup> Complications include bleeding, inflammation, perforation, obstruction or strangulation due to polyps, volvulus, inversion or intussusception of the diverticulum.<sup>7</sup> While in children MD is suspected quite frequently, in adults where complications are less common, the possibility of MD is rarely considered before surgery.<sup>8</sup> The symptoms prevailing in adults include inflammation and

obstructive ileus of the small bowel due to volvulus and strangulation by the fibrous cord connecting MD to the anterior abdominal wall. Obstructive ileus can be easily detected by an ultrasonography of the abdomen (abdominal US) in the case of suspected acute abdomen.

### Case presentation

A 25 year old man presented with a sudden onset of pains in his right lower abdomen and vomiting. On clinical examination the affected area was tender to palpation. An elastic cylindrical formation was palpated deeply in the abdomen. Blumberg's sign was positive while the laboratory findings were still within normal limits.

Abdominal US revealed an ileocaecal fluid



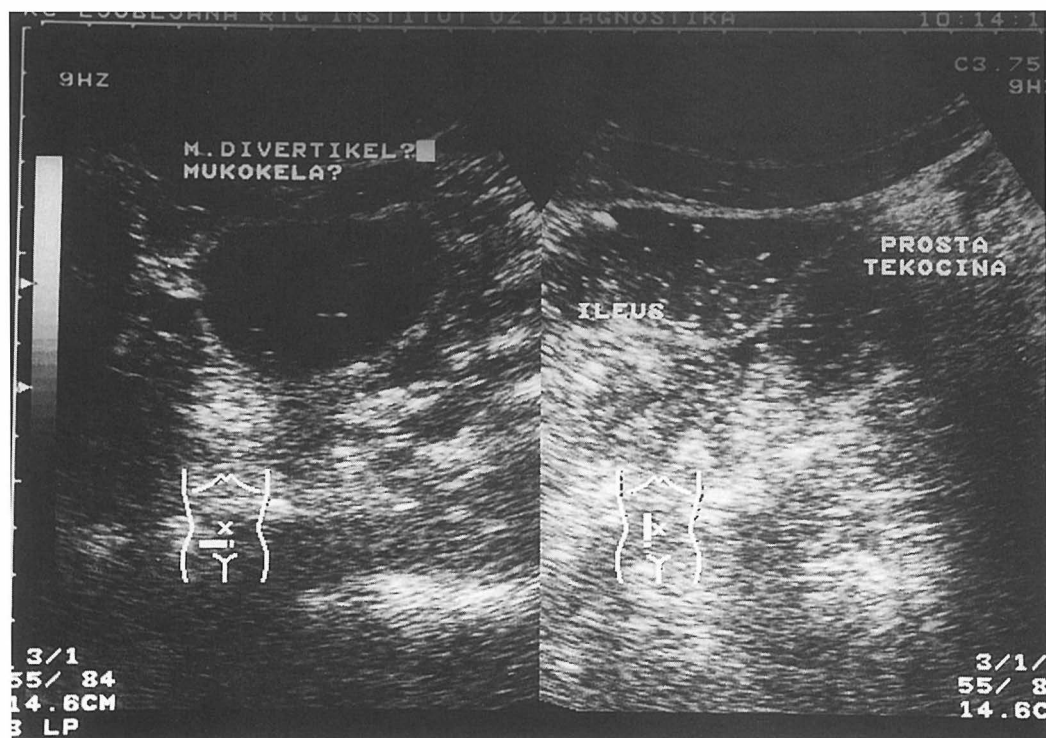


Figure 2. Meckel's diverticulum on the left side. Ileus of the small bowel proximally from MD on the right side.

collection, 6 x 3.5 x 6 cm of size, with a thicker and more echogenic residue in the bottom (Figure 1), which was suspicious for MD, or a duplicate cyst and ileus of the small bowel situated proximally from the described formation (Figure 2). Doppler sonography showed evidence of hyperemia in the area of the cystic wall. The findings of other abdominal organs were within normal limits. There was no evidence of acute appendicitis.

Native radiogram (X-ray) of the abdomen in the supine position confirmed the presence of obstructive ileus at the level of the distal part of the small bowel.

On surgery, intussusception of the distal part of the small bowel due to the presence of edematous MD and the associated obstructive ileus of the proximally situated small bowel were found. A resection of edematous MD and appendectomy were performed.

The postoperative course was uneventful.

Pathohistological analysis of the resected diverticulum showed an edematous wall with moderate a mononuclear infiltration which was most probably due to ischemia. In the top of the diverticulum, transition of the small bowel mucosa into the heterotopic gastric mucosa with individual chronic erosive changes was found.

## Discussion

Morphologically, MD is a blind diverticulum found most frequently in the anti-mesenteric side of the ileum, within a 90 cm distance from the ileocaecal valvula in more than 90% of cases, while the minority of cases can be situated even within 180 cm distance from the ileocaecal valvula.<sup>8</sup> The average size of MD is 3 cm in width (range 1.5 - 12.5 cm) and 4.5 cm in length (range 2 - 10 cm).<sup>2, 8</sup> They

occur more frequently in males than in females, the ratio being 1.7 vs. 1 respectively, and the frequency of complications in males is higher as well, which further increases the ratio to 2.8 vs. 1.8. Generally clinically silent diverticula have a broader basis and rarely contain heterotopic tissue of the gastric or pancreatic mucosa.<sup>8</sup> MD is a true diverticulum since its wall contains all the layers of the ileal wall. 6 - 40% of MD contain ectopic tissue: gastric mucosa in 62% and pancreatic tissue in 6%, while mucosa of other parts of the gastrointestinal tract, *i.e.* the colon, duodenum, jejunum and other tissues, is found less frequently.<sup>6, 8</sup> In symptomatic cases, the percentage of heterotrophic tissue can increase to 79.4%. MD is supplied by remnant of the primitive vitelline artery arising from an ileal branch of the superior mesenteric artery or, less commonly, from the ileocolic artery.<sup>9</sup>

MD related complications occur more frequently before the age of 2 years, and decrease with age. The main symptom in children is gastrointestinal bleeding, while adults will mostly present with symptoms resulting from inflammation or obstruction. In adult women symptoms occur much later, the mean age being 70 years, and less frequently than in men, whose mean age is 40 years.<sup>8</sup>

MD becomes clinically detectable only in patients with complications; with incidence according to the reports from literature in 20-30%.<sup>4, 5</sup> The possibility of MD should be considered in the differential diagnosis of pain and tenderness to palpation in the right lower quadrant, vomiting, borderline leukocytosis and silent bleeding from the gastrointestinal tract. Clinically the symptoms may mimic appendicitis, ileal diverticulitis, mesenteric lymphadenitis and other rarer conditions.

The most frequent complication is obstructive ileus, which represents 34-53% of all complications.<sup>2, 8, 9</sup> Obstructive ileus can be caused by the fibrous cord that connects MD with the anterior abdominal wall and can

cause intestinal obstruction and volvulus with strangulation of the bowel. Obstruction is further caused by intussusception of an inflamed or inverted MD, an internal herniation and adhesions.

A frequent complication is gastrointestinal bleeding, which occurs in 12-25% as a result of the presence of ectopic tissue in MD.<sup>2, 8, 9</sup> This causes ulcerations in the surrounding intestinal mucosa of the ileum. A case of spontaneous intraperitoneal bleeding from a necrotic MD, without evidence of intraluminal bleeding has been reported as well.<sup>2, 10, 11</sup> Bleeding is most common in children where it is the most frequent sign of MD.

Acute diverticulitis occurs in 13-31%, either with or without perforation.<sup>2, 6, 8</sup> The signs as well as associated complications can resemble those seen in appendicitis, and may include perforation and peritonitis. Acute diverticulitis is generally resulting from a peptic effect of the gastric mucosa on the surrounding intestinal mucosa. Other causes are comparable to those seen in acute appendicitis, or those associated with enteroliths closing the diverticular lumen.

Incarcerations with incarceration are less frequent; according to the data from literature they are found in 2-5%, most often inguinally or femorally, on the right, and generally do not cause obstruction.<sup>2, 6, 8</sup>

Malignant tumors represent only 3% of all complications.<sup>2, 6</sup> The most frequent malignant types include sarcomas, carcinoids and adenocarcinoma, originating from the gastric mucosa. Among the benign ones, leiomyomas, angiomas, neurinomas and lymphomas are seen most frequently.

Preoperative diagnosis of MD is rare, particularly owing to its small size, content of feces and small orifice. In the largest known study of 600 cases by Yamaguchi *et al.*, preoperative diagnosis was established in as little as 6% of cases.

In advanced cases, a plain radiogram of the abdomen in supine position reveals prevail-

ingly non-specific signs of obstruction in the distal part of the small bowel, where complication is present. Very rarely we can see laminar type of enteroliths (11%) and more common ring shaped Meckel's enteroliths (89%) with calcinated margins and radiolucent center.<sup>12</sup> Meckel's enteroliths are mostly (57%) situated in the right lower quadrant of the abdomen.<sup>12</sup> Rare cases of diverticulitis show gas-fluid levels.<sup>2</sup>

Among the X-ray diagnostic procedures employing a contrast medium for verification of MD in adults, enteroclysis is found to be the most sensitive since it can most clearly image the meeting point of MD with the small bowel wall.<sup>13</sup> Radiological signs indicative of MD presence are as follows: a collection of contrast in the diverticulum in a typical site, a filling defect due to the presence of concrement, fold pattern in the small bowel wall at the MD orifice, the mucosal "triangular plateau" which marks the site where the diverticulum orifice meets with the intestinal wall when the latter is dilated, and a "triradiate" fold pattern when the loops are collapsed.<sup>2,8</sup>

Frequent presence of the ectopic gastric tissue in MD (6-40%) enables its detection by means of <sup>99m</sup>Tc-pertechnetate based scintiscan, and in the case of bleeding, the use of <sup>99m</sup>Tc-sulfur colloid labeled erythrocytes, will also image possible hemorrhage. In adults, the sensitivity of 62.5% and specificity of only 9% has been established due to numerous false-positive findings attributable to inflammatory processes in other organs, arteriovenous malformations, and false-negative results which were mainly due to circulatory disorders and massive bleedings.<sup>2,6,14</sup>

In the diagnosis of MD, CT scan is hardly of any use, as it is generally impossible to distinguish between the intestinal loops and MD.

Angiography is often indicated in active bleeding from the gastrointestinal tract. The selective angiography of the superior mesen-

teric artery using digital subtraction technique is required. The arterial, capillary and venous phases as well as the mucosal blush are evaluated. The image includes the bowel and the pelvis. In order to prove the presence of extravasation, the bleeding flow should be at least 0.5 ml/min. Sometimes, a superselective imaging of the vitelline artery is made possible by means of magnification technique.<sup>2</sup>

In the diagnosis of abdominal symptoms, US is frequently the first method used, its sensitivity to detect any pathological changes in the ileocaecal area largely depending on the expertise of the investigator. There is little information available on the US features of MD, since the incidence of this pathological condition is low, and the specificity and sensitivity of US in the diagnosis of MD related pathological changes is probably small. No exact data could be found in the existing literature. Nevertheless, US proved to be first diagnostic modality for the detection of symptomatic MD related complications because it is simple and fast. In the case of MD lumen obliteration, an US image of MD appears as a hypoechogenic, cystic, possibly tubular and solid formation. Its axis is perpendicular to the intestinal wall. In the presence of inflammation the wall is thickened, and a Doppler sonography reveals hyperemia with free exudate in the surroundings. US is hardly able to distinguish between an MD and appendicitis, while it can reliably image early signs of ileus: more than 3-4 cm wide liquid-filled loops of the small bowel with either intense or already failing peristalsis. The threatening discontinuation of circulation in the wall in the site of intussusception is assessed by Doppler sonography.

We believe that the role of US in the diagnosis of MD is prevailing in the exclusion of other acute abdominal conditions and MD related complications, reduced need of additional radiological examinations, and a shorter way to diagnosis. The sensitivity of detec-

tion increases the targeted screening for MD and its related complications in patients with corresponding symptoms. Often, any further radiological investigations fail to contribute significantly to the final diagnosis.

Due to their similar features, it is necessary to exclude more frequent duplication cyst, which is situated parallel with the ileum axis, as well as diverticula of the small bowel, which are more numerous in the jejunal area (66%).<sup>14</sup> Unlike MD, both are situated in the side of the mesentrium.

The treatment for symptomatic MD is surgery. MD is removed together with a part of the ileum. Opinions on the procedure based on incidentally detected asymptomatic MD are controversial. When the surgical procedure is simple, it is indicated in these cases as well. However, in the diverticula with a broad base, which are unlikely to cause any complications, surgery is not simple and is therefore frequently contraindicated; such cases may rarely become symptomatic later on.<sup>8</sup>

### Conclusion

Diagnosis of symptomatic MD is difficult. Frequent use of US in suspected cases of acute abdomen, as well as consideration of the possibility of MD related complications in the differential diagnosis may contribute to fast and accurate evaluation of the cause of condition. The sensitivity and specificity of US are probably low, the role of this investigation being prevailing in the exclusion of other accompanying diseases and complications, in the reduced need for additional exposure of the patient to X-rays, and finally, in shortened way to diagnosis.

Scarce data in the available literature call for further investigations which would determine more accurately the role of US in the diagnosis of MD and this condition related complications.

### References

1. Gray SW, Skandalakis JE. *Embriology for surgeons*. Philadelphia: Saunders 1972: 156-67.
2. Rossi P, Courtsyiannis N, Bezzi M et. al. Meckel's diverticulum: Imaging diagnosis. *AJR* 1996; **166**: 567-73.
3. DiSantis DJ, Siegel MJ, Katz ME. Simplified approach to umbilical remanent abnormalities. *Radio Graphica* 1991; **11**: 59-66.
4. Mackey WC, Dineen P. A fifty - year experience with Meckel's diverticulum. *Surg Gynecol Obstet* 1978; **156**: 56-64.
5. Rubesin SE, Herlinger H, De Gaete L. Interlude. Test your skills. Inverted Meckel diverticulum with intussusception. *Radiology* 1990; **176**: 636-44.
6. Yamaguchi M, Takeuchi S, Awazu S. Meckel's diverticulum: investigation of 600 patients in Japanese literature. *Am J Surg* 1978; **136**: 247-9.
7. Donnelly LF, Johnson III. JF. Case report: Inverted Meckel's diverticulum With Associated Microcolon. *Clinical Radiology* 1998; **53**: 226-7.
8. DiGiacomo CJ, Cottone JF. Surgical treatment of Meckel's diverticulum. *South Med J* 1993; **86**: 671-75.
9. Rutherford RB, Akers DR. Meckel's diverticulum: a review of 148 pediatric patients, with special reference to the pattern of bleeding and to mesodiverticular vascular bands. *Surgery* 1966; **59**: 618-26.
10. Torgerson CL, Young DW, Yoginder N. et al. Intestinal duplication: Imaging with Tc-99m sodium pertechnetate. *Clin Nucl Med*. 1996; **21**: 968.
11. Sitaram V, Fox JN. Haemoperitoneum caused by Meckel's diverticulum. *Postgrad Med J* 1991; **67**: 94-5.
12. Pantograg-Brown L, Levine MS, Buetov PC, Buck JL, Elsayed AM: Meckel's enteroliths: Clinical, radiologic and pathologic findings. *AJR* 1996; **167**: 1447-50.
13. Maglinte DDT, Elmore MF, Isenberg M. Meckel diverticulum: Radiologic demonstration by enteroclysis. *AJR* 1980; **134**: 925-32.
14. Maglinte DDT, Cheruich SM, DeWeese R et al. Acquired jejunoileal diverticular disease: Subject review. *Radiology* 1986; **158**: 577-81.

## When do heterogeneous splenic enhancement patterns occur in contrast-enhanced CT studies of the abdomen?

Reinhard Groell<sup>1</sup>, Rainer Rienmüller<sup>1</sup>, Martin M. Uggowitzner<sup>1</sup>,  
Christian Kugler<sup>1</sup>, Rudolf E. Stauber<sup>2</sup>, Peter Fickert<sup>2</sup>

<sup>1</sup> Department of Radiology, University Hospital Graz, Austria

<sup>2</sup> Department of Internal Medicine, University Hospital Graz, Austria

---

**Background.** This study determines when heterogeneous splenic enhancement patterns occur in contrast-enhanced CT in patients with and without liver cirrhosis.

**Patients and methods.** Electron-beam CT of the abdomen was performed in 195 patients following intravenous injection of contrast agent according to one of three injection protocols (protocol 1: n=132, 120 ml, 2 ml/sec, scan delay: 50 sec; protocol 2: n=30, 90 ml, 3 ml/sec, scan delay: 10 sec; protocol 3: n=33, 50 ml, 5 ml/sec, scan delay: 10 sec). Thirty-four of these patients had liver cirrhosis.

**Results.** A heterogeneous splenic enhancement pattern was observed in 77% (protocol 2) and 65% (protocol 3) of the patients without liver disease and in 23% (protocol 2) and 20% (protocol 3) of the patients with liver cirrhosis. A heterogeneous enhancement pattern was visible between 14 and 58 sec after the administration of contrast agent. In all patient groups and protocols it never occurred later than 58 sec following the contrast agent application. Three patients had a splenic lesion (hemangioma, lymphoma, metastasis), these lesions were also visible after 58 sec following the injection.

**Conclusions.** These results indicate that heterogeneous splenic enhancement patterns do not occur later than 58 sec after the contrast agent injection, even when the contrast agent is still being injected at that time.

**Key words:** tomography, X-ray computed, electron-beam, enhancement; splenomegaly, liver cirrhosis

---

### Introduction

With the advent of fast imaging methods providing high temporal and spatial resolution (fast magnetic resonance imaging, helical- and electron-beam computed tomography) a

heterogeneous splenic enhancement pattern is frequently observed after the administration of iodinated or gadolinium-based contrast agents.<sup>1-3</sup> These heterogeneous enhancement patterns are regarded as reflecting the pathways of splenic microcirculation.<sup>3</sup> The interpretation of these heterogeneous patterns may be a matter of concern, as they may mimic focal or diffuse splenic lesions such as metastases, hemangiomas, lymphatic infiltration, or infarction.

The objectives of this study were to deter-

Received 13 January 1999

Accepted 25 March 1999

Correspondence to: Reinhard Groell, MD, Department of Radiology, University Hospital Graz, Austria, Auenbruggerplatz 9, A - 8036 Graz, Austria; Phone: +43 316 385 2411; Fax: + 43 316 385 3231; E-mail: reinhard.groell@kfunigraz.ac.at

mine how long heterogeneous splenic enhancement patterns normally persists, and beyond which time the radiologist should worry about focal or infiltrative splenic diseases.

Methods

The study group consisted of 195 patients who were referred for electron-beam CT (Evolution, Siemens, Erlangen, Germany) of the abdomen. The patients were examined according to one of 3 different contrast agent injection protocols using the same non-ionic contrast agent (iopromide 300mgI/ml, Ultravist, Schering, Berlin, Germany) which was applied by power injector (Angiomat 6000, Liebel-Flarsheim, Cincinnati, Ohio) (Table 1). The non-dynamic CT-protocol 1 rep-

quired in mid-inspiration using an incremental „single-slice mode” in the cranio-caudal direction (exposure time: 500 msec, inter-scan delay: 1.3 sec, slice thickness: 6 mm). The scans were taken after intravenous application of 120 ml of contrast agent at a flow rate of 2 ml/sec. The scan was taken with a delay of 50 sec after the contrast agent injection had been started. The exact time of image administration was documented automatically on each CT image.

Protocol 2

Dynamic electron-beam CT of the abdomen was performed in 30 patients of whom 13 patients (8 male, 5 female, mean age: 61±10 years) had biopsy proven liver cirrhosis. Seventeen patients (4 male, 13 female, mean age = 42±14 years) without liver cirrhosis were

Table 1. Protocols of contrast agent injection

	Amount of CA (ml)	Injection rate (ml/sec)	Bolus duration (sec)	Scan delay (sec)	Scan mode
Protocol 1	120	2	60	50	SSM
Protocol 2	90	3	30	10	MSM
Protocol 3	50	5	10	10	MSM

SSM=single-slice mode. MSM=multi-slice mode. CA=contrast agent

resented the routine protocol for patients referred to our department for CT studies of the abdomen. This protocols mimics that in use for spiral CT of the abdomen. The dynamic CT-protocols 2 and 3 were used in patients with suspected focal or diffuse liver lesions to evaluate hepatic perfusion.

Protocol 1

The study group consisted of 121 patients (66 male, 45 female, mean age: 56±15 years) without and 11 patients (7 male, 4 female, mean age 60±10 years) with clinical and biochemical signs of liver cirrhosis. In 4 patients the diagnosis of cirrhosis was also confirmed by biopsy. The electron-beam CT images were

examined because of suspected liver lesions (later proven by biopsy as: focal nodular hyperplasia n=12, hepatic adenoma n=1, hepatic hemangioma n=2). All 30 patients were studied using a „multi-slice mode” for „flow studies” with 6 levels covering a volume of 5.6 cm in the z-axis without table movement (exposure time 50 msec, slice thickness 8 mm, 6 levels). Ninty ml of non-ionic contrast agent was injected into an antecubital vein with a flow of 3ml/sec. Scans were taken 10, 12, 14, 16, 20, 24, 28, 38, 48, 58, 88, 118, 148 sec after the injection had been started. The scans were performed in inspiration, therefore the patients were asked to hold their breath for the first 18 sec and were instructed to breathe between the subsequent scans.

*Protocol 3:*

Thirty-three patients with suspected liver lesions were examined using identical electron-beam CT image acquisition parameters as described in protocol 2. However, contrary to protocol 2, a contrast agent flow of 5ml/sec and a volume of 50ml were used. Ten patients (8 male, 2 female, mean age:  $54 \pm 5$  years) had clinical and biochemical signs of liver cirrhosis, in 6 of these patients cirrhosis was also confirmed by biopsy. In 23 patients (13 male, 10 female, mean age:  $53 \pm 12$  years) neither clinical signs nor CT-evidence of liver cirrhosis were found. Six of these 23 patients revealed a liver lesion (focal nodular hyperplasia:  $n=2$ , hemangioma:  $n=1$ , metastasis:  $n=3$ ).

*Image analysis*

Each study was qualitatively analyzed on a digital image workstation (DRC104, Siemens, Erlangen, Germany) independently by consensus of two radiologists. In addition to the standard window settings (window center: 30 HU, window width: 300 HU) the readers changed the center and width of the windows as they felt necessary. Any visible irregular or

non-homogenous enhancement of the spleen visualized on any image level was defined as a heterogeneous enhancement pattern. Additionally, in the dynamic CT studies using protocol 2 and 3 the times were documented when a heterogeneous enhancement pattern became visible and when it disappeared.

A Wilcoxon rank sum test ( $p=0.05$ ) was used to compare the aortic enhancement and the time frames of splenic enhancement patterns of protocol 2 and 3 in cirrhotic and in non-cirrhotic patients.

**Results**

In 3 patients examined with protocol 1, splenic cysts were seen with a diameter of 1-3 cm which were later confirmed by sonography. In three of the patients examined with protocol 2, one patient had splenic hemangioma, one patient had biopsy proven splenic lymphoma and a third patient had splenic metastasis of a breast carcinoma. The hemangioma was confirmed by sonography and by prior conventional CT studies. The metastasis was confirmed by follow-up examinations.

**Table 2.** Times of the occurrence of heterogeneous splenic enhancement patterns on electron-beam CT of the abdomen

				Visualization of heterogeneous splenic enhancement patterns		
	n		n	Start [sec]	End [sec]	Duration [sec]
Protocol 2	30	non-cirrhotic	17	$22.5 \pm 2.5$ (20-28)	$33.1 \pm 6.7$ (24-58)	$10.6 \pm 7.6$ (4-34)
		Cirrhotic	13	$25.3 \pm 4.3$ (24-28)	$41.3 \pm 4.7$ (38-48)	$16.0 \pm 5.9$ (14-24)
Protocol 3	33	non-cirrhotic	23	$21.7 \pm 3.5$ (14-28)	$29.9 \pm 5.1$ (24-38)	$8.1 \pm 5.6$ (4-24)
		Cirrhotic	10	$19.0 \pm 1.0$ (18-20)	$33.0 \pm 5.0$ (28-38)	$14.0 \pm 4.0$ (10-18)
p-value*		cirrhotic vs. non-cirrhotic		0.65	0.04	0.08

The times are calculated in seconds from the start of injection. The numbers indicate the mean times and their standard deviation (mean $\pm$ SD), the time range (minimum-maximum) is listed in the parentheses below.

\*Wilcoxon rank test.



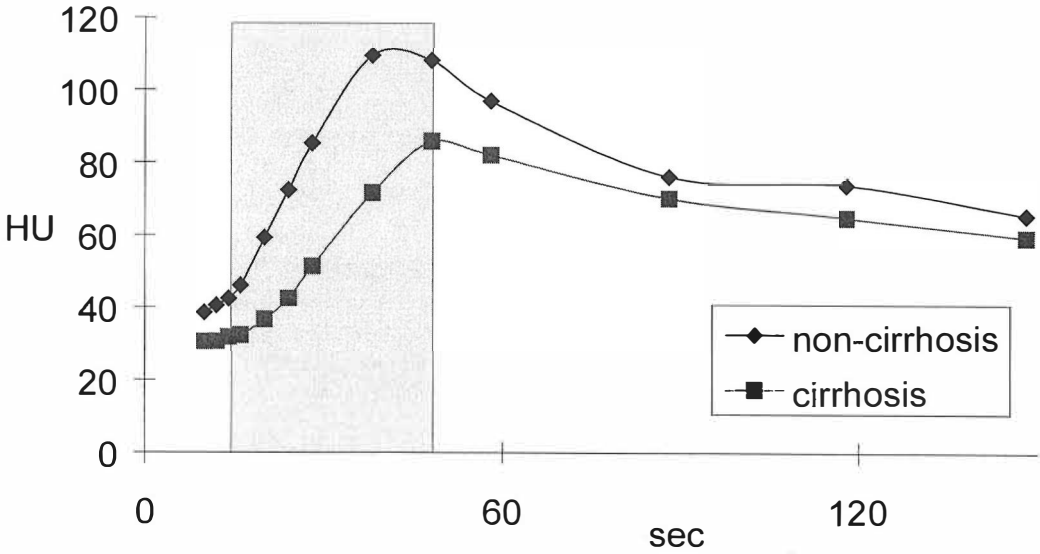


**Figure 1a.** Mean time-density-curves of the spleen for the patients studied according to protocol 2. In none of the patients did a heterogeneous enhancement pattern (marked area) occur later than 60 sec after the contrast agent injection had been started.

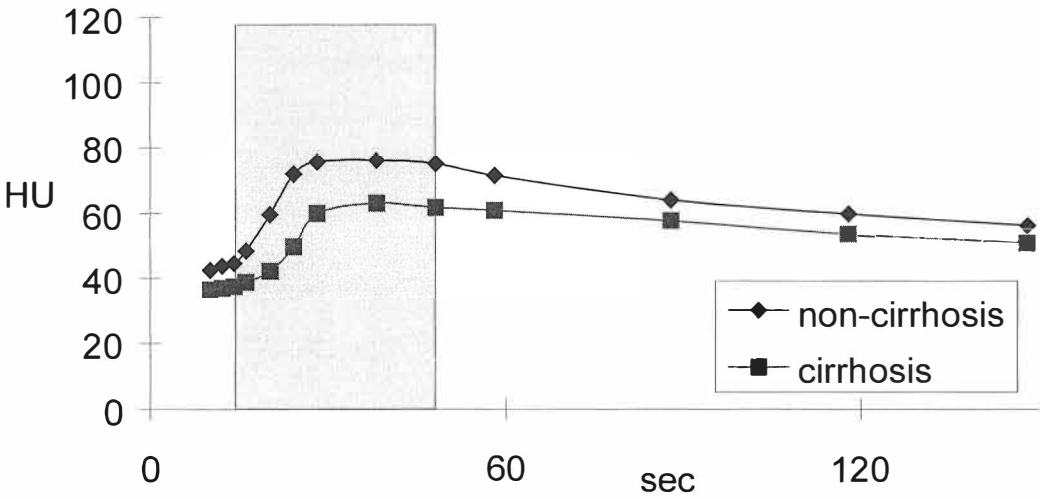


**Figure 1b.** Mean time-density-curves of the spleen for the patients studied according to protocol 3. In none of the patients did a heterogeneous enhancement pattern (marked area) occur later than 60 sec after the contrast agent injection had been started.

In all 132 patients examined according to protocol 1, the spleen appeared homogeneously enhanced on all CT-levels regardless of the presence or absence of liver cirrhosis.

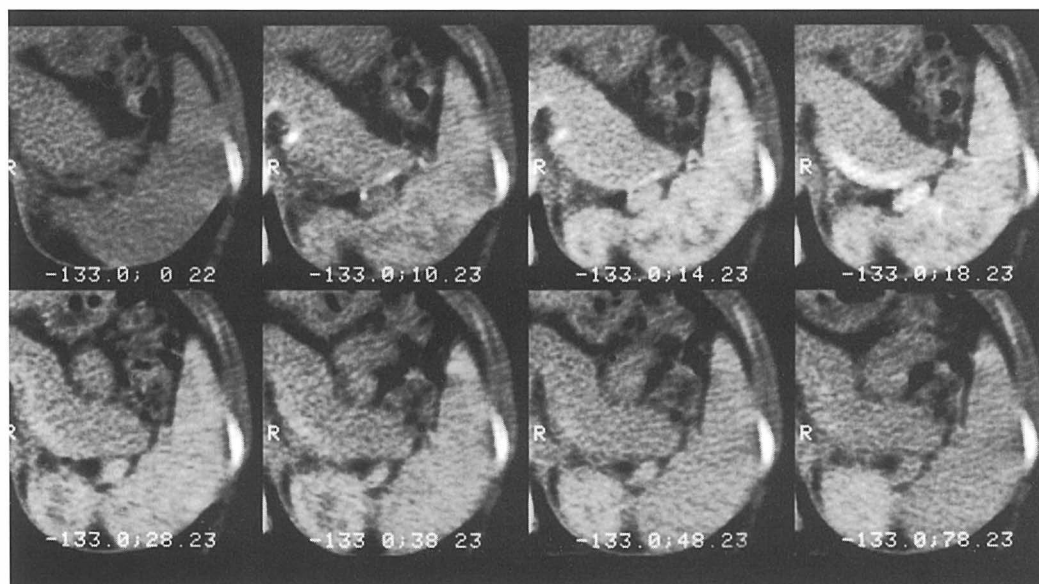


**Figure 2.** One level scanned over 90 sec after the injection of contrast agent. A heterogeneous enhancement pattern occurs in the early arterial phase.

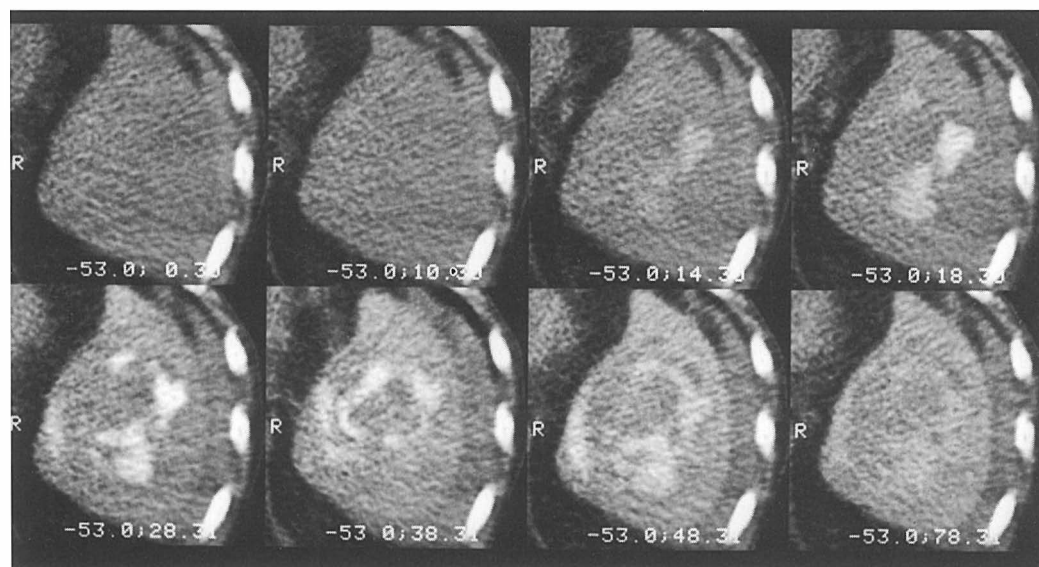


**Figure 3.** Splenic lymphoma also visible in the later bolus phase.

The time frames of heterogeneous enhancement patterns could be determined in the dynamic studies (protocols 2 and 3). Figure 1 shows the mean time-density-curves of the spleen of all patients studied according

to protocol 2 (Figure 1a) and 3 (Figure 1b). The time-density-curve of the spleen examined according to protocol 2 showed a later maximum and a higher value of peak enhancement when compared to protocol 3.

The times when heterogeneous enhancement patterns occurred are listed in Table 2. A heterogeneous enhancement patterns appeared between 14 and 28 sec and disappeared between 24 and 58 sec after the contrast application had been started (Figure 2). In all patients studied by protocol 1, 2 and 3 (n=195), the splenic parenchyma became homogeneous beyond 58 sec after the bolus injection had been started, except for the 3 above mentioned patients with splenic cysts and for the 3 patients with splenic hemangioma, metastasis and lymphoma (Figure 3), respectively.

Heterogeneous enhancement patterns were visible more frequently in non-cirrhotic than in cirrhotic patients ( $p < 0.01$ ). During the dynamic CT studies of the patients without liver cirrhosis (n=40) using protocol 2 and 3, a heterogeneous enhancement pattern was observed in 76.5% (13/17) and 65.2% (15/23), respectively. A heterogeneous splenic enhancement pattern was only observed in 23.1% (3/13) and 20% (2/10) of the patients with cirrhotic liver disease as examined by protocol 2 and 3, respectively.

### Discussion

Heterogeneous enhancement patterns of the spleen as observed on contrast-enhanced CT and in gadolinium-enhanced MRI examinations were assumed to reflect the mechanism of slow and fast blood flow in the pathways of splenic microcirculation.<sup>1-5</sup> However, heterogeneous enhancement patterns may also simulate pathoanatomical changes of the spleen.<sup>1-3,4</sup> It is therefore important to define the possible variations in normal splenic appearance.

Histologically the spleen comprises the white and red pulp. The white pulp consists of lymphatic tissue encasing the splenic arteries. It also forms the lymphoid follicles. The red pulp is a reticular meshwork where red

blood cells are conditioned before their destruction. The fast splenic pathway bypasses the reticular meshwork of the red pulp. It takes its route via direct capillary-venous connection inside the lymphoid follicles of the white pulp. This pathway accounts for 80-90% of total splenic blood flow. The slow pathway constitutes 10-20% of total splenic perfusion. After having passed the white pulp, the blood is filtrated into the splenic chords of the red pulp where abnormal blood cells are labeled for their destruction.

In a recent study using „functional CT“ imaging, Miles *et al*<sup>3</sup> showed that splenic regions with early enhancement revealed higher arterial perfusion values than those with delayed contrast enhancement. These early enhancing areas of the spleen are thought to reflect the regions in which the fast pathway is predominant and vice versa.<sup>3</sup>

With the advent of fast imaging techniques the spleen is often scanned within this early phase of enhancement showing a heterogeneous pattern.<sup>1-3</sup> To our knowledge no exact time frames have been reported when these patterns occur and whether they vary with different contrast agent injection protocols or different pathophysologies as may happen in patients with liver cirrhosis.

Advanced cirrhosis may increase portal venous pressure, consecutive chronic splenic venous hypertension and an elevated splenic sinus pressure. Miles *et al.* showed that splenic arterial blood flow is slower in patients with liver cirrhosis compared to those without cirrhosis.<sup>3</sup>

This study, using 3 different injection protocols with the same contrast agent, showed that the heterogeneous enhancement patterns were never seen later than 58 sec after the bolus injection had been started, even if the contrast agent was still being injected as in protocol 1, regardless of the presence or absence of liver cirrhosis. Using the two dynamic protocols with different amounts (50 vs. 90 ml) and flow rates (3 vs. 5 ml/sec) of

contrast agent, the time frames of heterogeneous enhancement patterns did not change significantly. The injection protocol 1 is similar to that used for spiral CT of the abdomen. Therefore, we suppose that the results of our study (heterogeneity should not be visible beyond 58 sec after the contrast injection had been started) may also be relevant for the interpretation of spiral CT studies of the abdomen.

In conclusion, the results of our study show that heterogeneous splenic enhancement patterns are visible more frequently in patients without than in patients with liver cirrhosis, probably due to decreased splenic blood flow in patients with liver cirrhosis. Regardless of the presence of liver cirrhosis, heterogeneous splenic enhancement patterns appear between 14 and 58sec after the contrast agent administration had been started. After 58 sec, the spleen is homogeneously enhanced, even when the contrast agent is still being injected at that time.

## References

1. Semelka RC, Shoenut JP, Lawrence PH, Greenberg HM, Madden TP, Kroeker MA. Spleen: dynamic enhancement patterns on gradient-echo MR images enhanced with gadopentetate dimeglumine. *Radiology* 1992; **185**: 479-82.
2. Mirowitz SA, Brown JJ, Lee JKT, Heiken JP. Dynamic gadolinium-enhanced MR imaging of the spleen: normal enhancement patterns and evaluation of splenic lesions. *Radiology* 1991; **179**: 681-6.
3. Miles KA, McPherson SJ, Hayball MP. Transient splenic inhomogeneity with contrast-enhanced CT: mechanisms and effect of liver disease. *Radiology* 1995; **194**: 91-5.
4. Taylor AJ, Dodds WJ, Scott JE, Steward ET. CT of acquired abnormalities of the spleen. *AJR* 1991; **157**: 1213-9.
5. Glazer GM, Axel L, Goldberg HI, Moss AA. Dynamic CT of the normal spleen. *AJR* 1981; **137**: 343-6.



## Value of F-18-FDG PET in patients with cervical lymph node metastases of unknown origin

Karl H. Bohuslavizki<sup>1</sup>, Susanne Klutmann<sup>1</sup>, Ralph Buchert<sup>1</sup>, Sabine Kröger<sup>1</sup>,  
Jochen A. Werner<sup>2</sup>, Janos Mester<sup>1</sup>, Malte Clausen<sup>1</sup>

<sup>1</sup>Department of Nuclear Medicine, University Hospital Eppendorf, Hamburg,

<sup>2</sup>Clinic of Otorhinolaryngology, Philipps University, Marburg, Germany

---

**Background.** Cancer of unknown primary is still a major diagnostic problem in patients with lymph node metastases despite a large variety of imaging modalities. Therefore, the aim of this study was to evaluate the impact of F-18-FDG positron emission tomography (PET) in these patients.

**Materials and methods.** A total of 28 patients aged 39 to 84 years with cervical lymph node metastases of squamous cell carcinoma (n=24) or an undifferentiated carcinoma (n=4) were investigated. Prior to PET a complete history, physical examination, ultrasound of the neck, panendoscopy, and CT of the head and neck region were performed in all patients without detection of the primary tumour site. All patients received 370 MBq F-18-FDG intravenously, and whole-body images were acquired at 60 min p.i. using an ECAT EXACT 47 (921) (Siemens, CTI). All lesions were evaluated either by histology or by subsequent CT/MRI.

**Results.** In 16/28 patients PET showed focal tracer accumulations corresponding to potential primary tumour sites located in the lungs (n=7), in the region of the palatine tonsil (n=5), the submandibular gland (n=1), the nasopharynx (n=1), the larynx (n=1), and at the base of the tongue (n=1). In 9 out of these 16 patients the primary tumour could be confirmed in the lungs (n=5), in the larynx, at the base of the tongue, the nasopharynx and the palatine tonsil in one patient each, respectively. In 6/16 patients PET lesions were false positive, predominantly located in the palatine tonsil (n=3). One patient denied further evaluation of PET findings. However, in 12/28 patients PET did not reveal tumour-suspicious lesions.

**Conclusions.** Since F-18-FDG PET detected the primary tumour site in approximately one third of the patients with cervical node metastases from an unknown primary (CUP-syndrome), F-18-FDG PET is a valuable diagnostic tool which might help to select a potentially curative treatment protocol in these patients.

**Key words:** neoplasm, unknown primary; lymphatic metastasis, CUP-syndrome; tomography, emission-computed, fluorine radioisotopes, F-18-FDG PET

---

Received: 5 January 1999

Accepted: 9 February 1999

Correspondence to: Dr. Karl H. Bohuslavizki, Department of Nuclear Medicine, University Hospital Eppendorf, Martinistr. 52, D-20246 Hamburg, Germany; Phone: +49 40 42 803 4047; Fax: +49 40 42 803 6775; E-mail: bohu@uke.uni-hamburg.de

### Introduction

The enlargement of cervical lymph nodes is often the first manifestation of a tumour disease.<sup>1</sup> The palpation and localisation of these

enlarged lymph nodes may be helpful in determining their dignity and the origin of the primary tumour site.<sup>2</sup> An additional ultrasound-guided fine-needle aspiration cytology may give evidence of tumour cells in cervical masses.<sup>1,3</sup> Furthermore, morphological orientated imaging, *i.e.* MRI or CT is performed in order to assess the nodal status and to define the origin of the malignancy. However, despite an accurate diagnostic work-up the primary tumour site can not be detected in 1 to 12 % of all patients with cervical lymph node metastases.<sup>4-9</sup> They are called patients with CUP-syndrome (cancer of unknown primary). The cytological examination of patients often reveals squamous cell carcinomas or undifferentiated carcinomas.<sup>4</sup> This holds especially true for metastatic lymph nodes of the upper and middle cervical compartments, whereas lymph nodes of the inferior portion of the neck often bear adenocarcinoma cells.

In some cases the primary tumour is found *post mortem*. Common head and neck sites of lately diagnosed malignancies are the piriform sinus, the tonsils, the nasopharynx or the base of the tongue.<sup>10</sup> However, as much as 40 % of the occult primary tumours are located outside the head and neck region, predominantly in the lungs.<sup>11</sup>

Careful staging of patients with CUP-syndrome is of utmost importance since the therapeutic approach mainly depends on the extent of the tumour. The five-years-survival-rate of patients with an occult primary amounts to about 29-50 %.<sup>12-16</sup> In case of bilateral cervical lymph node metastases ( $T_XN_{2C}M_0$ ) the five-years-survival-rate decreases to 17 to 28 %.<sup>17-20</sup> In contrast, in patients with localised squamous cell carcinoma of the head and neck region and bilateral lymph node metastases five-years-survival-rates of 55 % are reported.<sup>21</sup> This emphasises the necessity for an accurate diagnostic work-up in patients with unknown primary.

The value of positron emission tomography (PET) has already been reported in staging of head and neck tumors<sup>22-24</sup> as well as in therapy monitoring after irradiation.<sup>25,26</sup> Therefore, the aim of our study was to evaluate the use of F-18-FDG PET in the detection of the primary tumour in patients with cervical lymph node metastases and CUP-syndrome.

### Materials and methods

In total, 28 patients (12 female, 16 male) aged from 39 to 84 years with cervical lymph node metastases of a squamous cell carcinoma (n=24) or an undifferentiated carcinoma (n=4) were included in the study. The diagnosis was established either by histology (n=10) or by fine-needle aspiration cytology (n=18). Seven patients underwent neck dissection prior to PET. Prior to PET a complete history, physical examination, ultrasound of the neck, panendoscopy as well as an additional computed tomography of the head and neck region were performed in each patient. However, the primary tumour site could not be detected. Thus, patients were assigned to have CUP-syndrome.

Patients fastened for at least 6 hours prior to PET-scanning in order to minimise blood insulin levels and glucose utilisation of normal tissue.<sup>27</sup> Whole-body images were acquired 60 min after i.v. injection of 370 MBq F-18-FDG using an ECAT EXACT 47 (921) scanner (Siemens/CTI) with an axial field-of-view of 16.2 cm. No attenuation correction was performed. Emission data were reconstructed by filtered back projection using a Hanning filter with a cut-off frequency of 0.4 of the Nyquist frequency. Thus, transaxial spatial resolution was approximately 12 mm. PET-images were printed on transparency film (Helios 810, Sterling) using a linear grey scale with highest activity displayed in black. Images were displayed with

an upper threshold of five times of the mean activity in the lung. Standardised documentation included both 20 transversal and 20 coronal slices with a slice thickness of 13.5 mm each, and Maximum-Intensity-Projections (MIPs) in anterior, left lateral, right-anterior-oblique, and left-anterior-oblique view as published previously.<sup>28</sup> Whole-body images were interpreted by simple visual inspection.

All lesions were evaluated either by histology or by subsequent conventional imaging.

## Results

In 16/28 patients PET showed pathological tracer accumulations corresponding to potential primary tumour sites (Table 1). In nine

mandibular gland in one patient. Moreover, three patients showed an increased tracer uptake of the larynx, the nasopharynx or the base of the tongue, respectively. In addition, seven patients demonstrated pathological tracer uptake outside the head and head region, *i.e.* in the lungs. Moreover, one patient with increased uptake of F-18-FDG in the lungs showed decreased tracer accumulations of both occipital lobes. However, in 12/28 patients PET did not reveal tumour-suspicious lesions (Table 1).

PET correctly identified the primary tumour site in four out of nine patients with tumour-suspicious lesions of the head and neck region (Figure 1). Based on biopsy findings, the primary cancer was confirmed in the nasopharynx, the larynx, the base of the

**Table 1.** PET-findings of 28 patients investigated correlated to localisation of tumour-suspicious lesions and to true positive (TP) and false positive (FP) results

F-18-FDG PET (number)	localisation (number)	TP	FP
Negative (12)			
Positive (16)	lungs (7)	5	2
	palatine tonsil (5)	1	4*
	submandibular gland (1)	Ø	1
	nasopharynx (1)	1	Ø
	larynx (1)	1	Ø
	base of the tongue(1)	1	Ø

\*one of these patient denied further investigations.

out of these patients F-18-FDG accumulations were localised in the head and neck region with an increase of FDG uptake in the palatine tonsils in five patients and in the sub-

tongue, and the palatine tonsil, respectively. However, PET was false positive in three patients with tumour-suspicious tracer accumulations of the palatine tonsil and in one

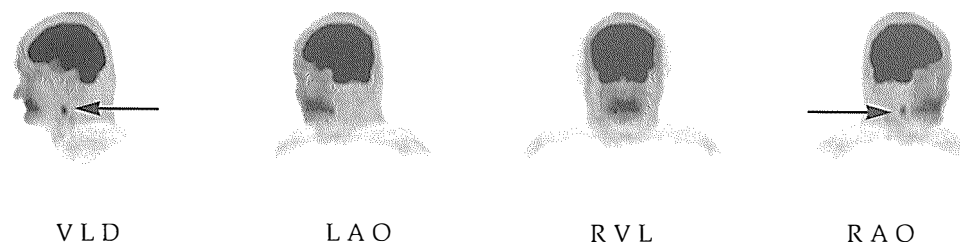


**Figure 1.** MIPs of a 58-year-old patient with histologically confirmed right-cervical lymph node metastases of a squamous cell carcinoma of unknown origin. Note focal uptake of F-18-FDG in the right palatine tonsil (arrows). Histological evaluation confirmed a squamous cell carcinoma of the right palatine tonsil.



patient with suspect for a primary tumour in the submandibular gland. One patient with increased uptake of F-18-FDG in the palatine tonsil refused biopsy. Thus, PET findings could not be evaluated in this patient.

In five out of seven patients with increased tracer uptake of the lungs PET correctly identified the primary tumour site (Figure 2). Moreover, in one patient with additional decreased tracer uptake of both occipital lobes, PET detected cerebral metastases which were confirmed by subsequent MRI imaging. In two out of the latter seven patients PET imaging was false positive concerning the localisation of the primary tumour site.

In 19 out of 28 patients investigated PET revealed a focal uptake of F-18-FDG in the neck region. These findings corresponded to known metastatic lymph nodes. Two out of the latter 19 patients underwent neck dissection prior to PET. However, PET findings turned out to be consistent with findings of physical examination of recurrent or remaining tumour tissue in the area pre-treated surgically.

PET showed no cervical lymph node uptake in nine patients. In five out of the latter nine patients a neck dissection was per-

formed prior to PET. Thus, PET findings confirmed total resection of cervical lymph node metastases. In four out of these nine patients diagnosis was established by complete resection of metastatic lymph nodes prior to F-18-FDG PET imaging.

## Discussion

In 1 to 12 % of all patients with cervical lymph node metastases the primary tumour site can not be detected despite an accurate diagnostic work-up.<sup>16</sup> Therefore, the therapeutic approach remains to be controversial in these patients.<sup>6</sup> The primary objective in patients with CUP-syndrome is the treatment of both cervical lymph node metastases and the primary tumour site. Therefore, the therapeutic approach includes an irradiation of both sides of the neck as well as an irradiation of potential sites of the tumour bearing mucosa. Other authors advocate an ipsilateral neck treatment alone either by irradiation or by surgery.<sup>29</sup> The variety of therapeutic approaches underlines the diagnostic and therapeutic difficulties in patients with CUP-syndrome. An important necessity is the accurate diagnostic work-up since the prog-

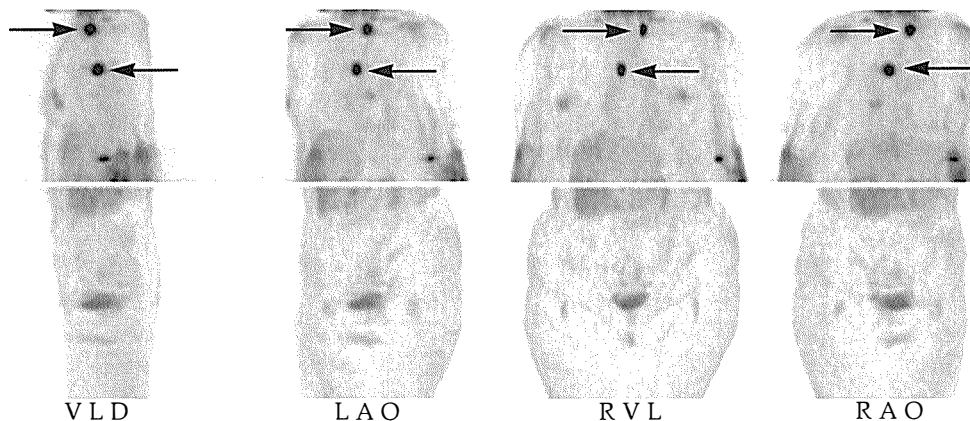


**Figure 2.** MIPs of a 59-year-old patient with cytologically confirmed left-supraclavicular lymph node metastases of a squamous cell carcinoma of unknown origin. Note focal uptake of F-18-FDG in the area of the known lymph node metastases (upper arrows) as well as a second focal tracer uptake in the right central lung (lower arrows). Histological evaluation confirmed a primary lung cancer.

nosis and the survival-rate mainly depend on the detection of the primary tumour site. Thus, five-years-survival-rates of patients with localised squamous cell carcinoma and bilateral cervical metastases are significantly higher as compared to patients with unknown primary tumour site and comparable lymph node status.<sup>15, 17-21</sup>

Initial studies using F-18-FDG PET showed its value in staging and therapy monitoring in patients with head and neck tumors.<sup>22,24-26</sup> The glucose analogue, F-18-FDG is accumulated and trapped within metabolic active cells. Thus, F-18-FDG can be used to identify higher glycolytic rates of many neoplasms when compared to normal glycolytic rates of non-malignant transformed tissue.

In 16 out of 28 patients PET revealed pathologic accumulations of F-18-FDG corresponding to potential primary tumour sites. In seven out of the latter 16 patients these tracer accumulations were localised outside the head and neck region, i.e. in the lungs. In nine out of 28 patients PET clearly identified the primary tumour lesion. In five patients lung cancer was confirmed as the primary tumour site. Thus, based on PET findings the therapeutic approach was changed in these patients. Of the nine patients with tumour-suspicious lesions of the head and neck region five were localised in the palatine tonsil. However, in three out of these patients PET was false positive, and one patient denied further evaluation of PET findings by biopsy. Thus, primary cancer of the palatine tonsil was only confirmed in one patient. The higher tracer accumulations of the palatine tonsils remained unclear. In contrast, PET clearly identified primary cancer of the larynx, the nasopharynx, and the base of the tongue in one patient, respectively. However, in 12 out of 28 patients PET could not identify tumour-suspicious lesions.

Moreover, PET findings were correlated to clinical findings of cervical lymph node metastases. In 19 out of 28 patients PET con-

firmed known tumour tissue, in nine patients with previous surgical resection of the metastatic lymph nodes PET findings corresponded to total resection of lymphatic tumour tissue. Thus, in the assessment of cervical metastases PET had no additional clinical impact in our patients. However, in this study PET imaging was helpful in approximately one third of all patients resulting in a change of the therapeutic approach.

Although F-18-FDG PET is an expensive diagnostic modality it allows the screening of the whole-body. This is especially important in patients with occult malignancies as in 40 % of malignant cervical lymph nodes the primary is localised below the clavicles with the most common site in the lungs.<sup>11</sup> However, the detection of the primary tumour site is the basis for an effective and curative therapy.

Previous reports suggested the usefulness of F-18-FDG PET in patients with CUP-syndrome. Braams and coworkers<sup>30</sup> investigated 13 patients with cervical lymph node metastases of unknown origin. PET was true positive in four patients detecting cancer of the oropharynx, of the larynx and of the lungs in one patient, respectively. Moreover, in one patient a plasmacytoma was identified as the primary tumour. Schipper and coworkers<sup>18</sup> reported a rate of 25 % true positive PET findings in 16 patients with cervical metastases of unknown origin.

## Conclusion

Since F-18-FDG PET detected the primary tumour site in approximately one third of the patients with CUP-syndrome, F-18-FDG PET is a valuable diagnostic tool which might help to select a potentially curative treatment protocol in these patients.

## References

- Liu YJ, Lee YT, Hsieh SW, Kuo SH. Presumption of primary sites of neck lymph node metastases on fine needle aspiration cytology. *Acta Cytol* 1997; **41**: 1477-82.
- Haynes BF. Enlargement of lymph node and spleen. In: Isselbacher KJ, Braunwald E, Wilson JD, Martin JB, Fauci AS, Kasper DL, editors. *Harrison's principles of internal medicine*. 13. Edition. New York: McGraw-Hill; 1994. p. 323-9.
- Van den Brekel MWM, Castelijns JA, Stel HV, Luth WJ, Valk J, Van der Waal I, et al. Occult metastatic neck disease: detection with US and US-guided fine-needle aspiration cytology. *Radiology* 1991; **180**: 457-61.
- De Braud F, Heilbrun LK, Ahmed K, Sakr W, Ensley JF, Kish JA, et al. Metastatic squamous cell carcinoma of an unknown primary localized to the neck. Advantages of an aggressive treatment. *Cancer* 1989; **64**: 510-5.
- Fried MP, Diehl Jr WH, Brownson RJ, Sessions DG, Ogura JH. Cervical metastasis from occult carcinoma. *Surg Gynecol Obstet* 1957; **104**: 607-17.
- Leipzig B, Winter ML, Hokanson JA. Cervical nodal metastases of unknown origin. *Laryngoscope* 1981; **91**: 593-8.
- Nordstrom DG, Tewfik HH, Latourette HB. Cervical lymph node metastases from an unknown primary. *Radiat Oncol Biol Phys* 1979; **5**: 73-6.
- Strasnick B, Moore DM, Abemayor E, Juillard G, Fu YS: Occult primary tumors. *Arch Otolaryngol Head Neck Surg* 1990; **116**: 173-6.
- Wang RC, Goepfert H, Barber AE, Wolf P. Unknown primary squamous cell carcinoma metastatic to the neck. *Arch Otolaryngol Head Neck Surg* 1990; **116**: 1388-93.
- Jacobs CD, Pinto HA. Head and neck cancer with an occult primary tumor [comment]. *N Engl J Med* 1992; **326**: 58-9.
- Jones AS, Cook JA, Phillips DE, Roland NR. Squamous carcinoma presenting as an enlarged cervical lymph node. *Cancer* 1993; **72**: 1756-61.
- Barrie JR, Knapper WH, Strong EW. Cervical nodal metastases of unknown origin. *Am J Surg* 1970; **120**: 466-70.
- Davidson BJ, Spiro RH, Patel S, Patel K, Shah JP. Cervical metastases of occult origin: the impact of combined modality therapy. *Am J Surg* 1994; **168**: 395-9.
- Glynn-Jones RGT, Anand AK, Young TE, Berry RJ, Phil D. Metastatic carcinoma in the cervical lymph nodes from an occult primary: a conservative approach to the role of radiotherapy. *J Rad Oncol Biol Phys* 1990; **18**: 289-94.
- Spiro RH, de Rose G, Strong EW. Cervical node metastasis of occult origin. *Am J Surg* 1983; **146**: 441-6.
- Yang ZY, Hu JH, Yan JH, Cai WM, Qin DX, Xu GZ, et al. Lymph node metastases in the neck from an unknown primary. Report on 113 patients. *Acta Radiol Oncol* 1983; **22**: 17-22.
- Jones AS, Phillips DE, Helliwell TR, Roland NJ. Occult metastases in head and neck squamous carcinoma. *Eur Arch Otorhinolaryngol* 1993; **250**: 446-9.
- Schipper JH, Schrader M, Arweiler D, M ller S, Sciuk J. Die Positronenemissionstomographie zur Prim rtumorsuche bei Halslymphknotenmetastasen mit unbekanntem Prim rtumor. *HNO* 1996; **44**: 254-7.
- Snee PM, Vyrarnuthu N. Metastatic carcinoma from unknown primary site: the experience of a large oncology centre. *Br J Radiol* 1985; **58**: 1091-5.
- Snow GB, Patel P, Leemans CR, Tiwari R. Management of cervical lymph nodes in patients with head and neck cancer. *Arch Otorhinolaryngol* 1992; **249**: 187-94.
- Clarke RW, Stell PM. Squamous carcinoma of head and neck in the young adult. *Clin Otolaryngol* 199; **17**: 18-23.
- Manusco AA, Drane WE, Mukherji SK. The promise FDG in diagnosis and surveillance of head and neck cancer tumor [editorial]. *Cancer* 1994; **74** (Suppl 1): 1193-5.
- Minn H, Lapela M, Klemi PJ, Grenman R, Leskinen S, Lindholm P, et al. Prediction of survival with fluorine-18-fluorodeoxyglucose and PET in head and neck cancer. *J Nucl Med* 1997; **38**: 1907-11.
- Rege S, Maass A, Chaiken L, Hoh CK, Choi Y, Lufkin R, et al. Use of positron emission tomography with fluorodeoxyglucose in patients with extracranial head and neck cancers. *Cancer* 1994; **73**: 3047-58.
- Anzai Y, Carroll WR, Quint DJ, Bradford CR, Minoshima S, Wolf GT, et al. Recurrence of head

- and neck cancer after surgery or irradiation: prospective comparison of 2-deoxy-2-[F-18] fluoro-D-glucose PET and MR imaging diagnoses. *Radiology* 1996; **200**: 135-41.
26. Greven KM, Williams DW, Keyes JW, McGuirt WF, Harkness BA, Watson Jr NE, et al. Distinguishing tumor recurrence from irradiation sequelae with positron emission tomography in patients treated for larynx cancer. *Int J Rad Oncol Biol Phys* 1994; **29**: 841-5.
  27. Minn H, Leskinen-Kallio S, Lindholm P, Bergman J, Ruotsalainen U, Teras M, et al. (18-F) fluorodeoxyglucose uptake in tumors: kinetic vs. steady-state methods with reference to plasma insulin. *J Comput Assist Tomogr* 1993; **17**: 115-23.
  28. Bleckmann C, Buchert R, Schulte U, Lorenzen J, Bohuslavizki KH, Mester J, et al. Onco-PET: lesion detection by computer display versus standardized documentation on film. *Nuklearmedizin*. In press.
  29. Reddy SP, Marks JE. Metastatic carcinoma in the cervical lymph nodes from an unknown primary site: results of bilateral neck plus mucosal irradiation vs. ipsilateral neck irradiation. *Int J Rad Oncol Biol Phys* 1997; **37**: 797-802.
  30. Braams JW, Pruim J, Kole AC, Nikkels PG, Vaalburg W, Vermey A, Roodenburg JL. Detection of unknown primary head and neck tumors by positron emission tomography. *Int J Oral Maxillofac Surg* 1997; **26**: 112-5.



## Renal transplant blood flow in patients with acute tubular necrosis

Dražen Huić<sup>1</sup>, Darko Grošev<sup>1</sup>, Ljubica Bubić-Filipi<sup>2</sup>, Sunčana Crnković<sup>1</sup>,  
Damir Dodig<sup>1</sup>, Mirjana Poropat<sup>1</sup>, Zvonimir Puretić<sup>2</sup>

<sup>1</sup>Clinical Department of Nuclear Medicine and Radiation Protection,

<sup>2</sup>Center for Dialysis, Clinic of Urology, University Hospital Rebro, Zagreb, Croatia

---

**Background.** Since there are contradictions in data, this study was aimed to investigate the quantity of renal transplant blood flow in patients affected by acute tubular necrosis (ATN).

**Subjects and methods.** During the four year period, 179 examinations were performed in 60 patients (31 female, 29 male, median age 37 years, range 11-62 years, 42 cadaveric and 18 living related transplants, median follow-up 21 months) using Tc-99m-pertechnetate and I-131-OIH. Renal blood flow was calculated from the first-pass time activity curves generated over the kidney and aorta and expressed as a percentage of cardiac output (RBF/CO).

**Results.** In 53 examinations of the patients with ATN, the mean RBF/CO was significantly lower than in 60 examinations of patients with normal graft function ( $6.5 \% \pm 3.4 \%$ ,  $11.4 \% \pm 3.4 \%$ , respectively,  $p = 9.6 \times 10^{-12}$ ), and similar to the mean values of 49 examinations with acute rejection (AR) and 17 examinations with the combination of ATN and AR ( $7.3 \% \pm 3.4 \%$ ,  $5.8 \% \pm 2.5 \%$ , respectively,  $p > 0.05$ ). In the patients with ATN, mean RBF/COs were significantly related to creatinin serum (CS) value ( $CS < 500 \mu\text{mol/l} - 8.0 \% \pm 3.0 \%$ ,  $CS > 1000 \mu\text{mol/l} - 5.2 \% \pm 2.2 \%$ ,  $p < 0.05$ ) and to I-131 OIH renogram patterns (some OIH excretion from renal parenchyma during the examination -  $7.0 \% \pm 3.5 \%$ , no excretion -  $5.1 \% \pm 2.2 \%$ ,  $p < 0.05$ ).

**Conclusions.** Renal transplant blood flow is clearly diminished in ATN, similarly as in AR, and significantly related to the graft function.

**Key words:** kidney transplantation; kidney tubular necrosis, acute, kidney-blood supply-radionuclide imaging; quantitative analysis; graft rejection

---

### Introduction

Received 12 April 1999

Accepted 24 April 1999

Correspondence to: Huić Dražen, MD, Clinical Department of Nuclear Medicine and Radiation Protection, University Hospital Rebro, Kišpatićeva 12, 10000 Zagreb, Croatia; Phone: ++385 1 23 33 850; Fax: ++385 1 23 35 785; E-mail: huić@mailexcite.com

Radionuclide methods, as non-invasive procedures, are very useful in detection of many complications, which affect renal transplants. It is necessary to study both renal perfusion and function to differentiate post-transplant complications.<sup>1,2</sup>

Acute tubular necrosis (ATN) is present in the majority of cadaveric transplanted kidneys, but only infrequently in transplants from living related donors. It arises in the immediate post-transplant period and usually resolves without therapy. The major pathologic changes in ATN are caused by ischemic damage to the kidney, which usually arises from prolonged ischemia caused by harvesting and implanting of the kidney or by reaction to X-ray contrast media.

Renal blood flow (RBF) in patients with ATN has been shown to be associated equally with both good and compromised perfusion and it has been usually described as "relatively good", always assumed better than in acute rejection (AR).<sup>1-6</sup>

Since the data are contradictory, the aim of our study was to investigate the quantity of renal transplant blood flow in patients affected by ATN.

## Subjects and methods

### Patients

During the four year period, 179 examinations were performed in 60 patients (31 female, 29 male, median age 37 years, range 11-62 years). Forty-two patients received the kidney from cadavers and 18 from living related donors. Median follow-up was 21 months (range 1-45 months). A baseline examination with Tc-99m pertechnetate (perfusion) and I-131-OIH (function) was performed in all patients within 48 hours of transplantation and additional examinations during post-transplant period in the patients in whom the transplant function impairment was suspected. All patients were treated with antirejection therapy.

### Diagnostic criteria

All examinations were classified by the following diagnostic criteria:

- A. Acute tubular necrosis (ATN)
  1. Delayed and prolonged peak of the OIH renogram.
  2. No signs and symptoms of rejection on the day of the examination and within the following week.
  3. Clinical and OIH renographic improvement after supportive therapy only.
- B. Acute rejection (AR)
  1. Signs and symptoms of AR (graft tenderness, pyrexia, rising serum creatinine level or decrease in the creatinine clearance).
  2. Evidence of rejection confirmed by biopsy (when available).
  3. Clinical improvement after specific treatment for acute graft rejection.
- C. Acute tubular necrosis complicated with acute rejection (ATN+AR)
  1. Criteria A+B.
- D. Normal functioning graft
  1. Good urine production of at least 150 ml/h.
  2. Serum creatinine level not more than 130  $\mu$ mol/l.
  3. No signs and symptoms of rejection on the day of the examination and within the following week.
  4. Normal appearance of OIH renogram.

### Radionuclide studies

The perfusion and subsequent dynamic graft scintigraphy were performed using 555 MBq of Tc-99m-pertechnetate and 8 MBq of I-131-OIH.

Tc-99m-pertechnetate was injected rapidly as a compact bolus. A gamma camera with low energy parallel collimator was used for

data acquisition. Flow images were collected at a frame rate of 1 per sec for 60 sec.

Pre- and post-dose syringe counts were measured on collimated gamma camera's face as 10 sec static frames for measuring the net injected dose. Dead time correction was performed as described previously.<sup>7</sup>

The distance between an anterior abdominal wall marker and the center of the transplanted kidney was obtained on a lateral view for depth correction factor measuring.

The dynamic examination with I-131-OIH was performed immediately after perfusion study using medium energy collimator and a frame rate of 1 per minute for 20 minutes for data acquisition.

#### Data analysis

The well known method for measuring RBF as a percentage of cardiac output (CO) was applied on blood flow studies.<sup>8,9</sup> One region of interest was placed around the kidney and three along the course of the abdominal aorta. Each aortic curve was corrected for recirculation using a gamma fit, integrated and multiplied by the ratio of the maximum upslope of the integrated gamma function aortic curve. The obtained curve represents the renal curve that would be recorded if the Tc-99m-pertech-netate was totally trapped in the vascular bed of the kidney on the first pass.

RBF as a fraction of CO was finally calculated from the formula:

$$\text{RBF/CO} = \frac{\text{gk} \times \text{A} \times \text{DCF} \times 100}{\text{ga} \times \text{D}}$$

where RBF/CO = RBF as a percentage of CO; gk = maximum upslope of the renal curve; ga = maximum upslope of the integrated aortic curve; A = plateau of the integrated aortic curve (cts/sec); D = net injected dose (cts/sec); DCF = depth correction factor ( $e^{\mu x}$ ); m = Tc-99m soft tissue linear attenuation coefficient ( $0.153 \text{ cm}^{-1}$ ).

A final RBF/CO value was expressed as an average value of three estimates from three aortic ROIs.

#### Statistical analysis

Comparative testing of more than two variables at a time was performed by the Kruskal-Wallis analysis of variance. Differences were considered significant if the respective probability values were less than 0.05. Testing of Kruskal-Wallis sub-groups was conducted by the Mann-Whitney-U test. The t - test was used for testing the differences between the two variables.

A summary statistics, including mean values, standard deviations, and minimal and maximal values was run on all data sets.

### Results

According to our diagnostic criteria 42 patients (33 cadaveric and 9 living related transplantations) were affected with ATN in the immediate post-transplant period.

In 53 examinations of the patients with ATN, the mean RBF/CO value was significantly lower than in 60 examinations of the patients with normal graft function ( $6.5\% \pm 3.4\%$ ,  $11.4\% \pm 3.4\%$ , respectively;  $p = 9.6 \times 10^{-12}$ ; Mann-Whitney-U test), but similar to the mean RBF/CO values of 49 examinations of the patients with AR and 17 examinations of the patients with the combination of ATN and AR ( $7.3\% \pm 3.4\%$ ,  $5.8\% \pm 2.5\%$ , respectively;  $p > 0.05$ ; Mann-Whitney-U test). These data are summarized in Table 1.

In patients with ATN, mean RBF/CO values were significantly related to the creatinine serum (CS) level and to OIH renogram patterns, as shown by the first examinations after transplantation. The mean RBF/CO was  $5.2\% \pm 2.2\%$  in nine examinations with CS  $> 1000 \mu\text{mol/l}$  and  $5.3\% \pm 3.2\%$  in 20 examinations with CS between 501 and  $1000 \mu\text{mol/l}$ ,



**Table 1.** Mean RBF/CO values, standard deviations and ranges in patients with normal graft function, ATN, AR, and ATN + AR

Diagnosis	Mean RBF/CO (%)	Standard deviation (%)	Range (%)	Number of examinations
ATN	6.5	3.4	1.4 - 19.2	53
AR	7.3	3.4	1.2 - 16.1	49
ATN + AR	5.8	2.5	1.9 - 13.2	17
Normal	11.4*	3.4	6.4 - 21.1	60

\* significantly different from all other mean values (Kruskal-Wallis analysis of variance,  $p = 4.8 \times 10^{-14}$ ).

as a contrary to higher RBF/CO values in 13 examinations with CS less than 500  $\mu\text{mol/l}$  ( $8.0 \% \pm 3.0 \%$ ;  $p = 0.044$ ; Kruskal-Wallis analysis of variance; Table 2).

$^{99}\text{Tc}$ -pertechnetate is preferable for simple routine studies because of its low price, high vascular transit and low kidney radiation.<sup>10</sup> At the same time, we perform quantitative analy-

**Table 2.** Mean RBF/CO values, standard deviations and ranges in patients with ATN according to creatinin serum values (CS)

CS ( $\mu\text{mol/l}$ )	Mean RBF/CO (%)	Standard deviation (%)	Range (%)	Number of examinations
< 500	8.0*°	3.0	5.6-14.3	13
501-1000	5.3*	3.2	1.5-12.2	20
> 1000	5.2°	2.2	1.4-8.5	9

\*  $p = 0.034$ ; °  $p = 0.025$  (Mann-Whitney-U test)

Some excretion of OIH from renal parenchyma during 22 I-131-OIH examinations was accompanied with better renal blood flow ( $\text{RBF/CO} = 7.0 \% \pm 3.5 \%$ ) in comparison with 20 cases without any hippuran excretion ( $\text{RBF/CO} = 5.1 \% \pm 2.2 \%$ ;  $p < 0.05$ , t-test).

In 13 patients affected with ATN graft function recovered and became normal in the second examination after transplantation. This improvement was followed with the mean RBF/CO rise of  $5.4 \% \pm 3.4 \%$  (range -0.2 % - 13.6 %). Only one patient did not show any flow improvement (Table 3.).

Discussion

At our department, we routinely use Tc-99 pertechnetate for assessing renal transplant perfusion. Since the renal handling of Tc-99m-DTPA, Tc-99m-MAG3 and I-123-OIH interferes on the downslope of the first-pass curve, these pharmaceuticals may be less useful in poorly or non-functioning kidneys. Tc-

sis of the transplant blood flow which is based on the principle of fractionation of cardiac output. This method depends minimally on bolus shape and is applicable with any recirculating gamma emitting tracer.<sup>8,9,11</sup>

The major pathologic changes in ATN are caused by prolonged ischemia, which usually arises during harvesting and implanting of the kidney. ATN is present in the majority of cadaveric kidneys and, in most cases, it will resolve without therapy in few weeks following the transplantation. Histologically, there is dilatation of the proximal as well as distal convoluted tubules lined by degenerative flattened or necrotic epithelial cells and there is disruption of the basement membrane. The glomeruli and vasculature are spared.<sup>5</sup>

In nuclear medicine literature, RBF in patients affected by ATN was described variously, from good and satisfactory to compromised.<sup>1-6</sup> The situation is somewhat clearer when renal function is being assessed by tubular agents. With tubular agents (I-131 or I-123-OIH and Tc-99m-MAG<sub>3</sub>), the most prominent finding in ATN is delayed transit

**Table 3.** RBF/CO changes in patients with normalization of renal transplant function after ATN.

Patient	First examination (ATN) RBF/CO (%)	Second examination (normal) RBF/CO (%)
1	14.3	19.0
2	6.5	8.8
3	3.0	7.6
4	7.5	21.1
5	1.6	8.7
6	6.6	6.4
7	4.1	12.2
8	9.5	11.7
9	12.2	16.8
10	7.4	11.4
11	6.4	13.4
12	5.7	11.8
13	1.8	7.6

with delayed T-max in severe cases without activity excreted into the bladder.

According to our results, RBF in renal transplant recipients with ATN is clearly diminished, on average amounting to more than 50 % of RBF in normal studies ( $6.5 \% \pm 3.4 \%$ ,  $11.4 \% \pm 3.4 \%$ , respectively). We did not observed any significant difference in the blood flow between ATN and AR ( $6.5 \% \pm 3.4 \%$ ,  $7.3 \% \pm 3.4 \%$ , respectively), what means that differentiation between these two post-transplant complications is not possible with RBF/CO values. With RBF/CO values both complications are obviously separated from normal functioning transplants.

Higher RBF/CO values in patients with lower CS values and in patients with some excretion of OIH during renography confirm the relation between the renal blood flow and transplants' function. Normalization of the renal function in 13 patients with ATN was accompanied with notable RBF improvement in 12 patients indicating a possible prognostic role of RBF/CO in the graft function recovery from ATN.

### Conclusions

In conclusion, renal transplant blood flow is

clearly diminished in ATN, similar as in AR, and significantly related to the graft function, which means that RBF/CO value could potentially serve as a prognostic factor in the graft function recovery from ATN.

### References

1. Dubovsky EV, Russel CD. Radionuclide evaluation of renal transplants. *Semin Nucl Med* 1988; **18**: 181-98.
2. Dubovsky EV, Russel CD, Erbas B. Radionuclide evaluation of renal transplants. *Semin Nucl Med* 1995; **25**: 49-59.
3. Chaiwatanarat T, Laorpatanaskul S, Poshyachinda M, Boonvisut S, Buachum V, Krisanachinda A, et al. Deconvolution analysis of renal blood flow: evaluation of postrenal transplant complications. *J Nucl Med* 1994; **35**: 1792-6.
4. Mange KC, Scheff A, Brayman K, Mozley D, Grossman RA, Naji A, et al. Focal acute tubular necrosis in a renal allograft. *Transplantation* 1997; **64**: 1490-2.
5. Dunn EK. Radioisotopic evaluation of renal transplants. *Urol Radiol* 1992; **14**: 115-26.
6. al-Nahhas AM, Kedar R, Morgan SH, Landells WN, al-Murrani B, Wright A, et al. Cellular versus vascular rejection in transplant kidneys. Correlation of radionuclide and Doppler studies with histology. *Nucl Med Commun* 1993; **14**: 761-5.

7. Huić D, Grošev D, Dodig D, Poropat M, Ivančević D. Renal blood flow measurement from first pass time-activity curves in patients undergoing routine bone scintigraphy. *Radiol Oncol* 1993; **27**: 31-5.
8. Peters AM, Gunasekera RD, Henderson BL, Brown J, Lavender JP, De Souza M, et al. Noninvasive measurement of blood flow and extraction fraction. *Nucl Med Commun* 1987; **8**: 823-37.
9. Huić D, Grošev D, Poropat M, Bubić-Filipi Lj, Dodig D, Ivančević D, et al. Quantitative analysis of blood flow in the estimation of renal transplant function. *Radiol Oncol* 1993; **27**: 105-10.
10. Thomsen HS. Renal transplant evaluation. In: Murray IPC, Ell PJ, editors. *Nuclear medicine in clinical diagnosis and treatment*. Edinburgh: Churchill Livingstone; 1994. p. 339-51.
11. Ash J, De Souza M, Peters M, Wilmot D, Hausen D, Gilday D. Quantitative assessment of blood flow in pediatric recipients of renal transplants. *J Nucl Med* 1990; **31**: 580-5.

# Cryosurgery combined with radiotherapy of tumors in mice

Albert P. Fras, Simona Kranjc, Maja Čemažar, and Gregor Serša

*Institute of Oncology, Ljubljana, Slovenia*

---

*The aim of this study was to determine antitumor effectiveness of cryosurgery alone and in combination with radiotherapy. Cryosurgery of subcutaneous fibrosarcoma SA-1 tumors in A/J mice was moderately effective treatment. Tumor growth delay was  $10.3 \pm 3.8$  days after 5 minute treatment with nitrogen filled cryo-probe. Shorter treatment times induced less, but dose dependent antitumor effect. In combined treatment, tumors were either first treated by cryosurgery for 3 minutes and then locally irradiated with 10 Gy for 5 minutes, or irradiated first and thereafter treated by cryosurgery. The antitumor effectiveness of combined treatment was sequence dependent; the irradiation of tumors before cryosurgery resulted in better antitumor effect than the irradiation after cryosurgery. These results indicate that radiosensitization may not be always expected, in spite of some reports demonstrating that cryosurgery may have radiosensitizing effect in vivo, and that some other mechanisms may be involved contributing to radiation damage when cryosurgery follows irradiation.*

**Key words:** sarcoma, experimental-surgery-radiotherapy; cryosurgery; mice

---

## Introduction

Cryosurgery is a form of cryotherapy that uses special instrumentation to produce freezing of tissue.<sup>1</sup> Whatever the approach is used, the basic cryosurgical technique has to devitalize the neoplastic tissue by freezing *in situ*. The same volume of the tissue has to be frozen as would have been excised with a conservative local excision. The nature of the tissue response varies with the intensity of the injury; that is, a minor cryogenic injury pro-

duces only an inflammatory response whereas greater cryogenic injury produces tissue destruction.<sup>2</sup>

Biological basis of tissue destruction by freezing of tissue is due to a number of factors which can be grouped into two major mechanisms, one immediate, the other delayed.<sup>1,2</sup> The immediate effect is due to injury such as crystallisation of the cells caused by freezing and warming.<sup>3</sup> The delayed effect is due to the progressive failure of microcirculation and ultimate vascular stasis, after the tissue has thawed.

Cryosurgery is being increasingly used in the treatment of malignant diseases as a potential alternative to conventional surgery or irradiation.<sup>1,4-7</sup> Its antitumor effectiveness has been demonstrated in many accessible

Received 20 March 1999

Accepted 19 April 1999

Correspondence to: Gregor Serša, Ph.D., Department of Tumor Biology, Institute of Oncology, Zaloška 2, SI-1000 Ljubljana, Slovenia. Tel/Fax: +386 61 133 74 10; E-mail: gserša@onko-i.si

cutaneous tumors of various types, as well as in the treatment of carcinomas of the pharynx, larynx, trachea, bronchi, lung, oesophagus, liver, as well as vulva, vagina and uterus.<sup>1</sup> Due to the biological basis of freezing effect on tumors, many clonogenic cells may survive in the margins of tumors, which may represent a source of tumor regrowth. Therefore, combined cryosurgery and radiotherapy of tumors may be a potential tool for elimination of the residual disease.

Reports dealing with radiosensitization of the cells with cryosurgery, demonstrate that, in certain conditions, hypothermia may predispose cells to irradiation damage.<sup>8,9</sup> There are only few reports dealing with cryosurgery combined with irradiation of tumors *in vivo*.<sup>5,10,11</sup> Most of these *in vivo* studies have dealt with radiotherapy as a means to eradicate the remaining viable cells in the tumors after cryosurgery. However, there are no reports comparing the sequencing of cryosurgery and radiotherapy. Therefore, the aim of this study was to determine antitumor effectiveness of cryosurgery on subcutaneous SA-1 fibrosarcoma tumors in mice performed either before or after local tumor irradiation.

## Materials and methods

### *Animals and tumors*

A/J mice of both sexes, were purchased from the Institute Rudjer Bošković, Zagreb, Croatia. They were maintained at 21°C with a natural day/night light cycle in a conventional animal colony. The mice were 8-12 weeks old at the beginning of the experiments. The tumor used was fibrosarcoma SA-1 (The Jackson Laboratory, Bar Harbour, ME). SA-1 cells for initiation of subcutaneous tumors were obtained from the ascitic form of the tumors in mice, which were serially transplanted twice per week. Subcutaneous tumors were implanted by injecting 0.1 ml NaCl

(0.9%) containing  $5 \times 10^5$  viable tumor cells under the skin on the rear dorsum. Six to 8 days after implantation, when the tumors reached approximately 40 mm<sup>3</sup> in volume (7 mm in diameter) the mice (5-10 per group) were randomly divided into experimental groups. Experiments were repeated twice.

### *Cryosurgery and radiotherapy of tumors*

Cryosurgery of the tumors was performed by Dewar/gas cylinder filled with liquid nitrogen. After a few minutes, the probe on the cylinder with a diameter of 8 mm was evenly cooled and pressed on the surface of the tumor. During treatment the mice were held in hand, therefore anaesthesia was not necessary. The treatment was performed either for 1, 3 or 5 minutes. The probe was placed on the same spot during the whole treatment with gentle pressure on the tumor not to loose contact.

A Darpac 2000 X-ray unit (Gulmay Medical Ltd. Shepperton, UK), operated at 220 kV, 10 mA, and with 0.55 mmCu and 1.8 mm Al filtration, was used for local tumor irradiation. The tumors were irradiated at a dose rate of 2.1 Gy min<sup>-1</sup>. A holder for 6 mice was mounted on the X-ray with the aperture for the irradiation of the tumors, the rest of the body of the mice was shielded by lead block, and by the lead holders for the mice. To ensure uniform dose through the tumor volume, the tumors were exposed to irradiation by two opposing treatment fields through each of which 50% of the dose was delivered.

In experiments with combined treatment, the tumors were either irradiated before or after cryosurgery. Interval between the treatments was 5 minutes.

### *Assessment of antitumor effectiveness*

Antitumor effectiveness of cryosurgery and radiotherapy was assessed by measurements of the tumor diameters in three orthogonal directions using Vernier caliper on consecu-

tive days following treatment. Arithmetic means and standard error of the means were calculated for each experimental group. Tumor doubling time was calculated from the growth curve of individual tumors. Tumor growth delay was calculated from the mean tumor doubling time of the experimental groups compared to untreated tumors.

#### Statistical analysis

Statistical significance was evaluated by modified t-test (Bonferroni t-test) after one way ANOVA had been performed and fulfilled.

## Results

#### Antitumor effect of cryosurgery

Antitumor effectiveness of cryosurgery was evaluated on subcutaneous tumors in mice. The treatment was performed by cryoprobe with a diameter of 8 mm, cooled by liquid nitrogen. The probe was firmly pressed on the tumor for 1, 3 or 5 minutes. Uniformity of the treatment was inspected visually. The results in Table 1 demonstrate that antitumor effectiveness of cryosurgery was dependent on the duration of the treatment. One minute treatment induced 0.8 days tumor growth delay, whereas 3 and 5 minutes 3.8 and 10.3 days, respectively. Significant tumor growth retardation was observed only after a 5 minute cryosurgical treatment ( $p < 0.05$ ). It induced early reduction of tumor size which was reflected also in tumor growth curves (Figure 1). The treatment did not result in tumor exulceration or any other side effects.

**Table 1.** Antitumor effectiveness of cryosurgery on SA-1 tumors in A/J mice

Group	n	Tumor doubling time*
Control	16	$2.0 \pm 0.2$
Cryosurgery 1 min.	14	$2.8 \pm 0.2$
Cryosurgery 3 min.	19	$5.8 \pm 1.0$
Cryosurgery 5 min.	14	$12.3 \pm 3.8$

\* Tumor doubling time  $\pm$  SE

#### Effect of cryosurgery combined with radiotherapy

Local tumor irradiation was performed either before or after cryosurgery of subcutaneous tumors. The tumors were treated for 3 minutes with cryosurgery, and after 5 minute interval, locally irradiated with 10 Gy, or in inverse sequence, irradiated first and after 5 minutes treated with cryosurgery. Tumor irradiation was effective, antitumor effectiveness, as measured by tumor growth delay was  $19.8 \pm 7.4$  days. When the tumors were irradiated first and cryosurgery was performed thereafter, tumor growth delay was  $28.8 \pm 6.5$  days. However, tumors that were treated by cryosurgery first and then irradiated responded similarly as those treated only by radiotherapy. Tumor growth delay of those tumors was prolonged for  $19.1 \pm 6.1$ . This observation is evident also from the growth curves of the tumors (Figure 2). Local tumor irradiation followed by cryosurgery induced early tumor volume reduction, that resulted in overall better antitumor effectiveness than radiotherapy only or cryosurgery followed by radiotherapy. No exulceration of the tumors or other side effects of single or combined treatments were observed.

**Table 2.** Antitumor effectiveness cryosurgery combined with radiotherapy (RT)

Group	n	Tumor doubling time*
Control	16	$2.0 \pm 0.2$
Cryosurgery 3 min.	19	$5.8 \pm 1.0$
RT 10 Gy	11	$21.8 \pm 7.4$
Cryosurg. + RT	11	$21.1 \pm 6.1$
RT + Cryosurg.	11	$30.8 \pm 6.5$

\* Tumor doubling time  $\pm$  SE

## Discussion

Our study shows that cryosurgery is effective when combined with radiotherapy in treatment of tumors. However, antitumor effectiveness of combined treatment was se-

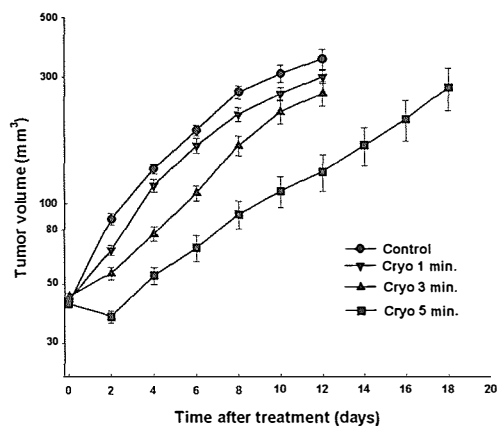


**Figure 1.** The antitumor effect of cryosurgery on subcutaneous fibrosarcoma SA-1 tumors in A/J mice. Cryosurgery was performed with 8 mm probe cooled by liquid nitrogen for 1, 3 and 5 minutes. Symbols, mean tumor volume; vertical bars, standard error of the mean.

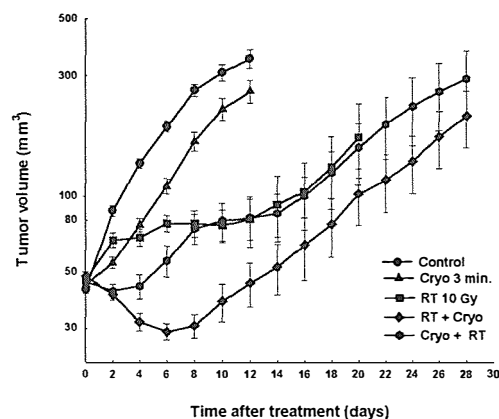


**Figure 2.** The antitumor effect of cryosurgery combined with radiotherapy on SA-1 tumors in mice. Cryosurgery was performed for 3 minutes and radiotherapy by local tumor irradiation with 10 Gy. The interval between cryosurgery and radiotherapy was 5 minutes. Symbols, mean tumor volume; vertical bars, standard error of the mean.

quence dependent. We found that the tumor growth delay was prolonged when tumors were treated with irradiation before cryosurgery. The inverse combined treatment did not differ significantly compared to irradiation alone.

Cryosurgery is being increasingly considered as a treatment of choice for a number of malignant skin tumors.<sup>1</sup> Moreover, better

understanding of the mechanisms of tissue injury by cryosurgery has lead its way into broader clinical practice for treatment of the head and neck and gynecological tumors. It is known that tissue damage by freezing depends on both, freeze and thaw rates; in many instances, rapid freezing and slow thawing should be used.<sup>2</sup> Injury is increased by repeating freeze-thaw cycles.<sup>3</sup> The best results of cryosurgery have been obtained in the treatment of malignant skin lesions.<sup>1</sup> The overall cure rates obtained by cryosurgery compare favourably with those obtained by other treatment modalities.

The depth of freezing is approximately the same as the lateral spread of frost from the edge of the probe. However, when the volume of the tumor hampers the optimal freezing, cryosurgery can not be performed adequately. These advanced bulky tumors may require combined therapeutic technique, such as combined cryosurgery and radiotherapy. It can be predicted that cryosurgery may deal better with central portion of the tumor, that tends to be radioresistant, while radiotherapy would deal better with the peripheral parts of the tumor that are more radiosensitive due to better oxygenation.

However, there have been only limited studies of hypothermia dealing with response to subsequent irradiation, either to cells or tissues *in vivo*.<sup>5,8,9</sup> Generally, enhanced radiosensitivity of cells and tumors after hypothermia have been observed, but the magnitude was dependent on cell line used, cooling temperature, duration, and rewarming interval before irradiation. In this study, the importance of sequencing was examined, i.e. local irradiation of tumors either before or after cryosurgery. This is important, since the rationale of tumor irradiation after cryosurgery bears the notion that cryosurgery may predispose cells to radiation damage. However, cryosurgery after irradiation can have the rationale in the potentiation of sublethal radiation damage of cells.

Although the aim of this study was not to investigate the underlying mechanisms of antitumor effectiveness of combined cryosurgery and radiotherapy, the results show that in our experimental design, cryosurgery was more effective when given after radiotherapy.

### Acknowledgements

This work was supported by the Ministry of Science and Technology of the Republic of Slovenia.

### References

1. Gage A. Cryosurgery in the treatment of cancer. *Surg Gynecol Obstet* 1992; **174**: 73-92.
2. Gage AA, Baust J. Mechanisms of tissue injury in cryosurgery. *Cryobiology* 1998; **37**: 171-86.
3. Gage AA, Guest K, Montes M, Caruana JA, Whalen Jr DA. Effect of varying freezing and thawing rates in experimental cryosurgery. *Cryobiology* 1985; **22**: 175-82.
4. Kuflik EG. Cryosurgery for cutaneous malignancy. *Dermatol Surg* 1997; **23**: 1081-7.
5. Shibata T, Yamashita T, Suzuki K, Takeichi N, Micallef M, Hosokawa M, Kobayashi H, Murata M, Arisue M. Enhancement of experimental pulmonary metastasis and inhibition of subcutaneously transplanted tumor growth following cryosurgery. *Anticancer Res* 1998; **18**: 4443-8.
6. Zouboulis CC. Cryosurgery in dermatology. *Eur J Dermatol* 1998; **8**: 466-74.
7. Büchner SA. Kryochirurgie bei malignen Tumoren der Haut. *Therapeutische Umschau* 1993; **50**: 848-51.
8. van Rijn J, van den Berg J, Kipp JBA, Schamhart DHJ, van Wijk R. Effect of hypothermia on cell kinetics and response to hyperthermia and X rays. *Radiat Res* 1985; **101**: 292-305.
9. Burton SA, Paljug WR, Kalnicki S, Werts ED. Hypothermia-enhanced human tumor cell radiosensitivity. *Cryobiology* 1997; **35**: 70-8.
10. Vergnon JM, Schmitt T, Alamartine E, Barthelemy JM, Fournel P, Emont A. Initial combined cryotherapy and irradiation for unresectable non-small cell lung cancer. *Chest* 1992; **102**: 1436-1440.
11. Zogafos L, Uffer S, Bercher L, Gaillound C. Chirurgie, cryocoagulation et radiothérapie combinée pour le traitement des mélanomes de la conjunctive. *Klin Monatsbl Augenheilkd* 1994; **204**: 385-90.





## A modified half-block breast irradiation technique using a CT-simulator

Michael D.C. Evans<sup>1</sup>, Veronique Benk<sup>2</sup>, Carolyn Freeman<sup>2</sup>  
Micheline Gosselin,<sup>1</sup> Marina Olivares,<sup>1</sup> Ervin B. Podgorsak<sup>1</sup>

<sup>1</sup>Department of Medical Physics,

<sup>2</sup>Department of Radiation Oncology, McGill University Health Centre, Montreal, QC, Canada

---

**Purpose.** Over the past two decades numerous approaches with varying degrees of complexity have been proposed for radiation treatment of the breast and peripheral lymphatics. In our center a single isocenter, rotating half-block technique has been used since 1982, and the recent installation of a CT-simulator and a linear accelerator with asymmetric jaws has provided an impetus to improve our treatment technique by incorporating this new technology into the treatment planning and dose delivery process.

**Materials and methods.** Our breast irradiation technique requires no couch or patient motion when switching from one field to another, and provides a smooth and reproducible junction between the tangential chest wall fields and the supraclavicular fields. Before treatment, the patient is scanned on the CT-simulator, and with the aid of virtual simulation software the optimal isocenter, common to all radiation fields, is determined and marked on the patient's skin.

**Results.** Since 1997, 17 patients have been treated with the modified breast irradiation technique. The simulation time is reduced to about 30 minutes. The patient setup on the linear accelerator is straightforward, and the dose delivery is relatively simple because all fields, despite being half-blocked, use the same isocenter. The wedged tangential fields are produced with a dynamic wedge, and the asymmetric jaws enable us to determine the optimum isocenter common to all treatment fields.

**Conclusions.** Treatment planning for our breast irradiation technique is based on virtual simulation, and dose delivery is accomplished on a 6 MV linear accelerator incorporating a rotating half-block, asymmetric jaws, dynamic wedge, and a multileaf collimator. The technique is practical, meets the requirements for adequate irradiation of the breast and peripheral lymphatics, and is easy to implement on modern linear accelerators.

**Key words:** breast neoplasm-radiotherapy; radiotherapy dosage; rotating half-block, CT-simulation, beam matching

---

Received 11 January 1999  
Accepted 27 January 1999

Correspondence to: Michael D.C. Evans, M.Sc., FCCPM, Department of Medical Physics; McGill University Health Centre, 1650 Ave Cedar, Montreal, PQ, Canada H3G 1A4; Phone: +1 514 934-8052; Fax: +1 514 934-8229; E-mail: mevans@medphys.mgh.mcgill.ca; Internet: <http://www.medphys.mgh.mcgill.ca>

## Introduction

Since 1982 our center has used a single isocenter breast irradiation technique for treatment of the breast or chest wall and draining lymphatics. The technique as originally described,<sup>1,2</sup> uses a rotating half-block to achieve a match between the two tangential chest wall fields and the AP-PA fields used to treat the axilla and supraclavicular region. A single isocenter is used for all four fields, and no couch motion is required when switching from one field to another.

The acquisition in 1994 of a CT-simulator and a linear accelerator with asymmetric jaws provided an opportunity to improve the technique in terms of treatment planning and beam delivery. In this paper we describe the modified technique, which uses virtual simulation software for the determination of the optimal location of the treatment isocenter and relies upon a rotating half-block and asymmetric jaws to define the treatment fields. It has been established that the isodose distributions and matchline dosimetry that were performed for the original technique<sup>1</sup> have not changed for the modified technique, therefore this paper presents only the modification to the planning using the CT simulator.

## Materials and methods

Numerous techniques with varying degrees of complexity have been proposed for radiation treatment of the breast and peripheral lymphatics.<sup>3-10</sup> Our original technique was designed around the capabilities of linear accelerators without asymmetric jaws. The isocenter of the machine was placed onto the patient's skin on the matchline between the two treatment volumes and midway between the medial and lateral limits of the anterior supraclavicular field. While this isocenter position was appropriate for the supraclavicular region, it was not always optimal for the

two tangential chest wall fields, and often resulted in the isocenter for the two tangential fields being located medially with respect to the position which would be chosen for a simple set of opposed tangential chest wall fields.

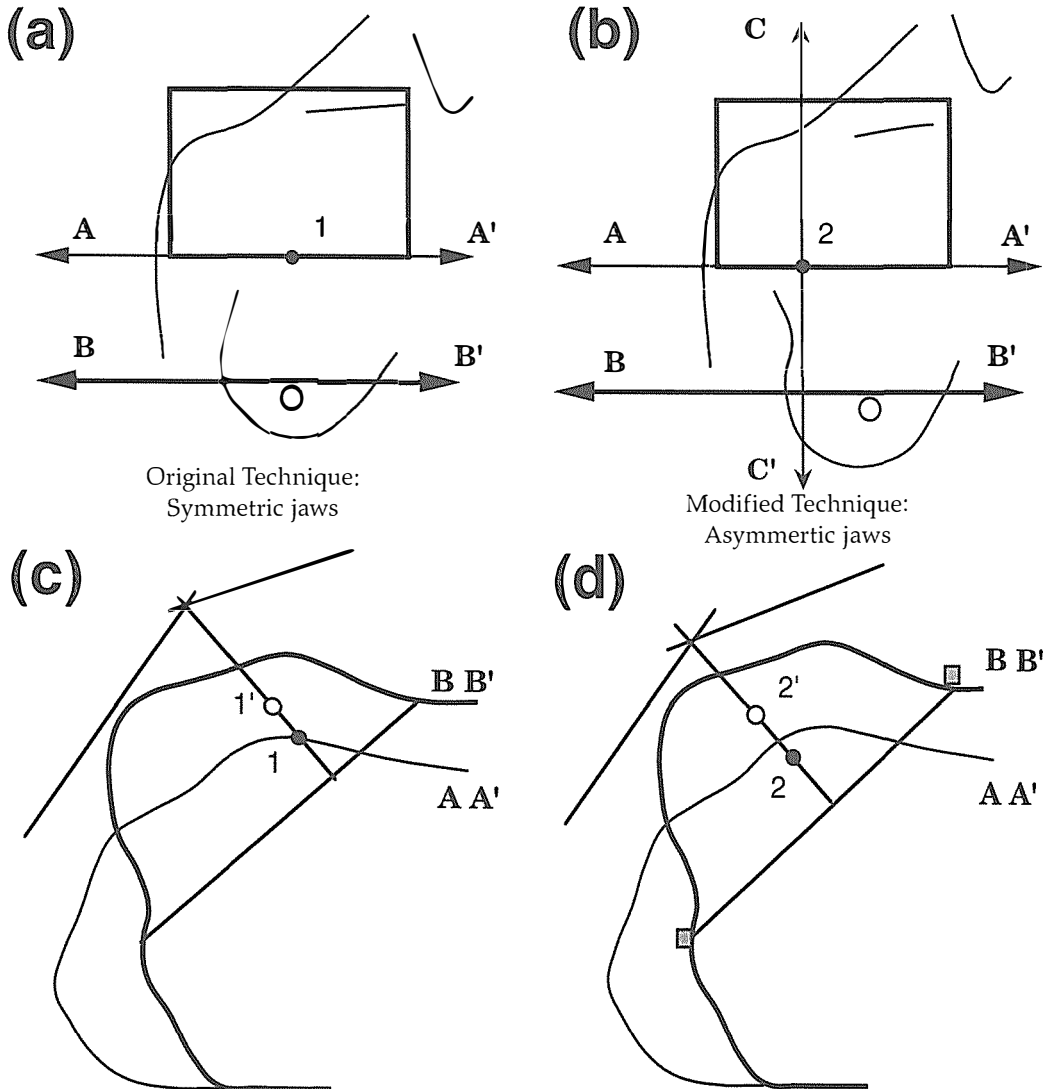
In our current technique the most appropriate isocenter is chosen for the tangential fields first, and then this isocenter is also used for the supraclavicular fields in conjunction with asymmetric jaws. Both our original and current breast techniques are shown schematically in Figure 1. For the original technique the solid dot (point 1 in Figure 1a) indicates the position of the treatment isocenter at the matchline of the fields, positioned midway between the medial and lateral limits of the supraclavicular field. The analogous isocenter point in our current technique (point 2 in Figure 1b) is shown shifted laterally. The placement of the isocenter using the symmetric jaws (point 1) was on the patient's skin, while typically point 2 will be positioned subcutaneously. The line CC' runs through point 2 along the coronal aspect of the patient.

Two transverse sections through the patient are shown for the original technique (Figure 1c) and the modified technique (Figure 1d). As indicated in Figures 1a and 1b, section AA' is at the level of the beam matchplane and section BB' is at a level midway through the tangential chest-wall volume. The constraints imposed by the linac with symmetric jaws required that the treatment isocenter (point 1) be placed medially, forcing the apparent isocenter (point 1') of the tangential fields to be off mid-volume and requiring unequal beam weights to produce an optimized dose distribution. Since these two tangential beams did not meet at midplane, the medial beam often had a large air splash, while the lateral beam was tight with respect to the patient's external contour. For the current technique (Figure 1d) the center of the chest wall volume to be treated at the level of

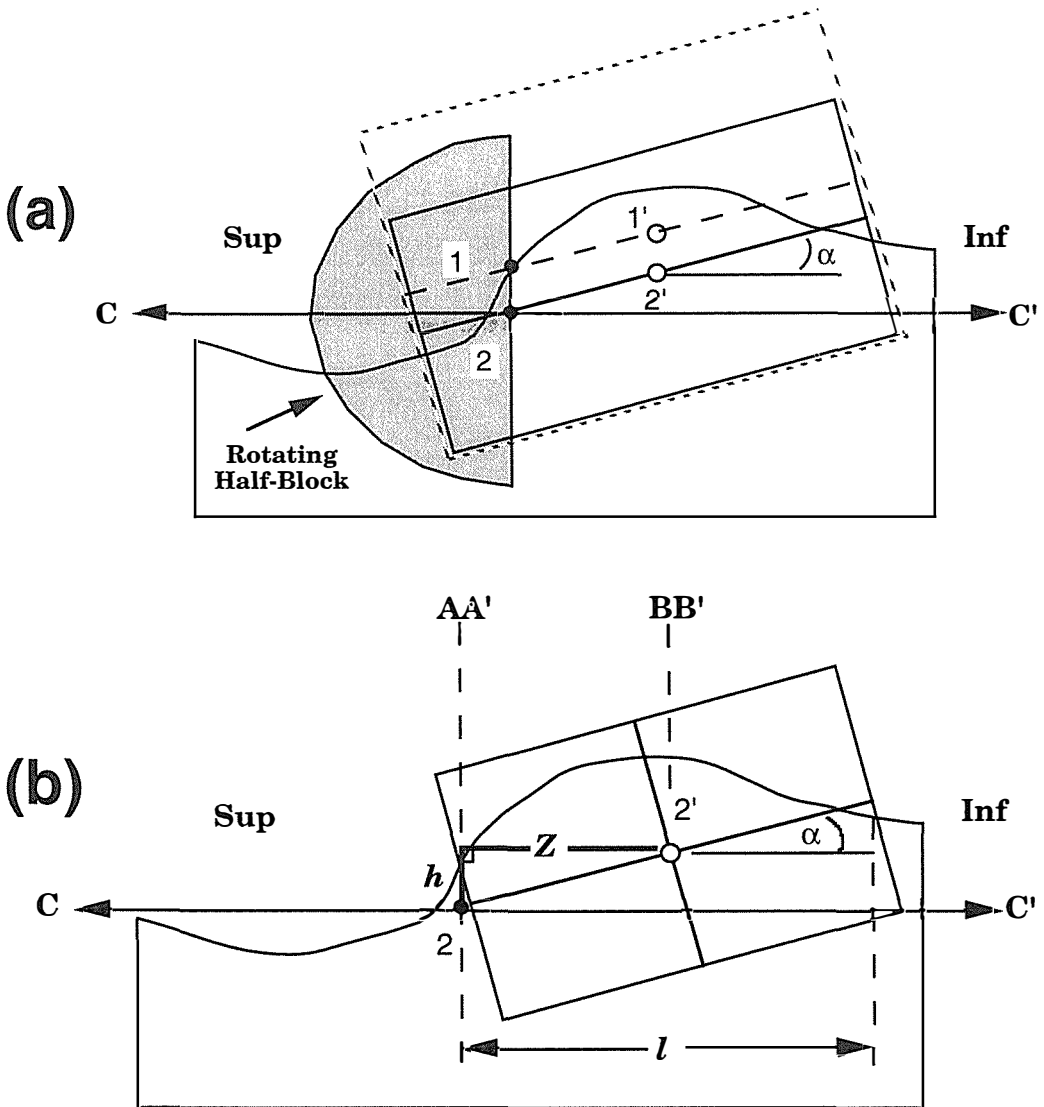
section BB' (point 2') is identified and then a simple calculation described in Equation (1) is carried out to determine the position of the treatment isocenter at the level of section AA' (point 2).

Figure 2a shows the current technique in the medial oblique beam's eye view containing the line CC' of Figure 1b and indicates the

position of the rotating half-block which compensates for the collimator angle  $\alpha$ . The field dimensions for the current technique are indicated by the rectangle with the solid line. The treatment isocenter (point 2) is located at a depth below the matchplane and the center of the tangential treatment volume (point 2') is located along the axis defined by the colli-



**Figure 1.** The original breast irradiation technique designed for use with symmetric jaws is shown on the left, the modified technique using asymmetric jaws on the right. Parts (a and b) show the coronal view, parts (c and d) two transverse sections, one at matchplane (AA') and the other at mid-tangential plane (BB').



**Figure 2.** The medial oblique beam's eye view containing the line CC' of Figure 1a is shown schematically. Part (a) shows the treatment isocenter and the mid-volume points for the original technique (1 and 1' respectively) and the current technique (2 and 2' respectively). The field dimensions for the original (dashed rectangle) and modified (solid rectangle) are also shown. Part (b) shows the geometry used to calculate the position of the isocenter (2').

mator rotation. For comparison, the treatment isocenter for the original technique is shown on the patient's skin (point 1), with the resulting position for the apparent mid-volume isocenter (point 1'). The field dimensions for the original technique are indicated by the rectangle with the dashed line.

A dedicated rotating half-block which attaches to the existing wedge slot on the linac (Clinac 2300 C/D, Varian, Palo Alto, CA) and accommodates a maximum field size of 20x40 cm<sup>2</sup> with a maximum collimator angle  $\alpha$  of 25° was constructed in our machine shop. The use of the wedge slot on our partic-

ular unit precludes the use of standard static wedges, so that tangential treatments are delivered with the use of a dynamic wedge. On the anterior and posterior axilla-supraclavicular fields humeral head shielding is achieved with a 26-pair multileaf collimator (MLC) provided that the field sizes are less than 13 cm in the half-blocked direction.

Patients are planned using CT-based virtual simulation (Picker AcQSim, Cleveland, OH) by placing them into an immobilization device on the CT stretcher with the both arms extended and abducted over the head. In order for the rotating half-block accessory on the linac to comfortably clear the patient, the ipsilateral arm is positioned as close as possible to the side of the patient. The borders of the tangential fields are determined clinically and identified with radio-opaque markers. The medial border is usually placed at mid-line, the lateral border at the mid-axillary line, the inferior border at 1.2 cm below the inframammary fold and the superior border corresponds to the matchplane for the tangential and supraclavicular fields, determined by using the AP scout view. The patient is CT scanned from below the level of the inferior limit of the tangential fields to a level superior to the limit of the supraclavicular fields.

The planning begins on the transverse CT slice (BB' of Figure 1) midway between the matchplane of the beams (AA' of Figure 1) and the inferior limit of the tangential fields. This slice contains the two radio-opaque markers indicating the medial and lateral limits of the chest wall treatment volume. The optimal isocenter position in this CT slice is identified using a software option overlaying a rectangle in such a way that the proximal edge connects the medial and lateral radio-opaque markers, while leaving a minimum air gap of 2 cm over the breast. The virtual simulation software then computes the center of this volume, as indicated in Figure 1d by the open circle (point 2'). The shift to the treatment machine isocenter (point 2) is then cal-

culated. The appropriate gantry angle and field size are chosen with respect to the anatomy and the radio-opaque markers as seen on the transverse CT slice (BB' of Figure 1d). The appropriate collimator angle is then determined for the lateral tangential field using the Digitally Reconstructed Radiograph (DRR) capability of the virtual simulation software. The field length  $l$  is known, having been determined clinically at the time of the CT scout imaging. The shift from isocenter 2' of the chest wall volume, to the treatment isocenter 2 is then decomposed into components  $Z$  and  $h$ , respectively. As shown in Figure 2b,  $h$  is simply given by:

$$h = Z \tan \alpha \quad (1),$$

where  $Z = l / 2$ .

By introducing the two shifts  $Z$  and  $h$  into the virtual simulator software, the position of the treatment isocenter may be displayed and verified on the central transverse slice containing the radio-opaque markers. An error in calculation or set-up becomes immediately apparent, as the beam edges will not intersect at the intended position, typically at the level of the radio-opaque markers.

## Results and discussion

Once the patient is placed into the immobilization device on the CT stretcher, the CT scan of the area of interest takes approximately 15 minutes. The CT-based virtual simulation takes another 15 minutes. The position of the treatment isocenter at the matchplane for the tangential and supraclavicular fields is marked on the skin, and the patient is released from the CT-simulator. Our technique is easily adaptable to CT-simulation as there is no tilt-board required for positioning, so that the patient fits comfortably into the CT tunnel. Figure 3 shows for a typical patient the anterior CT scout view used to determine the initial patient position and to identify the matchplane between the two tan-

gential and two supraclavicular fields, typically at the level of the posterior aspect of the 4th rib. The matchplane (AA') is identified with a radio-opaque marker, as are the medial and lateral borders (along BB') and the inferior border of the chest-wall volume.

In Figure 4a the transverse CT-slice taken at the middle of the chest-wall volume at the level of BB' in Figures. 1 and 3 is shown. The intended treatment volume is determined

with a rectangle defined by the medial and lateral radio-opaque markers of Figure 3 and a minimum air gap of 2 cm over all CT slices. The corresponding DRR for the lateral field of Figure 4a is shown in Figure 4b.

The position of the treatment isocenter is determined as follows: first the gantry angle and field width are adjusted on the transverse slice BB' with respect to the planning rectangle, as shown in Figure 4a. Next, based on the

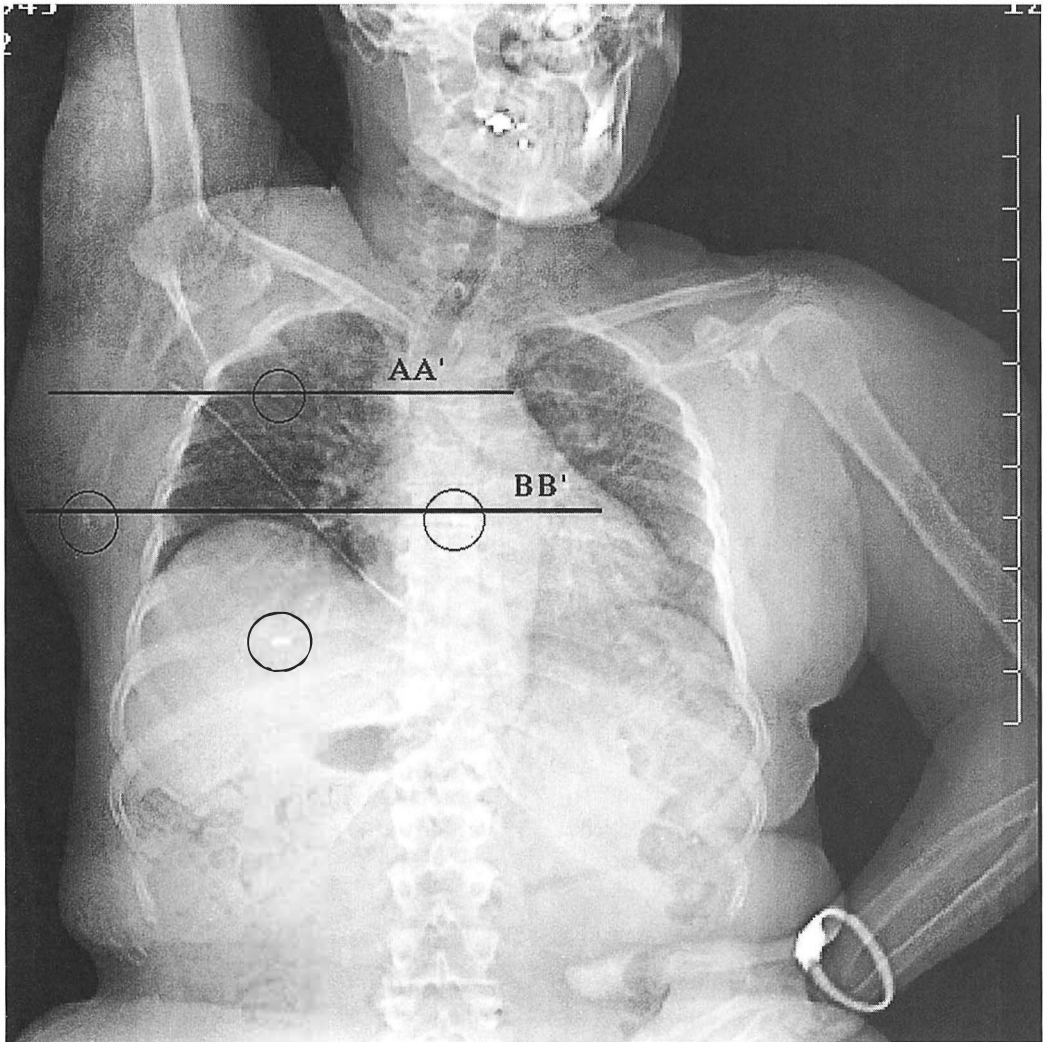


**Figure 3.** An AP CT scout view of the patient used to determine the matchplane (AA' of Figure 1) is shown. The location of the mid-tangential plane (BB' of Figure 1), as well the four radio-opaque markers used to identify the tangential volume are shown circled.

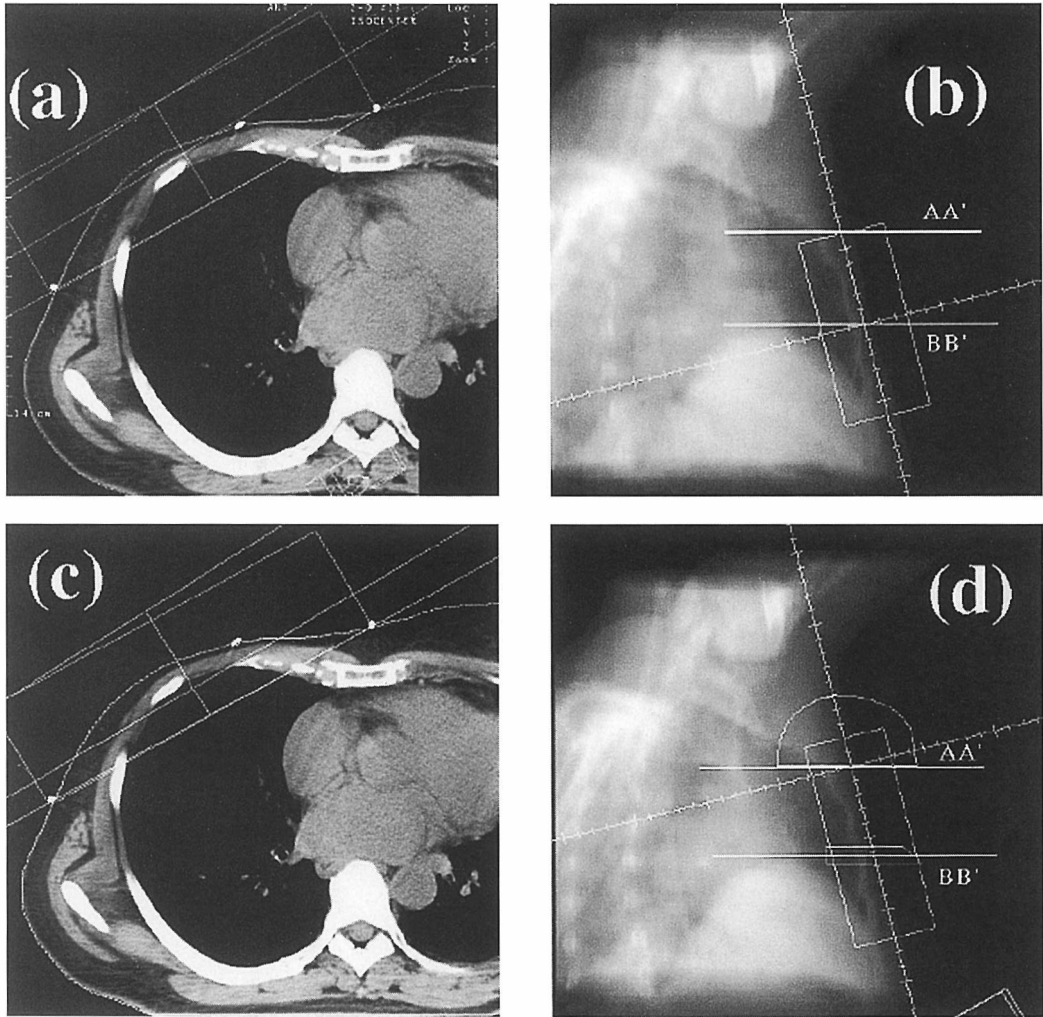


**Figure 4.** Part (a) shows the transverse CT section along the mid-tangential plane (BB' of Figure 1) with the isocenter located on BB', as well as the lateral radio-opaque markers. Part (b) shows the corresponding DRR and beam geometry. The transverse CT section along the mid-tangential plane (BB') with the isocenter located on AA' of Figure 1 is shown in part (c), and the corresponding DRR and beam geometry is shown in part (d).

DRR of Figure 4b, the collimator angle is then chosen with respect to the slope of the chest wall. Equation (1) is then used to determine the position of the treatment isocenter in the matchplane AA'. Figure 4c shows the transverse slice at the level of BB' with the treatment isocenter located on the matchplane AA'. The beam covers the same volume as in Figure 4a, although the fact that this slice is now off-axis is evident, as the isocenter pro-

jects more to the medial edge of the rectangle. The accuracy of the calculations can be assessed by verifying that the medial edge of the beam is still coincident with the medial border of the planning rectangle. Figure 4d shows the DRR for the oblique beam of Figure 4c centered at the matchplane, indicating the position of the semi-circular half-block. The planning rectangle passing through BB' off-axis is also shown.



The apex of the axilla and the supraclavicular region are typically treated with a pair of AP-PA opposed beams as shown in Figure 5. Contouring of structures such as supraclavicular and axillary lymph nodes can be done at a time convenient to the medical staff. The rotating block is lined up along the inferior border of the field on the matchplane AA' at the level of the isocenter, and the lateral borders of the field are defined with respect to

the contoured structures by using the asymmetric jaws. Humeral head shielding is achieved with the use of the MLC, and the AP-PA supraclavicular beams are typically angled 5 degrees off the spinal cord. The inset in Figure 5 shows the two AP-PA beams on the transverse slice at the matchplane. The posterior supraclavicular field may be treated at a fixed SSD to avoid the possibility of patient collision, although this introduces a

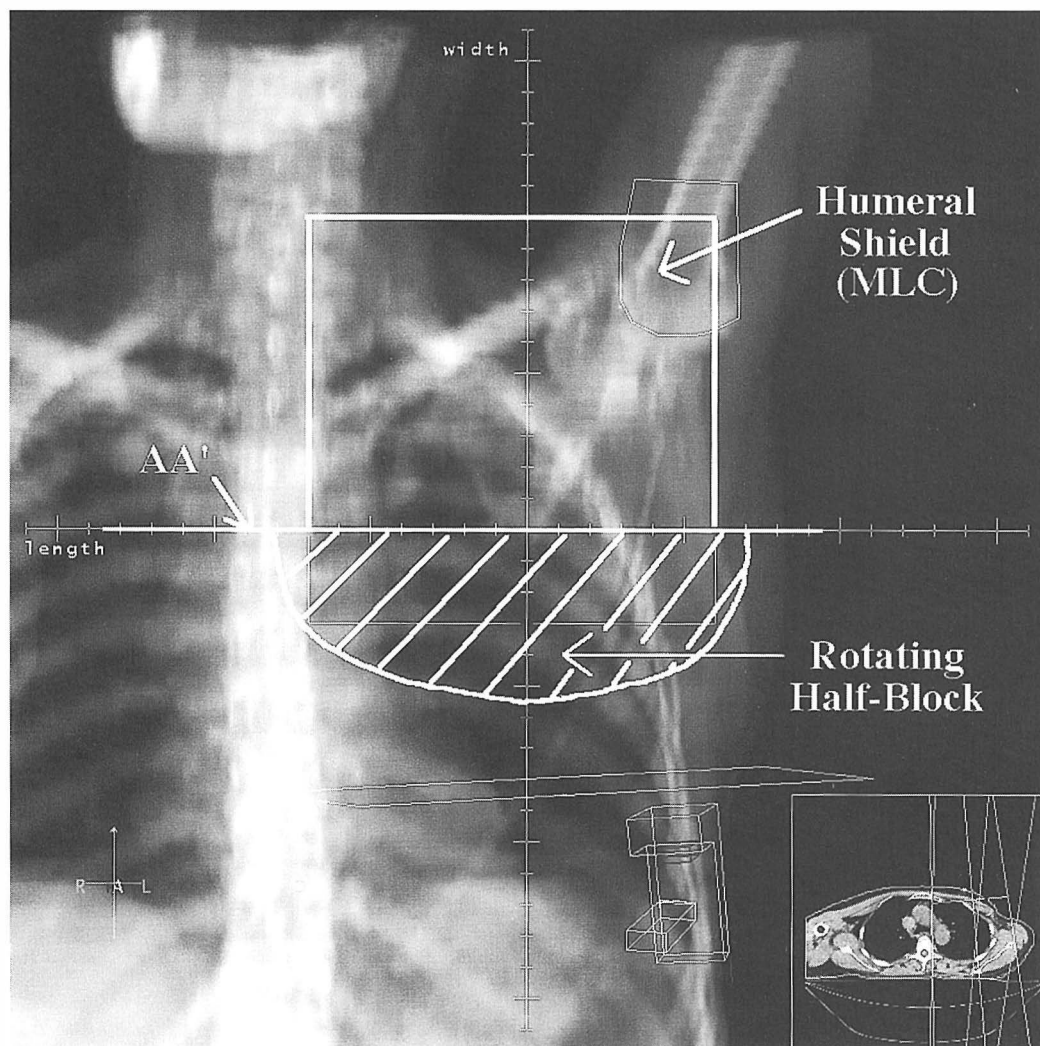


**Figure 5.** A typical anterior supraclavicular field is shown with the rotating block in the horizontal position. The humeral shielding is provided by an MLC. The inset shows the arrangement of both the AP and PA fields at the matchplane AA' of Figure 1.

field shift. DRRs of the supraclavicular and tangential fields are correlated with portal images obtained at the linac.

### Conclusions

The CT-simulated rotating half-block breast technique is a modification of an existing technique which has been in use since 1982. To date 17 patients have been planned and treated with this modified technique since 1997. As the technique is CT planned, there is a considerable reduction in time required by the patient. Previous planning sessions using a conventional fluoroscopic simulator required upwards of one hour, whereas the time required by the patient for CT scanning, virtual simulation and skin marking is on the order of 30 minutes. The decrease in planning time is an important advantage for patients having undergone an axillary node dissection as they often have problems extending their arm for long periods of time. Additionally, the use of CT-based simulation means that information with respect to other organs such as the lung and heart are available.

The current technique improves upon our original rotating half-block technique by taking advantage of the asymmetric jaw capabilities of the linac. By doing so the optimal position for both the tangential and supraclavicular-axillary field pairs can be incorporated in a set-up with a single isocenter which requires no patient movement. The original technique has been reliably used since 1982, and this modified breast technique builds on this experience to more adequately incorporate the capabilities offered by the CT-simulator and asymmetric jaw capabilities of the linac.

### References

1. Podgorsak EB, Gosselin M, Pla M, Kim TH, Freeman CR. A simple isocentric technique for the irradiation of the breast, chest wall and peripheral lymphatics. *Brit J Radiol* 1984; **57**: 57-63.
2. Podgorsak EB, Pla M, Gosselin M, Guerra JJ, Freeman CR. The McGill isocentric breast irradiation technique. *Med Dosim* 1987; **12**: 3-7.
3. Kelly CA, Wang X, Chu JCH, Hartsell WF. Dose to contralateral breast: a comparison of four primary breast irradiation techniques. *Int J Radiat Oncol Biol Phys* 1996; **34**: 727-32.
4. Klein EE, Taylor M, Michaletz-Lorenz M, Zoeller D, Umfleet W. A mono isocentric technique for breast and regional nodal therapy using dual asymmetric jaws. *Int J Radiat Oncol Biol Phys* 1994; **28**: 753-60.
5. Lederer EW, Schwendener H. A calculator based program to optimize the simulation of breast irradiation. *Med Dosim* 1997; **22**: 305-14.
6. Li C, Torigoe EW, Dunning A, Halberg F, Evans R. Three field breast irradiation technique using tangential quarter fields. *Med Dosim* 1994; **19**: 107-10.
7. Marshall M. Three-field isocentric breast irradiation using asymmetric jaws and a tilt board. *Radiat Oncol* 1993; **28**: 228-32.
8. Rosenow UF, Valentine ES, Davis LD. A technique for treating local breast cancer using a single set-up point and asymmetric collimation. *Int J Radiat Oncol Biol Phys* 1990; **19**: 183-8.
9. Siddon RL, Tonnesen GL, Svensson GK. Three-field technique for breast treatment using a rotatable half-beam block. *Int J Radiat Oncol Biol Phys* 1981; **7**: 1473-7.
10. Svensson GK, Bjarngard BE, Larsen RD, Levene MB. A modified three-field technique for breast treatment. *Int J Radiat Oncol Biol Phys* 1980; **6**: 689-94.



## Evaluation of silicon microstrip detectors as X-ray sensors in digital mammography

Tadej Mali<sup>1</sup>, Vladimir Cindro<sup>1</sup>, Marko Mikuž<sup>1,2</sup>,  
Urban Zdešar<sup>3</sup>, and Breda Jančar<sup>4</sup>

<sup>1</sup>Jožef Stefan Institute, <sup>2</sup>University of Ljubljana, Faculty of Mathematics and Physics,  
Departement of Physics, <sup>3</sup>Institute of Occupational Safety, Republic of Slovenia,  
<sup>4</sup>Institute of Oncology, Slovenia

---

**Background.** Position sensitive silicon microstrip detectors are used as sensors for X-rays in a digital imaging system. Silicon detectors were used in an edge-on geometry, yielding high X-ray detection efficiency.

**Material and methods.** A small detector system was assembled and tested. Images of a standard, 5 cm thick phantom were made and evaluated. It is demonstrated, that the use of silicon detectors in mammography could significantly contribute to a reduction of dose. All images were made with skin entrance doses lower than 1 mGy.

**Results and conclusion.** Microcalcifications with a diameter of 350  $\mu\text{m}$  could still be detected with skin entrance doses of about 0.25 mGy. It was demonstrated that a 5 lp/mm pattern can be detected. Image processing should further improve the image quality.

**Key words:** mammography; radiographic image enhancement; silicon

---

### Introduction

Silicon microstrip detectors are position sensitive detectors, intrinsically developed for high precision tracking in particle physics. Recently they were proposed to be used as X-ray detectors in full field digital mammography.<sup>1,2,3</sup>

Their advantage over screen-film is in

higher X-ray detection efficiency, leading to a reduction of the dose required per investigation. In addition, the proposed edge-on geometry suppresses the detection of radiation scattered in the tissue, thus increases the quality of radiographic images. The microstrip detectors operate in a single photon counting mode. If low noise electronics is used for photon counting, the noise in the image is due to statistical fluctuations of the number of detected photons only. However, the expected spatial resolution is somewhat lower than in the case of screen-film.

We have constructed and built a small test system. Several images of phantoms were

Received 14 April 1999

Accepted 21 July 1999

Correspondence to: Tadej Mali, Jožef Stefan Institute, Jamova 39, SI-1000 Ljubljana, Slovenia. Phone: +386 61 177 3832; Fax: +386 61 125 70 74; E-mail: Tadej.Mali@ijs.si

recorded and quality of images was evaluated to check the system performance.

## Material and methods

### Silicon microstrip detectors

The silicon microstrip detector is an array of closely spaced semiconducting p+n junctions - strips. Under reverse bias the p+n junction is depleted of free carriers and every photon interacting in the depleted region generates a current pulse which can be detected. In our system every strip of the detector is bonded to a readout circuit, where a fast preamplifier is followed by a discriminator and 16 bit counter. When the amplified signal exceeds a user defined threshold of the discriminator, the content of the counter is incremented by one.

The absorption length of X-ray photons in silicon in the energy range of interest (around 20 keV) is approximately 1 mm. In 3 mm of silicon as much as  $1 - e^{-3} = 95\%$  of radiation is absorbed. Therefore an active detector depth of a few millimeters is sufficient for high efficiency. Silicon detectors are typically fabricated on 200 to 300  $\mu\text{m}$  thick wafers while the length of strips can be up to several centime-

ters. If the incoming photons hit the detector from the side (Figure 1), the whole length of the strip is available for photon absorption. Practically all incoming radiation is absorbed in the detector and the detection efficiency is very high.<sup>1,2,3</sup> This is called an "edge-on geometry".

However, the active volume of the device cannot extend completely to the edge of the silicon substrate. Surface damage due to cutting would increase the dead current in the device, resulting in an increase of noise, leading to false photon counts.<sup>1</sup> Therefore a guard ring structure around the strips and a safety distance between the structures and cutting edge are required. They represent the inactive volume of the detector, because the photons, absorbed in the region between the cutting edge and the strips, cannot be detected (Figure 1). Detection efficiency ( $\eta$ ) is therefore limited by the thickness of dead volume ( $t$ ) as  $\eta = e^{-\mu t}$ , where  $\mu$  is the absorption coefficient for X-rays in silicon.

In the detector used for this experiment the dead region was 600  $\mu\text{m}$  thick, giving 55% efficiency at 20 keV. Measurements have shown, however, that the dead region could be reduced to values between 100 and 200  $\mu\text{m}$ , giving 90-80% efficiency at 20 keV.<sup>2,4</sup>

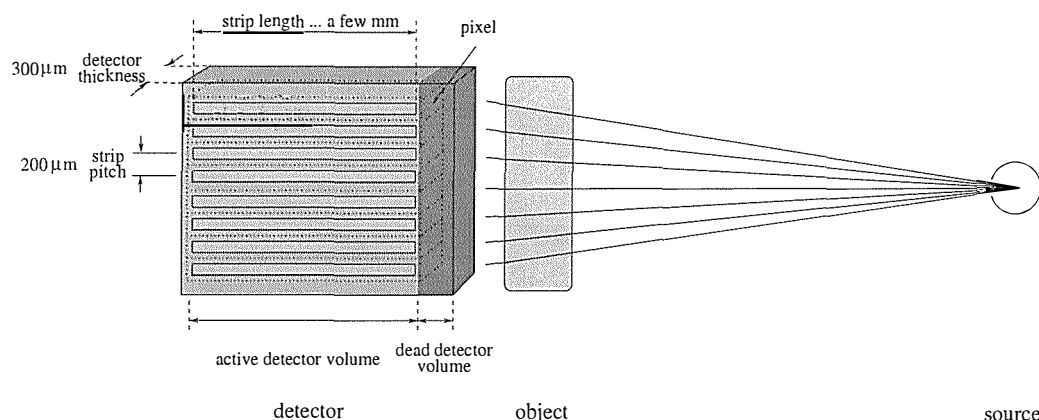


**Figure 1.** Silicon microstrip detector used in the 'edge-on' geometry. X-ray photons emerge from the source on the right hand side of the figure.

In the "edge-on geometry" a single microstrip detector acts as a linear pixel detector (one row of pixels) with the pixel dimensions given by the strip pitch (typically 25 to 200  $\mu\text{m}$ ) and the detector thickness (200 to 300  $\mu\text{m}$ ).

The pixel dimensions of the detector used in our study were  $100 \times 300 \mu\text{m}^2$  and the system consisted of 31 strips of a single microstrip detector, resulting in a row of pixels covering an area of  $3.1 \times 0.3 \text{ mm}^2$ . To obtain 2D images the object was moved in the direction perpendicular to the detector plane and an image of a narrow slice was taken at every step. To minimize the dose received by the patient during imaging, the X-ray beam must be collimated by a slit in such a way, that the radiation field fits the area covered by the detector. This imaging technique is called slit-scanning.

#### *Readout electronics*

The readout electronics of the device is a custom designed readout circuit CASTOR, developed by LEPSI, Strasbourg. CASTOR is a VLSI mixed analog-digital circuit consisting of 32 parallel independent channels, capable of single photon counting. The circuit enables photon counting without false photon hits for photon energies above 12 keV. The circuit and its operation are described in details elsewhere.<sup>5,6,7,8</sup>

#### *Imaging system*

As already mentioned, the silicon detector covered an area of  $3.1 \times 0.3 \text{ mm}^2$ , which is much smaller than objects under investigation. Therefore images of the objects were obtained by scanning the object positioned on a table, moved by a step motor. In this way images of narrow (3.1 mm in  $y$  direction), long (a few cm in  $x$  direction) regions were obtained (Figure 2).<sup>7,8</sup>

The spatial resolution depends on the pixel

size as well as on the sampling rate. The sampling rate in the direction along the detector ( $y$  axis in Figure 2) was determined by the strip pitch. The sampling rate in the direction of scanning ( $x$  axis in Figure 2) was equal to the scanning step and could be varied. Different scanning steps ranging from 50 to 300  $\mu\text{m}$  were used. The position of the detector and X-ray source were kept fixed. The scanning and readout of the device were controlled by a personal computer.

The X-ray source was an X-ray tube with a tungsten electrode operated at 32 kV<sub>p</sub> and the cathode current was 5 mA. The first half value layer of aluminum was measured to be 0.8 mm. Note that neither the operating voltage nor the anode material were optimal for mammography. Optimization of these parameters would result in even better contrast and lower dose.<sup>9</sup> The distance between the source and the phantom was 60 cm.

The entrance skin dose was measured on a 4.5 cm thick PMMA phantom using a thin window parallel plate ionization chamber PS-033 together with a Capintec WK 192 electrometer. The dose rate on the phantom at the given position was  $3.3 \pm 0.3 \text{ mGy/min}$ .

The phantom was a 5 cm thick "CIRS Tissue Equivalent Phantom Model 11". It was made of breast tissue equivalent plastic (30% gland, 70% adipose). Microcalcifications were modeled by irregularly shaped pieces of  $\text{CaCO}_3$  embedded in the phantom.

## **Results**

#### *Images of small, high contrast objects*

Contrast was studied by imaging a group of small, high contrast objects - microcalcifications with a diameter of 350  $\mu\text{m}$ . Their image was obtained at different levels of exposure in order to study the detection limit. The contrast of the objects,  $C$  was defined as:

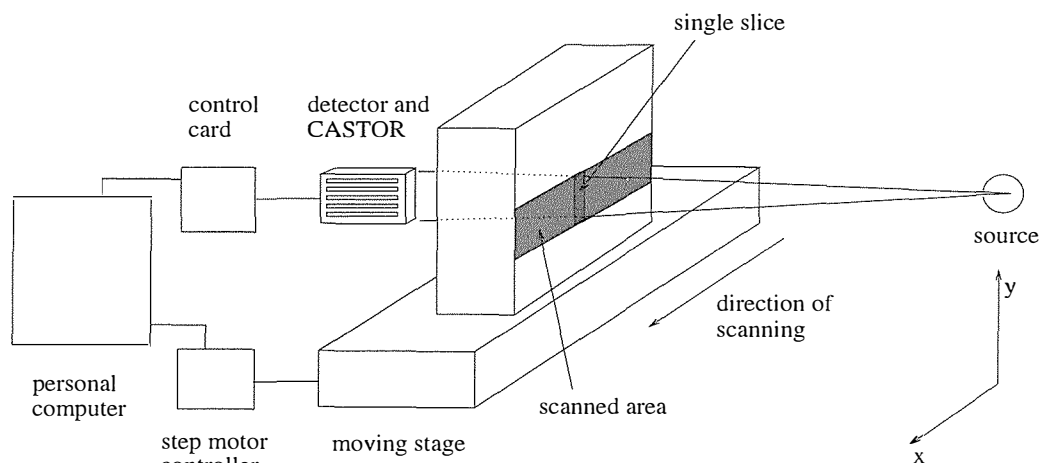


**Figure 2.** X-ray imaging setup. An object was positioned on the moving stage, while the position of the X-ray source and detector was fixed. An image of a narrow (3.1 mm in  $y$  direction) region of the object is obtained by scanning in  $x$  direction.

$$C = \frac{N_1 - N_2}{N_1}$$

where  $N_1$  is the number of detected photons per pixel in the region without microcalcifications (background region) and  $N_2$  is the minimum number of detected photons per pixel in the region, of the microcalcification (signal region).

A detail of the phantom, showing a cluster of microcalcifications is shown in Figure 3. The size of  $y$  axis was given by the number of channels and the strip pitch ( $31 \times 0.1$  mm) and the  $x$  axis was determined by the scanning direction and step size ( $50 \times 0.2$  mm). The image in Figure 3 was obtained at  $1.0 \pm 0.1$  mGy skin entrance dose. Figure 3a shows an image of three microcalcifications, which can be seen as white spots. Figure 3b shows the number of counts per pixel at  $y=2.1$  mm. Because of the amplifier gain variations between channels of the circuit, the number of detected photons varies too (up to 15%). Therefore the average number of hits in the background region of every single channel was calculated and the number of hits was normalized to this average.

The average number of detected photons

per pixel was about 26000 in the background and 24500 in the signal area. Using these numbers the contrast of the microcalcification at position  $x=3.5$ ,  $y=2.1$  was estimated to be

$$C = \frac{26000 - 24500}{26000} \approx 6\%.$$

One expects that the number of detected photons per pixel is given by the Poisson distribution, yielding the standard deviation of  $\sqrt{26000} \approx 160$ . Thus relative fluctuations of the background are about 0.6% in agreement with Figure 3.

The same detail was also observed with different levels of exposure, ranging from 1.0 to 0.16 mGy of skin entrance dose (Figure 4). The microcalcifications are clearly detectable at a dose of about 0.25 mGy and even at lower dose (0.16 mGy) they can still be recognized.

One can see in Figure 3 that the average number of detected photons at  $x>5$  is somewhat lower, which is due to the source intensity variations in time. Since the image is obtained by scanning, the instability of current in the X-ray source is manifested as the background variation along the  $x$  axis. The low exposure rate ( $3.3 \pm 0.3$  mGy/min) result-

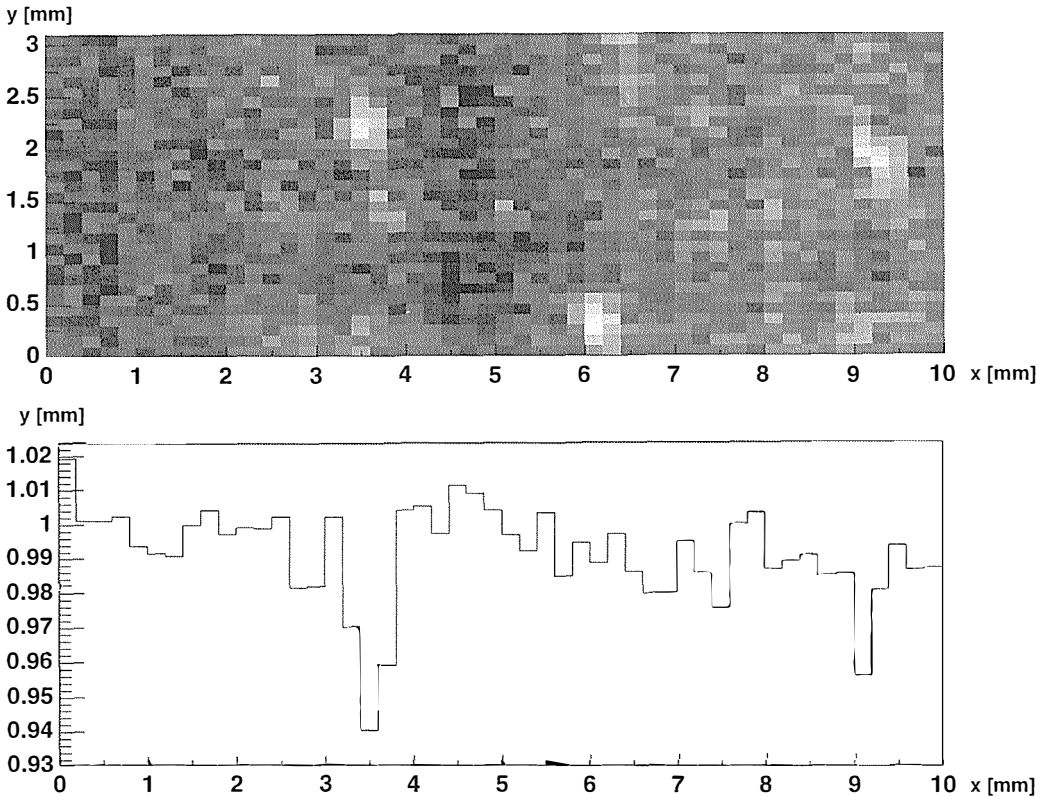


**Figure 3.** Microcalcifications with a diameter of 350  $\mu\text{m}$ . The contrast of the object at  $x=3.5$  is 6%. The image was obtained by scanning in  $x$  direction with a scanning step of 200  $\mu\text{m}$ ; the strip pitch of the detector was 100  $\mu\text{m}$ . The size of pixels is  $300 \times 100 \mu\text{m}^2$  ( $x \times y$  size). The image was obtained at a skin entrance dose of 1 mGy.

In Figure 3a three microcalcifications can be seen at positions: ( $x=6$ ,  $y=0.25$ ), ( $x=3.5$ ,  $y=2.15$ ) and ( $x=9.2$ ,  $y=1.8$ ). A cut through Figure 3a at  $y=2.15$  is shown in Figure 3b.

ed in an exposure time per step of 12 s and a total of 10 min was required for the whole image.

### Spatial resolution

Spatial resolution of the imaging system was studied by imaging a series of high contrast linepairs (lp) with different spatial frequencies. The spatial resolution of the system is characterized by the maximum spatial frequency ( $\nu$ ) of the linepair detail, that can still be detected. Among other it is limited by the size of the pixel which is relatively large -  $100 \times 300 \mu\text{m}^2$ . However, appropriate scanning steps could improve the spatial resolution in

one direction. The spatial resolution is limited by the Nyquist criteria<sup>10</sup>:

$$\nu_{\max} = \frac{1}{2d},$$

where  $\nu_{\max}$  is the maximal spatial frequency, which can be detected when a spatially variable signal is sampled at discrete, equidistant points, separated by distance  $d$ . In the direction along the detector, the maximum space frequency was limited by the strip pitch (100  $\mu\text{m}$ ), yielding the limit of 5 lp/mm in our case. The spatial resolution in the direction of scanning could be varied by changing the size of scanning step. The scanning step used for detection of microcalcifications in Figures 3



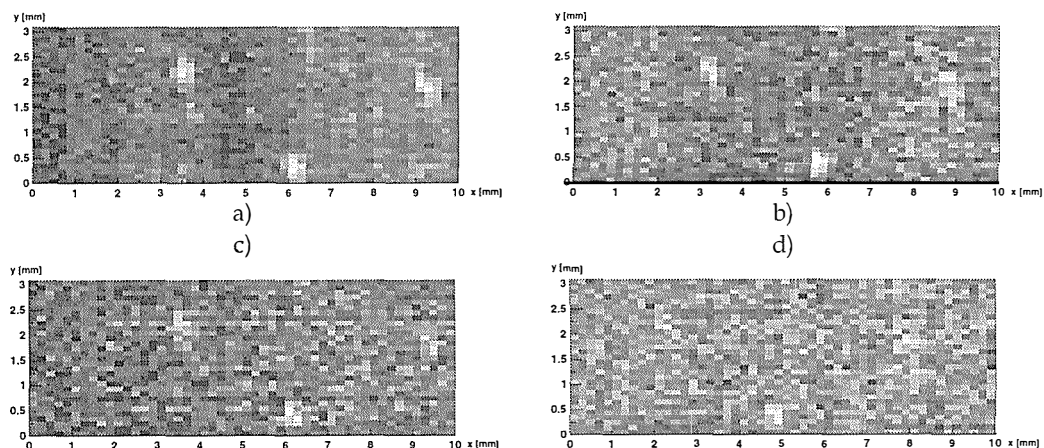


**Figure 4.** Cluster of microcalcifications with diameter of 350  $\mu\text{m}$  imaged at different level of exposure. Figure 4a: 1 mGy, Figure 4b: 0.5 mGy, Figure 4c: 0.25 mGy and Figure 4d 0.16 mGy. Microcalcifications are clearly visible at skin entrance dose of 0.25 mGy and can still be detected at a dose of 0.16 mGy.

and 4 was 200  $\mu\text{m}$ , giving the maximum frequency of 2.5 lp/mm in  $x$  direction. These numbers are significantly worse than in the case of screen-film (above 10 lp/mm). To enable the detection of 10 lp/mm spatial frequency, the strip pitch as well as the scanning step should be scaled down to 50  $\mu\text{m}$ .

In order to demonstrate the spatial resolution improvement by a finer scanning step, we made a measurement with a scanning step of 50  $\mu\text{m}$  (Figure 5), theoretically enabling detection of a 10 lp/mm pattern. Figure 5 shows the phantom detail, where a 5 lp/mm pattern is clearly visible.

However, the size of pixel (300  $\mu\text{m}$  in direction of scanning) distorts the image (Figure 5). Instead of five lines, standing out of the background, the figure shows a plateau and four lines standing out from the background. The plateau is obtained when a pixel covers a white-black-white pattern and the peaks are obtained when a pixel covers a black-white-black pattern of the phantom. Therefore the modulation transfer function (MTF) of the system should be evaluated and further image processing is required to achieve higher spatial resolution without distortion.

## Discussion

The presented results show that the silicon microstrip detectors, used in the edge-on geometry, can be successfully exploited as an X-ray detector in full field digital mammography.

Images of rather large (350  $\mu\text{m}$ ) microcalcifications were obtained. As expected, the noise in the image is mainly due to statistical fluctuations. The estimated contrast of the objects was low: 5-8%. This is mostly attributed to Compton scattering in the object. The contrast could be improved by using a slit, which would reject the Compton scattered photons. In addition the hardness of the radiation used was rather large. The first half value layer of Al was 0.8 mm, while in conventional mammograms it is 0.3-0.4 mm only<sup>12</sup>.

Even with this non optimized geometry (no slits for Compton scattering rejection), large edge cut (600  $\mu\text{m}$ ) and the non ideal radiation source (spectrum too hard), phantom objects were recognized with skin entrance doses lower than 0.25 mGy, which is significantly less than the dose required for the screen-film combination (>3 mGy). It is

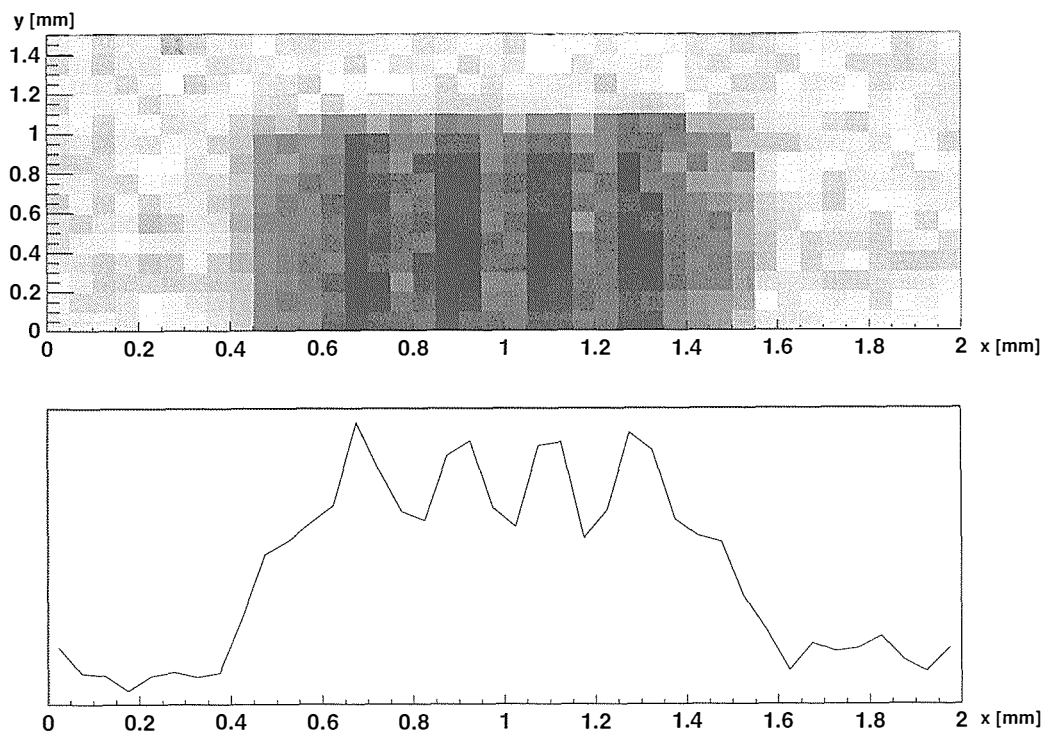


**Figure 5.** The 5 lp/mm detail from the phantom (Fig. 5a). Due to relatively large, finite size of pixel in  $x$  direction ( $300\ \mu\text{m}$ ), the image is distorted. Instead of five lines, separated by  $200\ \mu\text{m}$ , there are four lines separated by  $200\ \mu\text{m}$ , superimposed on a plateau (see text below). A  $x$  direction cut of Figure 5a at  $y = 0.5\ \text{mm}$  is shown in Figure 5b.

expected that the contrast of the images improves, when softer spectrum is used<sup>9</sup>, however at the moment such source is not available to our group.

As our results show, the high efficiency of microstrip detectors can reduce the required dose per investigation. However, when compared to the screen-film, their drawback is a lower spatial resolution. We demonstrated, that 5 lp/mm details (in  $x$  direction) can be detected if an appropriate scanning step is chosen. However, due to the large size of pixels, the signal is distorted (Figure 5).

There are still four main improvements which may be implemented. First, a wider and stacked detection system should be assembled in order to reduce imaging time. Stacking 4 to 6 layers of wider detectors would result in a detector covering the area of approx.  $1\ \text{mm} \times 5\ \text{cm}$ . This would enable imag-

ing of larger objects as well as a reduction of scanning time.

Next, detectors with a lower cutting distance could be used in order to improve efficiency. There are indications that a safe cutting distance could be below  $200\ \mu\text{m}$ , resulting in detector efficiency above 80% at 20 keV. In comparison, the efficiency of the described detector was about 55%.

The pixel size could be reduced by using thinner silicon substrates (e. g.  $200\ \mu\text{m}$ ) and a finer strip pitch (e. g.  $50\ \mu\text{m}$ ) leading to a better spatial resolution.

Finally, the transfer function of the system must be carefully evaluated and this information used for digital image processing, thus reducing the level of distortion due to the finite pixel size.

With the implementation of all these improvements, the dose required for mam-

mography may be reduced for a factor of about five compared to standard screen film.

### References

1. Arfelli F, Barbiellini G, Cantatore G, Castelli E, Cristaudo P, Dalla Palma L et al. Silicon X-ray detector for synchrotron radiation digital radiology. *Nucl Instrum Meth A* 1994; **353**: 366-70.
2. Arfelli F, Barbiellini G, Cantatore G, Castelli E, Cristaudo P, Dalla Palma L et al. Silicon detectors for digital radiography. *Nucl Instrum Meth A* 1995; **367**: 48-53.
3. Beuville E, Cederström B, Danielsson M, Luo L, Nygren D, Oltman E et al. High resolution X-ray imaging using a silicon strip detector. *IEEE T Nucl Sci* 1998; **45**: 3059-63.
4. Mali T, Cindro V, Mikuž M, Richter R. Effect of cutting distance on noise of silicon microstrip detectors. *Proceedings of MIDE 98 conference, Rogaška Slatina, Slovenia*, 1998: 199-204.
5. Comes G, Loddo F, Hu Y, Kaplon J, Ly F, Turchetta R. CASTOR a VLSI CMOS mixed analog-digital circuit for low noise multichannel counting applications, *Nucl Instrum Meth A* 1996; **377**: 440-5.
6. Colledani C, Comes G, Dulinski W, Hu Y, Loddo F, Turchetta R et al. CASTOR 1.0: A VLSI CMOS mixed analog-digital circuit for pixel imaging applications. *Nucl Instrum Meth A* 1997; **395**: 435-42.
7. Mali T. Postavitev sistema za rentgensko slikanje z mikropasovnimi silicijevimi detektorji. [Diplomsko delo], Ljubljana, Univerza v Ljubljani, 1997
8. Mali T, Cindro V, Mikuž M. X-ray imaging with a silicon microstrip detector. *Proceedings of MIDE 97 conference, Gozd Martuljek, Slovenia*, 1997: 347-52.
9. Dance DR. Diagnostic radiology with X-rays. In: Webb S, editor. *The physics of medical imaging*. Bristol and Philadelphia: Institute of Physics Publishing; 1988. p. 20-73.
10. Teuber J. *Digital Image Processing*. London: Prentice Hall; 1993.
11. Zavod RS za varstvo pri delu. Sevalna obremenjenost prebivalstva zaradi medicinske uporabe ionizirajočega sevanja v Republiki Sloveniji, poročilo za leto 1996. Ljubljana, 1997.

## Zdravljenje hiperfunkcijskih ščitničnih nodusov z ultrazvočno vodenim perkutanim vbrizgavanjem etanola - 30-mesečne izkušnje

Brkljačić B, Sučić M, Božikov V, Hebrang A

**Izhodišča.** V članku predstavljamo svojo tehniko perkutane vbrizgavanja etanola in rezultate po 30 mesecih zdravljenja ter jih primerjamo z rezultati, objavljenimi v literaturi.

**Bolniki in metode.** Metodo perkutane vbrizgavanja etanola smo uporabili na 40 bolnikih (37 žensk, 3 moški, starost od 28 do 76 let); od teh je bil pri 35 bolnikih ugotovljen solitaren in scintigrafsko 'vroč' nodus, pri 5 pa toksična nodularna golšavost. Volumen zdravljenih nodusov je znašal od 2,5 do 38 ccm (povprečni volumen  $20,7 \pm 14,1$  ccm). Etanol smo vbrizgavali s prosto roko, ultrazvočno vodeno z barvnim in energijskim Doplerjem, običajno v več ponovljenih postopkih. Celoten volumen vbrizganega etanola je bil 1,5-krat večji od volumna zdravljenega nodusa.

**Razultati.** Postopek je bil tehnično uspešen pri 37 bolnikih (92,5%). Vsi bolniki so tožili zaradi bolečine med vbrizgavanjem, podkožni hematoma je nastal pri 6 bolnikih, prehodna disfonija pa pri 1 bolniku. Daljnoročnih zapletov zdravljenja ni bilo. Pri 36 bolnikih smo 3 do 4 mesece po zdravljenju ocenili uspešnost zdravljenja s scintigrafijo, s hormonskim stanjem ter z ultrazvočno preiskavo. Ozdravljenih je bilo 22 bolnikov (61,1 %), delno ozdravljenih pa 10 bolnikov (27,8 %). Pri 4 bolnikih (11,1 %) so bili rezultati zdravljenja nezadovoljivi, ker je bila po zdravljenju ugotovljena le skromna hormonska remisija. Zadovoljivi rezultati zdravljenja so bili doseženi pri 32/36 bolnikih (88,9 %). V vseh primerih pa se je volumen nodusa močno zmanjšal. Boljše rezultate zdravljenja smo ugotovili pri manjših vozlih in avtonomnih adenomih. Hipertireoza se ni ponovila pri nobenem bolniku.

**Zaključki.** Ultrazvočno vodeno perkutano vbrizgavanje etanola je učinkovita in varna metoda zdravljenja avtonomnih ščitničnih nodusov, ki preprečuje hiperaktivnost nodusov z minimalnimi zapleti zdravljenja. Ti so prehodnega značaja in niso resni, kot jih lahko opazimo po zdravljenju z radioaktivnim jodom ali po operaciji.

## Ultrazvočno diagnosticiranje tujkov v mehkih tkivih pri otrocih

Roić G, Ercegović S, Vlahović T, Čop S, Bumčič I, Višnjić S

**Izhodišča.** Želeli smo ugotoviti uspešnost ultrazvočne metode pri diagnosticiranju tujkov mehkega tkiva.

**Bolniki in metode.** Analizirali smo ugotovitve ultrazvoka pri 14 otrocih s tujkom v strukturah mehkega tkiva. Predhoden klinični potek je bil pri bolnikih različen. Pri 6 bolnikih z rentgensko preiskavo niso našli tujka v telesu in sta bili identifikacija in odstranitev tujka neuspešni. Pri 5 bolnikih z manjšo površinsko prebodno rano sta po nekaj tednih do nekaj mesecev nastopili bolečina in oteklina struktur mehkega tkiva, rentgenski izvid pa je bil pravtako negativen. Pri 2 otrocih je nastal tujkov granulom, ko je bil tujek v mehkem tkivu že nekaj mesecev. Posumili smo na solidni tumor mehkega tkiva. Samo pri 1 bolniku je bil tujek (steklo) viden z rentgensko preiskavo, ni pa bilo mogoče določiti njegovega položaja in globine.

**Rezultati.** S pomočjo ultrazvoka smo natančno lokalizirali in označili položaj tujka v mehkih tkivih neposredno pred kirurškim posegom. Operacijo smo uspešno opravili pri vseh pregledanih bolnikih, le pri bolniku z več tujki je bilo potrebno kirurški poseg ponoviti, da bi odstranili preostale tujke.

**Zaključki.** Z ultrazvokom lahko uspešno dokažemo prisotnost tujka v mehkih tkivih, pa tudi okolišno granulomatozno vnetno reakcijo.

## Ultrazvočna diagnostika obstruktivnega ileusa pri bolniku z Meckelovim divertiklom

Višnar-Perović A in Koren A

**Uvod.** Kljub uporabi modernih slikovnih tehnik, zanesljiva preoperativna ocena Meckelovega divertikla in z njim povezanih komplikacij te redke prirojene anomalije prebavnega trakta mnogokrat ni mogoča.

**Predstavitev.** Predstavljamo primer 25 letnega moškega, pri katerem se je pojavila nenadna bolečina v spodnjem abdomnu desno. Klinično je bil predel občutljiv na palpacijo, ki je pokazala elastično, valjasto strukturo globoko v trebuhu. Blumbergov znak je bil pozitiven, laboratorijske vrednosti pa v mejah normale. Ultrazvok abdomna je ileocekalno pokazal tekočinsko kolekcijo z gosto vsebino, sumljivo za Meckelov divertikel ali duplikacijsko cisto in ileus ozkega črevesa proksimalno od opisane strukture. Nativni rentgenogram stoji je potrdil prisotnost obstrukcijskega ileusa v distalnem delu ozkega črevesa. Kirurški poseg je odkril ileus in kompresijo distalnega dela ozkega črevesa zaradi prisotnosti edematoznega Meckelovega divertikla.

**Zaključek.** Glede na pogosto uporabo ultrazvoka pri oceni akutnega abdomna, bi lahko racionalizirali diagnostični postopek in skrajšali čas do kirurške intervencije, če bi možne zaplete Meckelovega divertikla upoštevali v diferencialni diagnozi.

## Kdaj se pri slikanju trebušne votline s kontrastom pri računalniški tomografiji ojačijo heterogeni vzorci v vranici?

Groell R, Rienmüller R, Uggowitz MM, Kugler C, Stauber RE, Fickert P

**Izhodišča.** V študiji smo ugotavljali, kdaj se pri računalniški tomografiji trebušne votline s kontrastom pri bolnikih z diagnostično potrjeno cirozo jeter in pri osebah brez takšne diagnoze ojačijo heterogeni vzorci v vranici.

**Bolniki in metode.** Računalniško tomografijo trebušne votline z elektronskim snopom smo izvedli po vbrizganem kontrastu pri 195 bolnikih. Vbrizgavanja kontrastnega sredstva smo opravili v skladu s tremi protokoli: protokol 1 (n=132, 120 ml, 2 ml/sek, slikanje po 50 sek), protokol 2 (n=30, 90 ml, 3 ml/sek, slikanje po 10 sek) in protokol 3 (n=33, 50 ml, 5 ml/sek, slikanje po 10 sek). Od teh bolnikov jih je 34 imelo cirozo jeter.

**Rezultati.** Ojačenje heterogenih vzorcev v vranici smo opazili pri 77% bolnikov (protokol 2) in pri 65% bolnikov (protokol 3) z zdravimi jetri, ter pri 23% (protokol 2) in 20% (protokol 3) bolnikov s cirozo jeter. Ojačani heterogeni vzorci so postali vidni med 14 in 48 sek po vbrizganju kontrasta. Pri nobeni od skupin bolnikov in ob nobenem protokolu se ojačenje ni pojavilo kasneje kot v 48 sek po vbrizgu kontrastnega sredstva. Pri treh bolnikih smo odkrili lezije v vranici (hemangiom, limfom, metatstaze), ki so ostale vidne tudi 50 sek po vbrizgu kontrasta.

**Zaključki.** Iz rezultatov je razvidno, da ojačenje heterogenih vzorcev nastopi v času 50 sek po začetku vbrizgavanja kontrastnega sredstva. V enakem času nastopi ojačenje heterogenih vzorcev tudi v primerih ko kontrast še vbrizgavamo.

## Pomen priskave s F-18-FDG PET pri bolnikih z metastazami v vratnih bezgavkah neznanega izvora

Bohuslavizki KH, Klutmann S, Buchert R, Kröger S, Werner JA, Mester J, Clausen M

**Izhodišča.** Čeprav imamo danes več možnosti slikovne diagnostike, predstavljajo metastaze neznanega izvora še vedno velik diagnostičen problem. Zato je bil namen naše studije opredeliti pri teh bolnikih pomen preiskave s fluor-18-fluorodeoksiglukoza (F-18-FDG) in pozitronsko emisijsko tomografijo (PET)

**Material in metode.** Obravnavali smo 28 bolnikov, starih od 39 do 84 let, od katerih jih je imelo 24 v vratnih bezgavkah metastaze skvamoznoceličnega karcinoma, 4 pa metastaze nediferenciranega karcinoma. Pri vseh bolnikih smo naredili klinični pregled, ultrazvočno preiskavo vratu in CT glave. Ker nismo uspeli odkriti primarnega tumorja, smo se odločili za preiskavo s PET. Vsem bolnikom smo intravenozno aplicirali 370 MBq F-18-FDG, po 60. minutah pa smo naredili tomografski posnetek celega telesa z aparatom ECAT EXACT 47 (921) (Siemens, CTI). Lezije, ki smo jih odkrili s PET-om, smo skušali pri vseh bolnikih oceniti tudi histološko ali s CT/MRI.

**Rezultati.** Pri 16 od 28 bolnikov je PET pokazal žarišča kopičenja radiofarmaka, ki so ustrezala potencialnim primarnim ležiščem tumorja; pri 7 bolnikih v pljučih, pri 5 v tonzilah, po 1 bolnik pa je imel takšno žarišče v submandibularni žlezi, v nazofarinksu, v larinksu in v bazi jezika. Primarni tumor smo uspeli potrditi pri 9 od omenjenih 16 bolnikov; od tega 5 v pljučih, po enega pa v tonzili, v nazofarinksu, larinksu in v bazi jezika. Tako je pri 6 od 16 bolnikov preiskava dala lažno pozitiven rezultat, največkrat v tonzilah, to je pri 3 bolnikih, en bolnik pa je odklonil nadaljnjo evaluacijo, s katero bi potrdili ali ovrgli rezultat preiskave s PET. Pri preostalih 12 od 28 bolnikov preiskava PET ni pokazala za primarni tumor sumljivih lezij.

**Zaključki.** S preiskavo F-18-FDG PET lahko primarni tumor odkrijemo približno pri tretjini bolnikov z metastazami na vratu neznanega izvora (CUP-sindrom), zato lahko omenjeno preiskavo pri teh bolnikih smatramo za pomembno pomoč pri izbiri ustreznega zdravljenja.

## Krvni obtok v ledvičnih transplantatih pri bolnikih z akutno tubularno nekrozo

Huić D, Grošev D, Bubić-Filipi L, Crnković S, Dodig D, Poropat M, Puretić Z

**Izhodišča.** Zaradi nasprotujočih se podatkov smo so odločili za raziskavo ledvičnega krvnega obtoka (RBF) v ledvičnih transplantatih pri bolnikih z akutno tubularno nekrozo (ATN).

**Bolniki in metode.** V štirih letih smo opravili 179 preiskav s Tc-99m pertehnetatom in I-131-OIH na 60 bolnikih (od teh je bilo 31 žensk in 29 moških, njihova srednja starost je bila 37 let in sicer od 11 do 62 let, presajenih je bilo 42 kadavrskih ledvic in 18 ledvic od živih darovalcev sorodnikov, kontrolno sledenje je v povprečju trajalo 21 mesecev). Krvni obtok smo izračunali iz časovnih krivulj prvega pretoka skozi ledvice in aorto in ga izrazili v odstotkih iztisnega volumna krvi iz srca (RBF/CO).

**Rezultati.** V 53 preiskavah bolnikov z ATN je bil povprečni RBF/CO precej nižji kot pri 60 bolnikih z normalnim delovanjem transplantirane ledvice ( $6,5 \% \pm 3,4 \%$ ;  $11,4 \% \pm 3,4 \%$ ;  $p=9,6 \times 10^{-12}$ ) in enak srednjim vrednostim 49 preiskav bolnikov z akutnim zavračanjem transplantirane ledvice ter prav tako enak 17 preiskavam bolnikov z ATN in z akutnim zavračanjem transplantirane ledvice ( $7,3 \% \pm 3,4 \%$ ;  $5,8 \% \pm 2,5 \%$ ;  $p=0,005$ ). Pri bolnikih z ATN so bile vrednosti RBF/CO v sorazmerju z vrednostjo serumskega kreatinina (KS<500 mmol/l -  $8,0 \% \pm 3,0 \%$ ; KS >1000 mmol/l -  $5,2 \% \pm 2,2 \%$ ;  $p<0,05$ ) in z renogrami z I-131 OIH (delno izločanje OIH iz ledvičnega parenhima med preiskavo -  $7,0 \% \pm 3,5 \%$ ; brez izločanja -  $5,1 \% \pm 2,2 \%$ ;  $p=<0,005$ ).

**Zaključek.** Krvni obtok v transplantiranih ledvicah se očitno znatno zmanjša tako pri ATN kot pri akutnem zavračanju in je značilno odvisen od delovanja transplantirane ledvice.



## Kriokirurgija mišjih tumorjev SA-1 v kombinaciji z obsevanjem

Fras AP, Kranjc S, Čemažar M, Serša G

Namen naše raziskave je bil določiti protitumorsko delovanje kriokirurgije kot samostojne terapije in v kombinaciji z obsevanjem. Kriokirurgija podkožnih fibrosarkomskih tumorjev SA-1, ki smo jih nasadili v A/J miši, je bila učinkovita terapija. Zaostanek v rasti tumorjev po 5 minutnem zamrzovanju s tekočim dušikom je bil  $10.3 \pm 3.8$  dni. Časovno krajše zamrzovanje je bilo manj učinkovito, a odvisno od časa zamrzovanja. Pri kombinirani terapiji smo tumorje najprej zamrzovali 3 minute in jih po 5 minutah obsevali z 10 Gy, oziroma najprej obsevali in jih po 5 minutah zamrzovali. Protitumorsko delovanje je bilo odvisno od vrstnega reda kombinirane terapije, tumorji ki smo jih obsevali pred zamrzovanjem so rastle počasneje, kot tisti, ki smo jih obsevali po zmrzovanju. Kljub temu, da nekatere študije poročajo o povečani občutljivosti celic na obsevanje po kriokirurgiji, so naši rezultati pokazali, da te občutljivosti na sevanje *in vivo* ne moremo vedno pričakovati, ter da so v protitumorsko delovanje kombinirane terapije verjetno vpleteni tudi drugi mehanizmi, ki prispevajo k poškodbam zaradi obsevanja, če le-temu sledi kriokirurgija.

## Obsevanje dojke s prilagojeno tehniko polovičnega zapiranja polja in z uporabo CT simulatorja

Evans MDC, Benk V, Freeman C, Gosselin M, Olivares M, Podgorsak EB

**Izhodišča.** Zadnji dve desetletji so številni avtorji predlagali vrsto različnih načinov obsevanja dojk in regionalnih bezgavk. V naši ustanovi od leta 1982 uporabljamo izocentrično tehniko s polovičnim zapiranjem polja; novejša uporaba CT simulatorja in linearnega pospeševalnika z asimetričnimi čeljustmi sekundarnega kolimatorja pa je spodbudila prizadevanja za izboljšanje tehnike obsevanja z vključitvijo nove tehnologije v načrtovanje obsevanja in v samo izvedbo obsevanja.

**Material in metode.** Naša tehnika obsevanja ne zahteva premikanja obsevalne mize ali premikanje bolnika pri obsevanju dveh zaporednih polj. Omogoča natančno in ponovljivo združevanje tangencialnega polja na prsni steni in supraklavikularnega polja. Pred obsevanjem bolnico slikamo na CT simulatorju, s pomočjo programa za virtualno simulacijo pa določimo in narišemo na kožo bolnice optimalni izocenter, ki je skupen vsem obsevalnim poljem.

**Rezultati.** Od leta 1997 smo s prilagojeno tehniko obsevali dojke pri 17 bolnicah. Čas dela na simulatorju smo zmanjšali na 30 minut. Namestitev bolnice na obsevalno mizo linearnega pospeševalnika je bila enostavna, prav tako je bila enostavna, kljub polovičnemu zapiranju polj, izvedba obsevanja, saj so imela vsa polja isti izocenter. Oblikovanje polj smo izvedli z dinamičnimi klini, uporaba asimetričnih čeljusti na sekundarnem kolimatorju pa je omogočila optimalen izocenter, ki je bil skupen vsem obsevalnim poljem.

**Zaključki.** Načrtovanje obsevanja z opisano tehniko temelji na virtualni simulaciji, obsevanje pa omogoča 6 MV linearni pospeševalnik, ki je izpopolnjen z rotacijskim sistemom polovičnega zapiranja polj, z asimetričnimi čeljustmi na sekundarnem kolimatorju, z dinamičnimi klini in z večlistnim kolimatorjem. Takšna tehnika obsevanja je zelo uporabna, omogoča natančno obsevanje dojke in regionalnih bezgavk pri isti bolnici, prilagoditev sodobnega linearnega pospeševalnika pa ni težavna.

## Ovrednotenje silicijevih mikropasovnih detektorjev kot rentgenskih senzorjev za digitalno mamografijo

Mali T, Cindro V, Mikuž M, Zdešar U, Jančar B

**Izhodišče.** Pozicijsko občutljive silicijeve detektorje smo uporabili kot senzorje rentgenskih žarkov v sistemu za digitalno rentgensko slikanje. Silicijevi detektorje smo uporabili v t. i. geometriji "na rob", kjer rentgenski žarki zadenjejo detektor s strani, zato lahko dosežemo visok izkoristek detekcije - preko 80% pri energiji rentgenskih fotonov 20 keV.

**Material in metode.** Sestavili in testirali smo majhen sistem. Posneli smo slike standardnega, 5 cm debelega fantoma in jih ovrednotili.

**Rezultati in zaključki.** Silicijevi detektorji lahko znatno prispevajo k zmanjšanju doze pri mamografskih preiskavah. Vse slike so bile posnete pri vstopni kožni dozi do 1 mGy. Mikrokalcifikacije s premerom 350  $\mu\text{m}$  so še vedno vidne z vstopno kožno dozo 0.25 mGy. Pokazali smo, da z našim sistemom uspešno zaznamo testni vzorec črt z gostoto 5 parov na mm. Z nadaljno digitalno obdelavo lahko še dodatno izboljšamo kvaliteto slik.

## Notices

*Notices submitted for publication should contain a mailing address, phone and/or fax: number and/or e-mail of a Contact person or department.*

### Immunotherapy of cancer

*September 20-23, 1999*

The ESO training course will take place in Moscow, Russia.

**Contact** ESO Office for Russia and Community of Independent States, Blokhin Cancer Research Centre, L. Demidov, Kashirskoye shosse 24, 115478 Moscow, Russia; or call +70 95 3241184/3241504; or fax +70 95 3241504

---

### Gynecological oncology

*September 23- 24, 1999*

The ESO course on the occasion of the "7th Biennial Meeting of the International Gynecological Cancer Society" will take place in Rome, Italy.

**Contact** Triumph P.R. s.r.l., Via Proba Petronia 3, 00136 Rome, Italy; or fax +39 0639735195; or e-mail triumph@tin.it

---

### Gynecological oncology

*September 26-30, 1999*

The "7th Biennial Meeting of the International Gynecological Cancer Society" will be offered in Rome, Italy.

**Contact** Triumph P.R. s.r.l., Via Proba Petronia 3, 00136 Rome, Italy; or fax +39 0639735195; or e-mail triumph@tin.it

---

### Radiation oncology

*September 26-30, 1999*

ESTRO course on Evidence Based Radiation Oncology will be held in Bratislava, Slovakia.

As a service to our readers, notices of meetings or courses will be inserted free of charge.

Please sent information to the Editorial office, Radiology and Oncology, Vrazov trg 4, 1000 Ljubljana, Slovenia.

**Contact** ESTRO office, Av. E. Mounierlaan, 83/4, B-1200 Brussels, Belgium; or call +32 7759340; or fax +32 2 7795494; or e-mail info@estro.be; web: <http://www.estro.be>

---

### Breast cancer

*September-October, 1999*

The ESO training course will take place in Skopje, Macedonia.

**Contact** ESO office for Balkans and Middle East, N. Pavlidis, E. Andreopoulou Medical School, Department of Medical Oncology, University Hospital of Ioannina, 45110 Ioannina, Greece; or call +30 651 99394 or +30 953 91083; or fax +30 651 97505

---

### Surgical oncology

*October, 1999*

The ESO training course "Conservative Surgery and Combined Treatment" will take place in Sofia.

**Contact** ESO office for Balkans and Middle East, N. Pavlidis, E. Andreopoulou Medical School, Department of Medical Oncology, University Hospital of Ioannina, 45110 Ioannina, Greece; or call +30 651 99394 or +30 953 91083; or fax +30 651 97505

---

### Head and neck

*October 1-2, 1999*

The first International Chicago Symposium on Malignancies of the Chest and Head/Neck will take place in Chicago, IL, USA.

**Contact** Center for Continuing Medical Education, Chicago University, 950 East 61st Street, Chicago, IL 60637, USA; or call +1 773 402 1056; or fax: +1 773 702 1736; or e-mail marlen@delphi.bsd.uchicago.edu

---

### Radiation oncology and biology

*October 4-6, 1999*

Radiation Oncology and Biology Conference will be held on Bali, Indonesia.

**Contact** ISRO secretariat, Av. E. Mounier 83/12, 1200, Brussels, Belgium; or call +32 2 7759342; or fax +32 2 7795494; e-mail ISRO@estro.be

---

### Organ sparing treatment in oncology

*October 6-8, 1999*

The ESO training course will take place in Bled, Slovenia.

**Contact** ESO office for Central and Eastern Europe, Ms. Dagmar Just, Ärztekammer für Wien, Fortbildungssreferat, Weihburggasse 10-12, 4<sup>th</sup> floor, 1010 Vienna, Austria; or call +43 1 51501262; or fax +43 1 51501200; or e-mail just@aekwien.or.at

---

### Medical oncology

*October 7-9, 1999*

The ESO training course will take place in Milan, Italy.

**Contact** ESO Office, Viale Beatrice d'Este 37, 20122 Milan, Italy; or call +39 0258317850; or fax +39 0258321266; or e-mail esomi@tin.it

---

### Haematology and oncology

*October 9-13, 1999*

The Annual Meeting of German and Austrian Association of Haematology and Oncology will be offered in Jena, Germany.

**Contact** Dr.G.H. Sayer, Klinikum der Friedrich-Schiller-Universität Jena, Klinik für Innere Medizin II, 07747 Jena, Germany; or call +49 3641 639100; or fax +49 3641 639219; or e-mail HSAY(polkim.med.uni-jena.de); or see internet <http://www.weimar-cs.de/kuk/-dgho.htm>

---

### Radiotherapy

*October 10-13, 1999*

ESTRO meeting on Radiation for Benign Disease: Current Status and Possible Perspectives will take place in Brussels, Belgium.

**Contact** ESTRO office, Av. E. Mounierlaan, 83/4, B-1200 Brussels, Belgium; or call +32 7759340; or fax +32 2 7795494; or e-mail info@estro.be; or see internet <http://www.estro.be>

---

### Prostate cancer

*October 12-16, 1999*

The ESO training course "Prostate pathology - Oncology" will take place in Ioannina, Greece.

**Contact** ESO office for Balkans and Middle East, N. Pavlidis, E. Andreopoulou Medical School, Department of Medical Oncology, University Hospital of Ioannina, 45110 Ioannina, Greece; or call +30 651 99394 or +30 953 91083; or fax +30 651 97505

---

### Cancer management

*October 13-15, 1999*

The ESO training course "Innovations in Cancer Management" will take place in Alexandria; Egypt.

**Contact** ESO office for Balkans and Middle East, N. Pavlidis, E. Andreopoulou Medical School, Department of Medical Oncology, University Hospital of Ioannina, 45110 Ioannina, Greece; or call +30 651 99394 or +30 953 91083; or fax +30 651 97505

---

### Bladder cancer

*October 15-16, 1999*

The ESO training course will take place in Milan, Italy.

**Contact** ESO Office, Viale Beatrice d'Este 37, 20122 Milan, Italy; or call +39 0258317850; or fax +39 0258321266; or e-mail esomi@tin.it

---

### Leukaemia lymphoma

*October 16-20, 1999*

The ESO training course "Athens Postgraduate leukaemia lymphoma" will take place in Athens, Greece.

**Contact** ESO office for Balkans and Middle East, N. Pavlidis, E. Andreopoulou Medical School, Department of Medical Oncology, University Hospital of Ioannina, 45110 Ioannina, Greece; or call +30 651 99394 or +30 953 91083; or fax +30 651 97505

---

### Radiobiology

*October 17-21, 1999*

ESTRO course on Basic Clinical Radiobiology will be offered in Gdansk, Poland.

**Contact** ESTRO office, Av. E. Mounierlaan, 83/4, B-1200 Brussels, Belgium; or call +32 7759340; or fax +32 2 7795494; or e-mail info@estro.be; web: <http://www.estro.be>

---

### Melanoma

*October 25-26, 1999*

The ESO training course will take place in Milan, Italy.

**Contact** ESO Office, Viale Beatrice d'Este 37, 20122 Milan, Italy; or call +39 0258317850; or fax +39 0258321266; or e-mail [esomi@tin.it](mailto:esomi@tin.it)

Milan, Italy; or call +39 0258317850; or fax +39 0258321266; or e-mail [esomi@tin.it](mailto:esomi@tin.it)

---

### Ovarian cancer

*October 25-27, 1999*

The ESO training course "Ovarian Cancer and Trophoblastic Disease" will take place in Moscow, Russia.

**Contact** ESO Office for Russia and Community of Independent States, Blokhin Cancer Research Centre, L. Demidov, Kashirskoye shosse 24, 115478 Moscow, Russia; or call +70 95 3241184/3241504; or fax +70 95 3241504

---

### Radiation therapy

*October 31- November 3, 1999*

ASTRO Annual meeting will be held in San Antonio, TX, USA.

**Contact** American Society for Therapeutic Radiology and Oncology Office, 1891 Preston White Drive, Reston, VA 20191, USA.

---

### Skin cancer and melanoma

*November, 1999*

The ESO training course will take place in Tirana, Albania.

**Contact** ESO office for Balkans and Middle East, N. Pavlidis, E. Andreopoulou Medical School, Department of Medical Oncology, University Hospital of Ioannina, 45110 Ioannina, Greece; or call +30 651 99394 or +30 953 91083; or fax +30 651 97505

---

### Geriatric oncology

*November 3, 1999*

The ESO training course will take place in Tel Aviv, Israel.

**Contact** ESO office for Balkans and Middle East, N. Pavlidis, E. Andreopoulou Medical School, Department of Medical Oncology, University Hospital of Ioannina, 45110 Ioannina, Greece; or call +30 651 99394 or +30 953 91083; or fax +30 651 97505

---

### Antiangiogenic therapy

*November 8-10, 1999*

The ESO conference "Biological Basis for Antiangiogenic Therapy" will take place in Milan, Italy.

**Contact** ESO Office, Viale Beatrice d'Este 37, 20122

---

### Sentinel node

*November 25-26, 1999*

The ESO training course will be offered in Milan, Italy.

**Contact** ESO Office, Viale Beatrice d'Este 37, 20122 Milan, Italy; or call +39 0258317850; or fax +39 0258321266; or e-mail [esomi@tin.it](mailto:esomi@tin.it)

---

### Breast cancer

*November 26-27, 1999*

The ESO training course will take place in Nicosia, Cyprus.

**Contact** ESO office for Balkans and Middle East, N. Pavlidis, E. Andreopoulou Medical School, Department of Medical Oncology, University Hospital of Ioannina, 45110 Ioannina, Greece; or call +30 651 99394 or +30 953 91083; or fax +30 651 97505

---

### Breast cancer

*December, 1999*

The ESO training course "Breast Reconstructive and Cancer Surgery" will take place in Paris, France.

**Contact** ESO Office, Viale Beatrice d'Este 37, 20122 Milan, Italy; or call +39 0258317850; or fax +39 0258321266; or e-mail [esomi@tin.it](mailto:esomi@tin.it)

---

### Cancer and genetics

*December 2-4, 1999*

The ESO training course will take place in Athens, Greece.

**Contact** ESO office for Balkans and Middle East, N. Pavlidis, E. Andreopoulou Medical School, Department of Medical Oncology, University Hospital of Ioannina, 45110 Ioannina, Greece; or call +30 651 99394 or +30 953 91083; or fax +30 651 97505

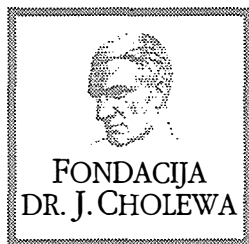
---

### Lung cancer

*December 3-4, 1999*

International Symposium on Staging of Lung Cancer: New Perspectives for the New Century will take place in Madrid, Spain.

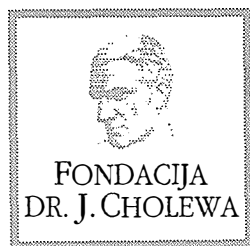
**Contact** Dr. A. López Encuenera, Servicio Neumología, Hospital Universitario 12 de Octubre, Carretera Andalucía 5.4, 284041 Madrid, Spain; or call +3491 3908335; or fax +34 91 39083558



FONDACIJA "DOCENT DR. J. CHOLEWA"  
JE NEPROFITNO, NEINSTITUCIONALNO IN NESTRANKARSKO  
ZDRUŽENJE POSAMEZNIKOV, USTANOV IN ORGANIZACIJ, KI ŽELIJO  
MATERIALNO SPODBUJATI IN POGLABLJATI RAZISKOVALNO  
DEJAVNOST V ONKOLOGIJI.

MESESNELOVA 9  
1000 LJUBLJANA  
TEL 061 15 91 277  
FAKS 061 21 81 13

ŽR: 50100-620-133-05-1033115-214779



## Activity of "Dr. J. Cholewa" Foundation for Cancer Research and Education - A Report for the Second Quarter of 1999

In the second quarter of 1999 the „Dr. J. Cholewa” Foundation for cancer research and education continued with its activities, as already outlined in previous reports. The activity of the Foundation is slowly adapting itself to the summer recess. World-wide financial crisis left its impact on the willingness of the donors to contribute to the Foundation, and the need for the reassessment of the strategies concerning financial contributions from private and constitutional donors is therefore obvious, making the summer recess even more welcome.

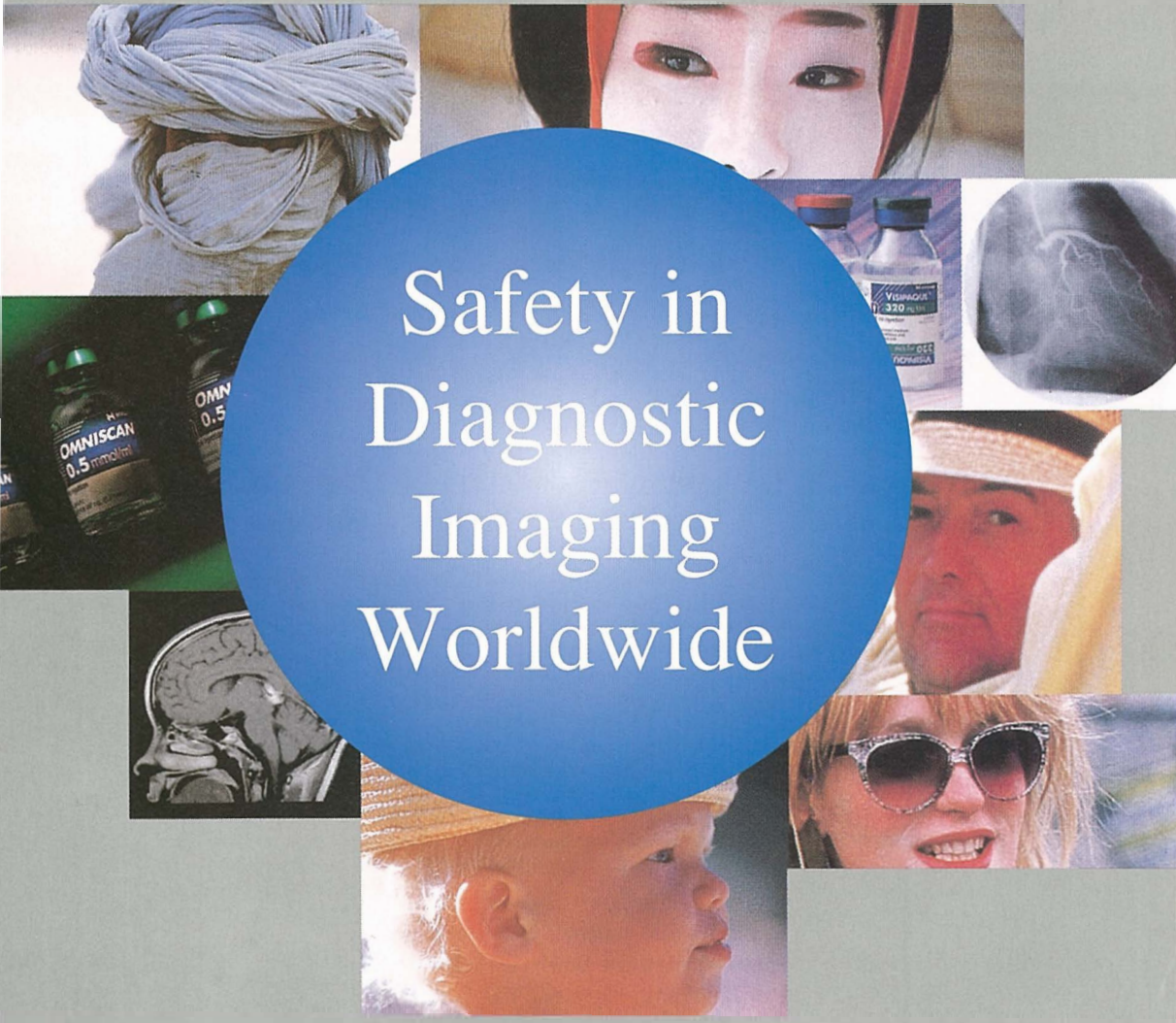
Despite the problems mentioned in the first paragraph, the Foundation continues to support the regular publication of „Radiology and Oncology” international scientific journal, and the regular publication of the „Challenge ESO Newsletter”, the newsletter of the European School of Oncology from Milan, Italy. Both medical journals mentioned are edited and published in Ljubljana, Slovenia. It is also worth mentioning the educational grants awarded to three oncologists for their training in foreign countries, as well as the support the Foundation granted to the Organising Committee of the 1st. Slovenian Congress of Surgery, held in the city of Maribor. All of this in addition to the grants and support mentioned before in the previous reports in „Radiology and Oncology” journal.

In the plan for the activity of the Foundation submitted to the members of its Executive board seven major points were presented. As such, the proposal also constitutes a viable framework for the activity of the Foundation for years to come. Besides editorial activity mentioned above, the Foundation will additionally concentrate on bestowing educational and study grants for the research work in oncology. Some of this research and educational work will probably be carried out in the clinical and research facilities in Ljubljana. Contrary to the research and education performed abroad that will continue to be financed by the Foundation, this grants will be of shorter duration of one or two months, thus benefiting a larger number of applicants in a shorter period of time. The Foundation will also try to sponsor a larger number of educational meetings and congresses in Slovenia than until recently, especially those with oncology as the main subject. In addition to those mentioned above, special attention will continue to be given to the requests coming from the regions of Slovenia outside Ljubljana, and the Foundation will especially try to help in the process of choosing and financing the visits of renowned lecturers on such meetings. The Foundation will also continue to provide grants for the participation of Slovenian oncologists and others interested in this subject on various educational meetings organised by the European School of Oncology from Milan, Italy, thus enhancing the collaboration with this internationally recognised educational and research organisation.

The Foundation continues to pursue its stated goals, as outlined at the meetings of its Executive and Advisory Boards.

Borut Štabuc, MD, PhD  
Andrej Plesničar, MD  
Tomaž Benulič, MD





# Safety in Diagnostic Imaging Worldwide

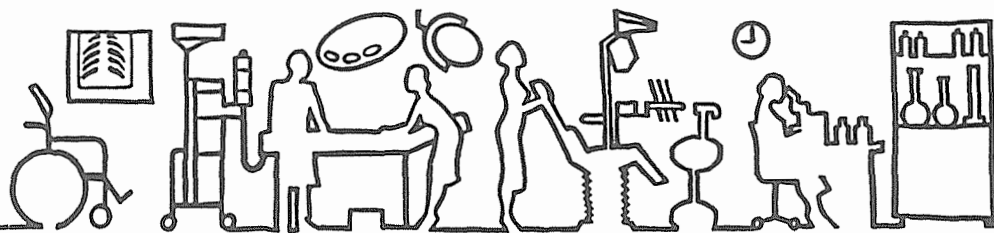
*Nycomed Imaging is proud  
of its role in providing  
for the early, accurate  
diagnosis of disease,  
thus improving patients'  
quality of life and  
prospect for effective  
treatment. The company is  
committed to the continuous  
development of innovative  
imaging product to enhance  
diagnostic procedures.*

**ZASTOPA**  
**HIGIEA d.o.o., Trzin**  
tel.: (061) 1897 225  
fax: (061) 1897 226

**Nycomed**  
**Amersham**

**DISTRIBUCIJA**  
**SALUS d.d. Ljubljana**  
tel.: (061) 1899 100  
fax: (061) 1681 420


# **SANOLABOR**



## **Pri nas dobite vse za rentgen!**

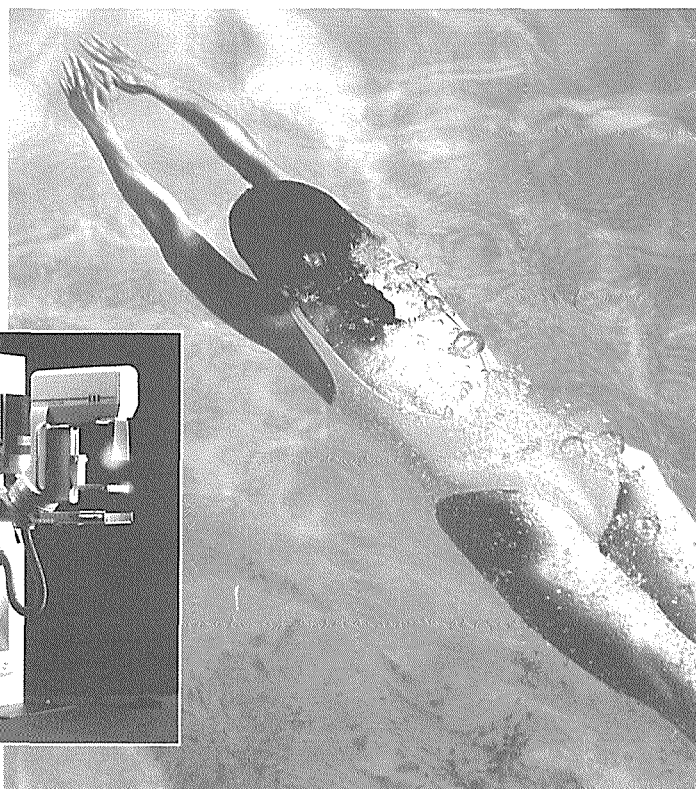
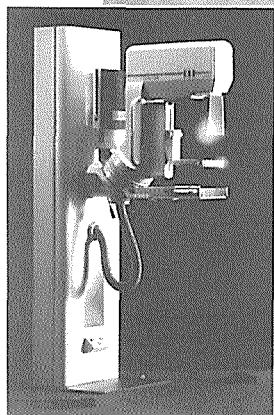
- KODAK • SIEMENS • GENERAL ELECTRIC •
- PHILIPS • BENNETT • HITACHI • POLAROID •
- XENOLITE • MAVIG • CAWO •

- rentgenski filmi in kemikalije
- kontrastna sredstva
- rentgenska zaščitna sredstva
- rentgenski aparati, aparati za ultrazvočno diagnostiko, stroji za avtomatsko razvijanje, negatoskopi in druga oprema za rentgen

** SANOLABOR**, Leskoškova 4, 1103 Ljubljana  
Tel.: 061 185 42 11 Fax: 061 140 13 04

# SIEMENS

## Rešitve po meri



M a m m o m a t 3 0 0 0 m o d u l a r

## Mammomat 3000 modular

- univerzalni sistem za vse vrste mamografije
- optimizacija doze in kompresije z OPDOSE in OPCOMP sistema
- modularna zgradba zagotavlja posodabljanje sistema
- servis v Sloveniji z zagotovljenimi rezervnimi deli in garancijo
- izobraževanje za uporabnike

SIEMENS d.o.o.  
Dunajska 22  
1511 Ljubljana  
Telefon 061/1746 100  
Telefaks 061/1746 135



Diagnostics

Elecsys, Reaching New Heights



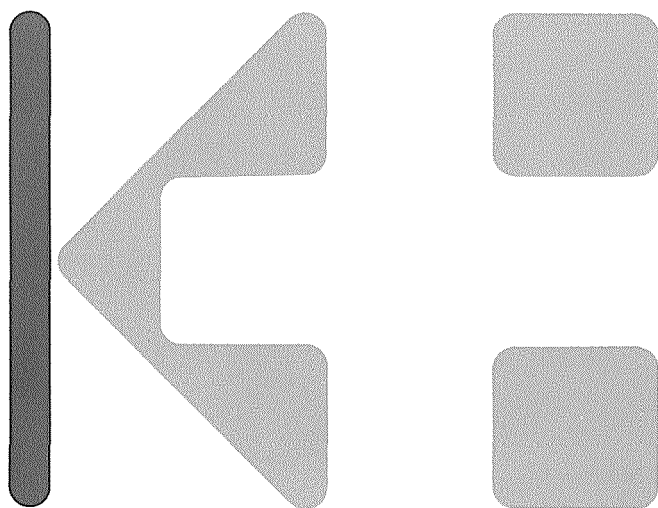
Roche and Boehringer Mannheim, two of the most experienced innovators in diagnostics, have joined forces to create a new, fully-integrated approach to health management worldwide.

**There are no limits to innovation at Roche Diagnostics.**

Roche Diagnostics  
Info Office Ljubljana

Parmova 53  
1000 Ljubljana  
Slovenia

tel.: \* 386 61 133 60 24  
\* 386 61 133 63 31  
fax: \* 386 61 130 92 02



# KEMOFARMACIJA

Lekarne, bolnišnice, zdravstveni domovi in  
veterinarske ustanove večino svojih  
nakupov opravijo pri nas.

Uspeh našega poslovanja temelji na  
kakovostni ponudbi, ki pokriva vsa  
področja humane medicine in veterine, pa  
tudi na hitrem in natančnem odzivu na  
zahteve naših kupcev.

KEMOFARMACIJA – VAŠ ZANESLJIVI DOBAVITELJ!



Veletrgovina za oskrbo zdravstva, d.d. / 1000 Ljubljana, Cesta na Brdo 100  
Telefon: 061 12-32-145 / Telefax: 271-588, 271-362

**ARROW<sup>®</sup>**  
INTERNATIONAL INC.



**EXTRUSION**

DISTRIBUTED  
BY  
**SIRION** s.r.l.  
34170 GORIZIA - ITALY  
Corso Italia 112  
Tel. (0481) 32073-32074  
Fax. (0481) 534753



*varno in učinkovito lajšanje bolečin, tudi ponoči*



*zmaga nad bolečino*

**Tramal<sup>®</sup>**  
RETARD

*samo 2x na dan*



**Sestava:** V lakirani tableti je 100 mg tramadol hidroklorida.

**Oprema:** Tramal retard 100 mg - Skatlica s 30 lakiranimi tabletami.

**Izdeluje:** Bayer Pharma d.o.o. Ljubljana po licenci Grünenthal GmbH



Bayer Pharma d.o.o.



Podrobnejše informacije o zdravilu dobite pri proizvajalcu.

# LABORMED

*laboratory & medical equipment*

LABORMED d.o.o. · SLO-1215 Medvode · Zg. Pirniče 96/c  
Telefon 061 / 621 098 · Telefax 061 / 621 415

Labormed v Sloveniji ekskluzivno zastopa naslednje firme:

## **KÖTTERMANN**

laboratorijsko pohištvo, varnostne omare za kisline, luge, topila, pline in strupe, ventilacijska tehnika in digestoriji

## **EHRET**

laminar flow tehnika, inkubatorji, sušilniki, suhi sterilizatorji in oprema za laboratorijsko vzrejo živali - kletke

## **DAKO**

testi za aplikacijo v imunohistokemiji, patologiji, mikrobiologiji, virologiji, mono- in poliklonalna protitelesa...

## **GFL**

laboratorijski aparati, omare in skrinje za globoko zamrzovanje

## **ROSYS ANTHOS**

fotometri, avtomatski pralni sistem za mikrotitrine plošče

## **CHARLES ISCHI Pharma-Prüftechnik**

specialna oprema za testiranje izdelkov v farmacevtski industriji; aparati za procesno kontrolo in kontrolo kvalitete

## **NOVODIRECT BIOBLOCK**

kompletna oprema in pripomočki za delo v laboratoriju

## **ANGELANTONI SCIENTIFICA**

hladilna tehnika in aparati za laboratorije, transfuziologijo, patologijo in sodno medicino

## **INTEGRA BIOSCIENCES**

laboratorijska oprema za mikrobiologijo, biologijo celic, molekularno biologijo in biotehnologijo

## **CORNINGCostar**

specialna laboratorijska plastika za aplikacijo v imunologiji, mikrobiologiji, virologiji, ipd., mehanske eno- in večkanalne pipete ter nastavki

## **BIOMERICA**

hitri testi za diagnostiko, EIA / RIA testi

## **Advanced BIOTECHNOLOGIES**

PCR tehnologija, potrošni material, reagenti, encimi

## **SVANOVA Biotech**

Elisa testi za diagnostiko v veterini

## **HÜRNER**

ventilacijska tehnika



# GEMZAR®

*gemcitabin hidroklorid*



## Nova *luč* v onkologiji

### INDIKACIJE

- nemikrocelični pljučni karcinom (NSCLC)
- karcinom pankreasa
- karcinom sečnega mehurja

Drugi terapevtski učinki opaženi pri karcinomih dojke, ovarijev, prostate in pri mikroceličnem pljučnem karcinomu (SCLC).

### Oblika in pakiranje

- injekcijska steklenička z 200 mg gemcitabina
- injekcijska steklenička z 1 g gemcitabina

### Sestavine

aktivna učinkovina (gemcitabin hidroklorid), manitol,  
natrijev acetat, natrijev hidroklorid

Dodatne informacije o zdravlilu so na voljo v strokovnih publikacijah, ki jih dobite na našem naslovu.



**Eli Lilly** (Suisse) S. A., Podružnica v Ljubljani,  
Ljubljana, Vošnjakova 2, tel.: (061) 319-648, faks: (061) 319-767

**KNOWLEDGE IS POWERFUL MEDICINE**



Think what you'd gain by giving  
your radiologists a free hand.

Are your radiographers' hands tied by equipment that slows them down? And what can you do about it? Nearly 70% of X-rays are made at a Bucky. A fact that has influenced the design of Philips' Bucky systems. It's led to technology without gadgetry, for uncomplicated, speedy work. Control units operated one-handed.

A display that eliminates trips to the generator. Tomography functions activated via a single button. All to speed patient throughput, for improved cost-efficiency. It's one way in which Philips Medical Systems is working with you to meet today's changing healthcare needs. For more information call 061 177 88 50.

website: [www.philips.com/ms](http://www.philips.com/ms)



**PHILIPS**

*Let's make things better.*





# iflazon®

kapsule

flukonazol

- *v svetu največ predpisovani sistemski antimikotik*
- *edini peroralni sistemski antimikotik za zdravljenje vaginalne kandidoze, ki ga je odobril FDA*

Skrajšano navodilo

Flukonazol je sistemski antimikotik iz skupine triazolov.

#### Odmerjanje pri različnih indikacijah:

vaginalna kandidoza	150 mg v enkratnem odmerku
mukozna kandidoza	50 do 100 mg na dan
dermatomikoze	50 mg na dan ali 150 mg na teden
sistemska kandidoza	prvi dan 400 mg, nato od 200 do 400 mg na dan Največji dnevni odmerek je 800 mg.
preprečevanje kandidoze	50 do 400 mg na dan
kriptokokni meningitis	prvi dan 400 mg, nato od 200 do 400 mg na dan
vzdrževalno zdravljenje	200 mg na dan

**Kontraindikacije:** Preobčutljivost za zdravilo ali sestavine zdravila. **Interakcije:** Pri enkratnem odmerku flukonazola za zdravljenje vaginalne kandidoze klinično pomembnih interakcij ni. Pri večkratnih in večjih odmerkih so možne interakcije s terfenadinom, cisapridom, astemizolom, varfarinom, derivati sulfonilureje, hidroklorotiazidom, fenitoinom, rifampicinom, ciklosporinom, teofilinom, indinavirom in midazolamom. **Nosečnost in dojenje:** Nosečnica lahko jemlje zdravilo le, če je korist zdravljenja za mater večja od tveganja za plod. Doječe matere naj med zdravljenjem s flukonazolom ne dojijo. **Stranski učinki:** Povezani so predvsem s prebavnim traktom: slabost, napenjanje, bolečine v trebuhu, driska, zelo redko se pojavijo preobčutljivostne kožne reakcije, anafilaksija in angioedem – v tem primeru takoj prenehamo jemati zdravilo. Pri bolnikih s hudimi glivičnimi obolenji lahko pride do levkopenije in trombocitopenije in do povečane aktivnosti jetrnih encimov. **Oprema in način izdajanja:** 7 kapsul po 50 mg, 28 kapsul po 100 mg, 1 kapsula po 150 mg. Na zdravniški recept: 1/99.

Podrobnejše informacije so na voljo pri proizvajalcu.



Krka, d. d., Novo mesto  
Šmarješka cesta 6  
8501 Novo mesto

## Instructions for authors

**Editorial policy** of the journal *Radiology and Oncology* is to publish original scientific papers, professional papers, review articles, case reports and varia (editorials, reviews, short communications, professional information, book reviews, letters, etc.) pertinent to diagnostic and interventional radiology, computerized tomography, magnetic resonance, ultrasound, nuclear medicine, radiotherapy, clinical and experimental oncology, radiobiology, radiophysics and radiation protection. The Editorial Board requires that the paper has not been published or submitted for publication elsewhere: the authors are responsible for all statements in their papers. Accepted articles become the property of the journal and therefore cannot be published elsewhere without written permission from the editorial board. Papers concerning the work on humans, must comply with the principles of the declaration of Helsinki (1964). The approval of the ethical committee must then be stated on the manuscript. Papers with questionable justification will be rejected.

**Manuscript** written in English should be submitted to the Editorial Office in triplicate (the original and two copies), including the illustrations: *Radiology and Oncology*, Institute of Oncology, Vrazov trg 4, SI-1000 Ljubljana, Slovenia; (Phone: +386 61 132 00 68, Tel./Fax: +386 61 133 74 10, E-mail: gersa@onko-i.si). Authors are also asked to submit their manuscripts on a 3.5" 1.44 Mb formatted diskette. The type of computer and word-processing package should be specified (Word for Windows is preferred).

All articles are subjected to editorial review and review by independent referee selected by the editorial board. Manuscripts which do not comply with the technical requirements stated

herein will be returned to the authors for correction before peer-review. Rejected manuscripts are generally returned to authors, however, the journal cannot be held responsible for their loss. The editorial board reserves the right to ask authors to make appropriate changes in the contents as well as grammatical and stylistic corrections when necessary. The expenses of additional editorial work and requests for reprints will be charged to the authors.

**General instructions** • Radiology and Oncology will consider manuscripts prepared according to the Vancouver Agreement (*N Engl J Med* 1991; **324**: 424-8, *BMJ* 1991; **302**: 6772; *JAMA* 1997; **277**: 927-34.). Type the manuscript double spaced on one side with a 4 cm margin at the top and left hand side of the sheet. Write the paper in grammatically and stylistically correct language. Avoid abbreviations unless previously explained. The technical data should conform to the SI system. The manuscript, including the references may not exceed 15 typewritten pages, and the number of figures and tables is limited to 4. If appropriate, organize the text so that it includes: Introduction, Material and methods, Results and Discussion. Exceptionally, the results and discussion can be combined in a single section. Start each section on a new page, and number each page consecutively with Arabic numerals.

**Title page** should include a concise and informative title, followed by the full name(s) of the author(s); the institutional affiliation of each author; the name and address of the corresponding author (including telephone, fax and e-mail), and an abbreviated title. This should be followed by the *abstract page*, summarising in less than 200 words the reasons for

the study, experimental approach, the major findings (with specific data if possible), and the principal conclusions, and providing 3-6 key words for indexing purposes. Structured abstracts are preferred. If possible, the authors are requested to submit also slovenian version of the title and abstract. The text of the report should then proceed as follows:

*Introduction* should state the purpose of the article and summarize the rationale for the study or observation, citing only the essential references and stating the aim of the study.

*Material and methods* should provide enough information to enable experiments to be repeated. New methods should be described in detail. Reports on human and animal subjects should include a statement that ethical approval of the study was obtained.

*Results* should be presented clearly and concisely without repeating the data in the tables and figures. Emphasis should be on clear and precise presentation of results and their significance in relation to the aim of the investigation.

*Discussion* should explain the results rather than simply repeating them and interpret their significance and draw conclusions. It should review the results of the study in the light of previously published work.

**Illustrations and tables** must be numbered and referred to in the text, with appropriate location indicated in the text margin. Illustrations must be labelled on the back with the author's name, figure number and orientation, and should be accompanied by a descriptive legend on a separate page. Line drawings should be supplied in a form suitable for high-quality reproduction. Photographs should be glossy prints of high quality with as much contrast as the subject allows. They should be cropped as close as possible to the area of interest. In photographs mask the identities of the patients. Tables should be typed double spaced, with descriptive title and, if appropriate, units of numerical measurements included in column heading.

**References** must be numbered in the order in which they appear in the text and their corresponding numbers quoted in the text. Authors are responsible for the accuracy of their references. References to the Abstracts and Letters to the Editor must be identified as such. Citation of papers in preparation, or submitted for publication, unpublished observations, and personal communications should not be included in the reference list. If essential, such material may be incorporated in the appropriate place in the text. References follow the style of Index Medicus. All authors should be listed when their number does not exceed six; when there are seven or more authors, the first six listed are followed by "et al.". The following are some examples of references from articles, books and book chapters:

Dent RAG, Cole P. *In vitro* maturation of monocytes in squamous carcinoma of the lung. *Br J Cancer* 1981; **43**: 486-95.

Chapman S, Nakielnny R. *A guide to radiological procedures*. London: Bailliere Tindall; 1986.

Evans R, Alexander P. Mechanisms of extracellular killing of nucleated mammalian cells by macrophages. In: Nelson DS, editor. *Immunobiology of macrophage*. New York: Academic Press; 1976. p. 45-74.

**Page proofs** will be faxed to the corresponding author whenever possible. It is their responsibility to check the proofs carefully and fax a list of essential corrections to the editorial office within 48 hours of receipt. If corrections are not received by the stated deadline, proof-reading will be carried out by the editors.

Reprints: Fifty reprints are free of charge, for more contact editorial board.

---

For reprint information in North America Contact:  
International Reprint Corporation 968 Admiral  
Callaghan Lane, # 268 P.O. Box 12004, Vallejo; CA  
94590, Tel: (707) 553 92 30, Fax: (707) 552 95 24.

# Za mirno potovanje skozi kemoterapijo

**Navoban**  
tropisteron

- preprečevanje slabosti in bruhanja pri emetogeni kemoterapiji
- učinkovito zdravilo, ki ga odrasli in otroci dobro prenašajo
- vedno 1-krat na dan
- vedno 5 mg

**Skrajšano navodilo za uporabo:** Navoban® kapsule, Navoban® raztopina za injiciranje 2 mg in 5 mg. Serotoninski antagonist. **Oblika in sestava:** 1 trda kapsula vsebuje 5 mg tropisetronovega hidroklorida. 1 ampula po 2 ml vsebuje 2 mg tropisetronovega hidroklorida. 1 ampula po 5 ml vsebuje 5 mg tropisetronovega hidroklorida. **Indikacije:** Preprečevanje slabosti in bruhanja, ki sta posledici zdravljenja s citostatiki. Zdravljenje pooperativne slabosti in bruhanja. Preprečevanje pooperativne slabosti in bruhanja pri bolnicah, pri katerih je načrtovana ginekološka operacija v trebušni votlini. **Odmerjanje in uporaba:** Preprečevanje slabosti in bruhanja, ki sta posledici zdravljenja s citostatiki. **Odmerjanje pri otrocih:** Otroci starejši od 2 let 0,2 mg/kg telesne mase na dan. Največji dnevni odmerek ne sme preseči 5 mg. Prvi dan kot intravenska infuzija ali kot počasna intravenska injekcija. Od 2. do 6. dne naj otrok jemlje zdravilo oralno (raztopino v ampuli razredčimo s pomarančnim sokom ali koka kolo). **Odmerjanje pri odraslih:** 6-dnevna kura po 5 mg na dan. Prvi dan kot intravenska infuzija ali počasna intravenska injekcija. Od 2. do 6. dne 1 kapsula na dan. **Zdravljenje in preprečevanje pooperativne slabosti in bruhanja:** **Odmerjanje pri odraslih:** 2 mg Navobana z intravensko infuzijo ali kot počasna injekcija. Glej celotno navodilo! **Kontraindikacije:** Preobčutljivost za tropisetron, druge antagoniste receptorjev 5-HT<sub>3</sub> ali katerokoli sestavino zdravila. Navobana ne smemo dajati nosečnicam; izjema je preprečevanje pooperativne slabosti in bruhanja pri kirurških posegih, katerih del je tudi terapevtska prekinitev nosečnosti. **Previdnostni ukrepi:** Bolniki z nenadzorovano hipertenzijo; bolniki s prevodnimi ali drugimi motnjami srčnega ritma; ženske, ki dojijo; bolniki, ki upravljajo s stroji ali vozili. **Medsebojno delovanje zdravil:** Rifampicin ali druga zdravila, ki inducirajo jetrne encime. Glej celotno navodilo! **Stranski učinki:** Glavobol, zaprtje, redkeje omotica, utrujenost in prebavne motnje (bolečine v trebuhu in driska), preobčutljivostne reakcije. Zelo redko kolaps, sinkopa ali zastoj srca, vendar vzročna zveza z Navobanom ni bila dokazana. **Način izdajanja:** Kapsule: uporaba samo v bolnišnicah, izjemoma se izdaja na zdravniški recept pri nadaljevanju zdravljenja na domu ob odpustu iz bolnišnice in nadaljnjem zdravljenju. Ampule: uporaba samo v bolnišnicah. **Oprema in odločba:** Zloženka s 5 kapsulami po 5 mg; številka odločbe 512/B-773/97 z dne 10. 11. 1997. Zloženka z 1 ampulo po 2 ml (2 mg/2 ml); številka odločbe 512/B-772/97 z dne 10. 11. 1997. Zloženka z 10 ampulami po 5 ml (5 mg/5 ml); številka odločbe 512/B-771/97 z dne 10. 11. 1997. **Izdelovalec:** NOVARTIS PHARMA AG, Basel, Švica. **Imetnik dovoljenja za promet z zdravilom:** NOVARTIS PHARMA SERVICES INC., Podružnica v Sloveniji, Dunajska 22, 1511 Ljubljana, kjer so na voljo informacije in literatura. **Preden predpišete Navoban, prosimo preberite celotno navodilo.**

 **NOVARTIS**



